TEMPORAL VARIATION IN THE ALLOCATION OF ACID MINE DRAINAGE CONTAMINANTS IN THE WATERS AND SEDIMENTS OF THE ENGINEERED REMEDIATION REED BEDS ALONG THE VARKENSLAAGTE STREAM:
AN AUTUMN – WINTER STUDY

By

Patricia. N. Omo-Okoro

784744

A research report submitted to the Faculty of Science, University of the Witwatersrand in partial fulfillment of the requirements for the degree of Masters

(MSc. by Course work and Research Report)

30th September, 2015

Supervisor: Prof. Christopher Curtis (School of Geography, Archaeology & Environmental Studies)

Advisor: Isabel Weiersbye (School of Animal, Plant & Environmental Sciences)

Dedication

To God Almighty, who gave me strength, good health, resilience, direction and protection throughout the entire period, it was tough but Lord, your Mercy and Grace saw me through.

Declaration

I declare that this research report is my own unaided work. It is being submitted for the degree of Master of Science at the University of the Witwatersrand, Johannesburg, South Africa. It has not been submitted before for any degree or examination at any other university.

Patricia N. Omo-Okoro (Mrs.)
School of Geography, Archaeology and Environmental Studies
University of the Witwatersrand, Johannesburg,
30/09/2015.

Abstract

Acid Mine Drainage (AMD) refers to the seepage or runoff of acidic water from abandoned mines into the surrounding environment. Acid mine drainage is considered a serious long term environmental threat associated with mining. This study was conducted on the Varkenslaagte canal or stream which flows from north to south within the AngloGold Ashanti West Wits gold mining operation, 75 km west of Johannesburg, and receives AMD from tailings storage facilities (TSFs) located on both the northern aspect and the western aspect of the catchment. On the Varkenslaagte, 17 reed beds were planted between 1-12-2011 and 12-9-2012, in a series of shallow excavated depressions. This study was conducted in 2013 and 2014, and aimed to ascertain: (i) whether there is any temporal difference (autumn – end of the rainy season, versus winter – mid-dry season, for 2013 and 2014 combined) in selected fresh-water quality parameters and concentrations of AMD contaminants in the flowing waters in the engineered reed beds; - this was observed, as higher concentrations were recorded in winter than in autumn, for some of the selected water quality parameters, in both survey years; (ii) to determine if vertical changes exist in the elements down the sediment profile from the surface to a depth of approximately half a metre; - conspicuous vertical changes were not evident; and also; (iii) to provide a baseline for monitoring the post clean-up state of the upper Varkenslaagte, and conclude whether the reed bed system is retaining AMD contaminants (major ions, trace and major elements). Chemical variations in water and sediment samples were measured *in situ* in April/May 2013 and July 2014, and water samples and sediment cores collected for laboratory analyses. Water samples were collected from three points (inflow, middle and outflow) at each of 15 reed beds (RBs, numbered RB 1 -15) in receipt of AMD from two directions (downstream and laterally from TSFs on the northern and western aspects). Ion Chromatography was used to detect chloride (Cl^-) and sulphate (SO_4^{2-}), Inductively Coupled Plasma Optical Emission Spectroscopy (ICP-OES) and Inductively Coupled Plasma Mass Spectrometry (ICP-MS) were used to identify major and trace elements; iron (Fe), magnesium (Mg), manganese (Mn), potassium (K), cobalt (Co), nickel (Ni), lead (Pb), copper (Cu) and zinc (Zn) in the water samples whereas X-Ray Fluorescence (XRF) analysis for elements was conducted on surface sediments (0-2cm; additional analyses of sediment core samples at depths 2-5 cm, 5-10 cm, 10-20 cm and 20 -30 cm were analyzed but were not considered further).

The water in the reed beds was moderately acidic to within the target range. It ranged from pH 5.17 to 6.51 in April, 2014 (approaching the end of the wet season) ($P < 0.05$) ($P = 0.0001$) to slightly higher values of pH 5.45 to 6.82 in July, 2014 (mid-dry season) ($P = 0.0053$). Marginal acidity is above pH 6. A pH of 6.5 – 7.5 is within the target water quality range (TWQR) on the Highveld. High electrical conductivity (EC) values were found, ranging from 3500 – 4600 µs/cm in April and 2600 – 5500 µs/cm in July, though EC values can be higher on much of the South African gold mining Highveld. Lateral influx of AMD from the western TSFs was visually observed into two of the southernmost Varkenslaagte stream reed beds (at RBs13 and 15) during both April and July sampling. In 2014, the Varkenslaagte was still flowing from reed bed to reed bed, although very slowly, similar to 2013. Chloride, sulphate and metal concentrations were high relative to target water quality ranges in most of the reed beds in during April and July, 2014. Although higher concentrations in the sediment suggest that the reed beds are effective in capturing and retaining contaminants in sediment and root mass, the concentrations in the water in reed beds 1-15 still exceeded the target water quality ranges for aquatic ecosystems in South Africa (DWAF, 1996) and the World Health Organization (WHO) guidelines for drinking water quality (WHO, 2004). However use of the water from the Varkenslaagte by humans and livestock is prohibited by the Department of Water and Environmental Affairs, and the National Nuclear Regulator.

The bar charts comparing 2013 and 2014 selected water quality data showed that during winter/drier periods with no rains, the rate of evaporation exceeded dilution; this was observed by the slightly lower pH values recorded across the reed beds in July, 2013 and 2014, in comparison with the slight higher pH values recorded across the reed beds in May, 2013 and April, 2014. The bar charts also showed that the highest EC was recorded in the winter of 2014. It was also observed from the principal component analyses (PCAs) that EC, sulphate and pH, in combination with Mg and Fe, were responsible for most of the variation in the water quality data for the two survey years, 2013 and 2014. Following the findings from this study, it is recommended that monitoring of the site should also address whether the reed beds and other control measures that have been put in place (riparian woodlands and windmill pumps) will be adequate to control the lateral seepage from the Western TSFs at some of the southernmost reed beds.

Acknowledgements

First of all, my profound gratitude goes to the Almighty God for His protection and guidance throughout this period and for making it possible for me to complete this study, I would not have achieved this on my own.

I would like to thank my supervisor Prof. Chris Curtis who tirelessly guided me through this project and to my advisor Isabel Weiersbye, your timely advice, suggestions and corrections are invaluable. I am very grateful to Maxine Joubert, who was with me at each site visit and whose Honors project contributed the 2013 data. To Prof. Fethi, thank you for the encouragement and advice.

Many thanks to Innocent Rabohale and Chris Davies for your help while I was working at the EEPP laboratory, to Alexandra Wald and Shena Kennedy of the EEPP team for your support and encouragement, to Dr. Julien Lusilao and Dr. Hlanganani Tutu of the Environmental and Analytical Chemistry Group for conducting some of the water chemistry analysis. To Sabelo, Mbuli and Siyamcella, thank you for helping out with the soil core pipes at the site. I would also like to thank the Ecological Engineering and Phytotechnology Programme (EEPP), in the School of Animal, Plant and Environmental Sciences and AngloGold Ashanti for the MSc bursary and project running costs through the THRIP Grant (Department of Trade and Industry and the National Research Foundation) to Isabel Weiersbye and Prof. Edward Witkowski.

To Donna Koch of the School of Geography and Environmental Studies and friends like Dr. Shola Shonubi, Thibedi Moshoeu, Eromsele Ebhuoma, Julius Osayi, Cynthia Nnaji, Chiedu Nwokolo, Shemo Akpene, Victoria Nwafor, Vivian Ezekobe, Elo Okudo and Yemisi Bakare, thanks for being there throughout this period.

Lastly, I am greatly indebted to my parents, Mr. and Mrs. Udechukwu, my husband and kids, my brothers IK and Charles, my sister Chinwe and to my in laws Mummy Warri, aunty Yule, Ada and Tina for your constant support and check on my progress throughout this programme.

Table of Contents

List of Abbreviations

AGA:	AngloGold Ashanti
AMD:	Acid Mine Drainage
CRM:	Certified Reference Material
DWA:	Department of Water Affairs (of South Africa)
IC:	Ion Chromatography
ICP-MS	Inductively Coupled Plasma Mass Spectrometry
ICP-OES:	Inductively Coupled Plasma Optical Emission Spectroscopy
LOD:	Limit of Detection
RB:	Reed bed
RSD:	Relative Standard Deviation
TSF:	Tailings Storage Facility
USEPA:	United States Environmental Protection Agency
WHO:	World Health Organization
XRF:	X-ray Fluorescence
TWQR:	Target Water Quality Range

List of Figures

List of Tables

Chapter 1: Introduction

This chapter introduces the problem, which is the heavily contaminated Varkenslaagte canal and stream which starts under a tailings storage facility (TSF) on AngloGold Ashanti (AGA) mining operations. How AGA and the University of the Witwatersrand have tried to remedy this situation is explained. The objectives, key questions, motivation for this study and the overall hypothesis are also given in this chapter

1.1 General overview

Mining is an important factor contributing towards the current level of human civilization in South Africa and in other countries, where mining drives their economies. Mining has environmental impacts, one of which is acid mine drainage (AMD). The impact of mining on the environment includes the release of many chemical contaminants into water sources by way of AMD production. These chemical contaminants can cause environmental damage and threaten the health and safety of nearby communities who rely on the water long after mine closure. This pollution is so persistent that, in the absence of effective remediation techniques, in many cases the contaminated sites may never be rehabilitated (CSIR, 2009). Hence there is the need for continuous studies on techniques to prevent, control and mitigate AMD.

Acid mine drainage is the generation of sulphuric acid that occurs when the mineral pyrite comes in contact with oxygen, water and sulphur oxidizing bacteria, as a result of the mining and processing activities of the gold and coal mining industries (Zamzow, 2014). Acid mine drainage causes environmental pollution that affects many countries having historic or current mining industries that rely on sulphide ores (Johnson and Hallberg, 2005). The process of acid mine drainage formation involves the oxidation of iron disulphide (also known as iron pyrite), in a two-stage process. The first stage produces sulphuric acid and ferrous sulphate and the second stage produces orange-red ferric hydroxide and more sulphuric acid (McCarthy, 2011). The tailings storage facilities (TSFs), also known as mine dumps, in the Highveld of South Africa contain pyrite minerals because gold occurs in association with these in the Witwatersrand Basin

ores. The influx of AMD into streams can severely degrade both habitat and water quality often producing an environment devoid of most aquatic life and unfit for desired uses (Fadiran *et al.*, 2014).

The pollution of surface waters from mines is a global problem wherever mineral ores have been exploited (Chapman *et al*., 2013). It is a problem in China (He *et al*., 1997), North America (Wren and Stephenson, 1991), South America (Van Damme *et al*., 2008), United Kingdom (Johnson and Hallberg, 2005; Smith, 1997; Neal *et al*., 2005), Australia (Battaglia, 2005) and South Africa (Tutu *et al*., 2008; McCarthy, 2011). According to the United States Environmental Protection Agency (USEPA) regulations, acid mine drainage is drainage water from a mine which before any treatment has a pH of less than 6 or a total iron concentration of 10 mg/l or greater. The chemistry of AMD is very complex and dependent on a number of factors and controls both geological and geochemical, including the amount and type of sulphide mineral being oxidized (Ziemkiewicz *et al*., 2003; Berger *et al*., 2000). The most common sulphides are iron sulphides but other metal sulphide minerals may also be acid generating (Akcil and Koldas, 2006).

Remediation techniques are available to treat acid mine drainage, most of which are very expensive or require large operating budgets. In some situations, a more cost effective remediation technique may be the use of the passive wetland remediation technique, for example the reed beds system. Wetland remediation is a successful and low maintenance method to remediate AMD. The reed beds or wetland water treatment system is a proven technology that has been employed in countries like the United Kingdom, United States of America, Australia and South Africa (Neal *et al*., 2004; Smith, 1997).

The study area in this research is the heavily polluted Varkenslaagte canal which originates under and around a large TSF complex, constructed in the 1950s, and located within the AngloGold Ashanti's mining operational area (Figure 1). AngloGold Ashanti (AGA) is a mining company in South Africa. During the period 2011 to 2012, AGA cleaned approximately 180,000 cubic metres of spilled tailings from the canal and the area below the TSFs where this study is conducted. The original wetland soils were mapped and the canal was reshaped into a small drainage line on its original pathway, with a series of 17 reed beds established in shallow depressions between 2012 and 2013 by EMPR Services (Johannesburg), an environmental

rehabilitation company. The aim of this study is to assess the early performance of the reed bed system in retarding AMD contaminants (selected ion, trace and metal elements), through the measurement of water and sediment quality.

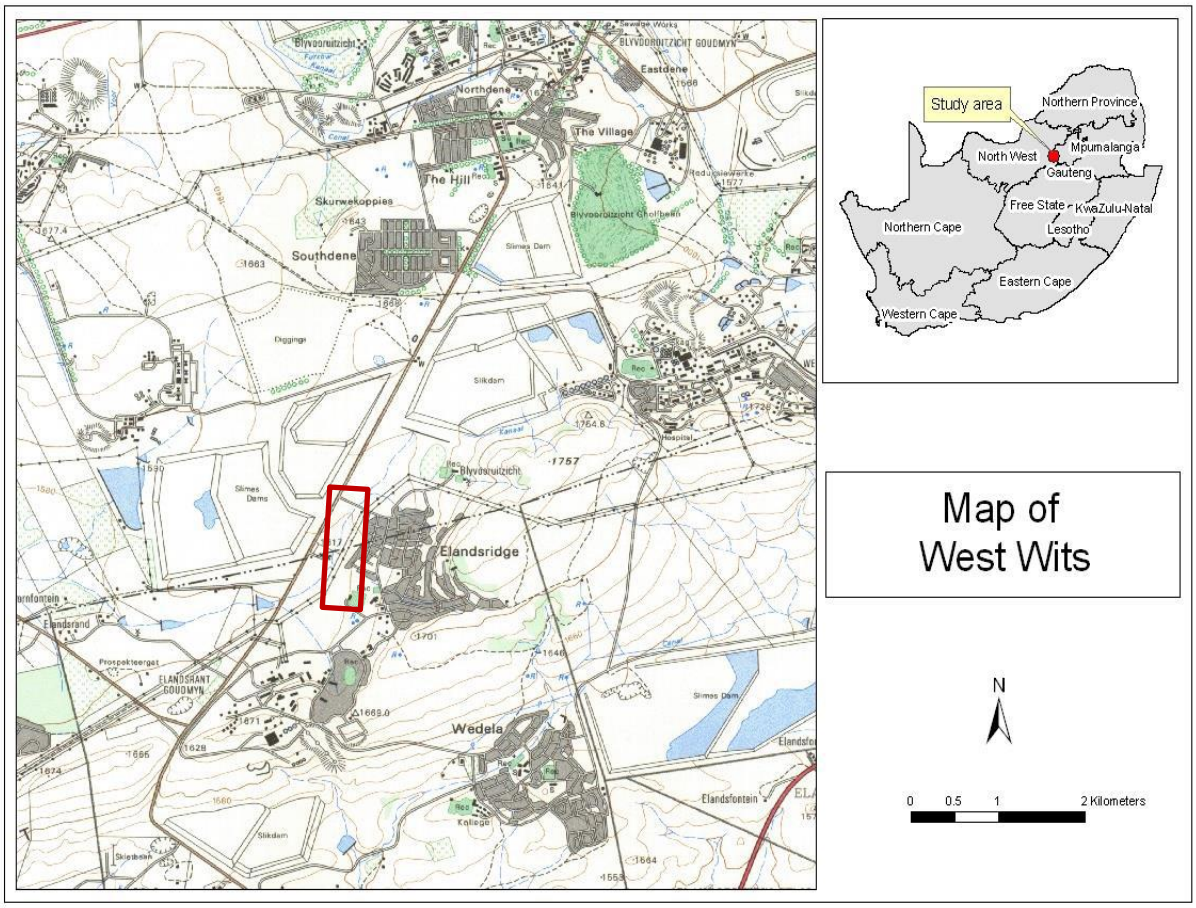

Figure 1: A map showing the study area outlined in red on AngloGold Ashanti West Wits gold mining operations (redrawn from Joubert, 2013).

1.2 Motivation for study

In spite of the fact that water is a scarce resource in South Africa, AMD contributes about 88% of the total wastewater produced (CSIR, 2009). Hence there is the need for technologies that

treat wastewaters and also do so in an eco-friendly way, in South Africa, so as to conserve this limited resource.

Wetland and reed beds systems have been widely used in countries like the United Kingdom, U.S.A., South Africa, Australia, Canada, Denmark, Germany and other European countries due to their low cost of operation and maintenance, availability regardless of seasons, ability to reduce, sequester, adsorb, absorb, uptake and accumulate metals to significant levels (Smith, 1997; Neal *et al*., 2004).

Reed beds systems are robust and well proven, requiring only a fraction of the maintenance of traditional methods of treatment. The use of reed beds systems in treating contaminated effluents does not require the application of chemicals like other remediation techniques. In the past, sludge, both in the liquid and solid form could be disposed of to landfill at reasonable costs but recent legislative measures have been instigated making landfill an increasingly expensive and time- limited disposal option (Johnson and Hallberg, 2005).

The use of reed beds increases of the retention time of a stream influx, thereby slowing the flow of water and ultimately filtering the water. This is a type of phytoremediation technique known as rhizofiltration. Rhizofiltration acts as an organic filter, reducing downstream transport of contaminants. In the case of this study site, the contaminant-loaded biomass may later need to be harvested and disposed of as organic mulch as cover for TSFs (Dye and Weiersbye, 2013). Engineered reed bed systems do not require the use of power, as with other physical and chemical methods of effluent remediation. AngloGold Ashanti has invested greatly in the cleanup of tailings and rehabilitation of the Varkenslaagte canal, including a polishing mechanism for AMD in the form of the engineered remediation reed beds in the study area (Figure 2). These reed beds are located on the exact same sites where reed beds historically occurred on the wetland soils along the drainage line. The AMD generated on the Varkenslaagte stream is depicted by the whitish, crystalline mineral encrustations (efflorescence) seen at the sides of the stream (Figure 2). This study will serve to monitor the progress of this development in retarding AMD contamination and also produce useful recommendations for future studies on the study site.

Figure 2: A photograph showing acid mine drainage at the foot of the Old North Complex TSF and mineral efflorescence (as white encrustations) on the catchment of the Varkenslaagte stream in July, 2013 (Courtesy of Chris Curtis).

1.3 Objectives of the research

The objectives of the current study are:

1. To test the early performance of the 6- to 18-month old engineered reed beds in mitigating water acidity, sequestering contaminants in the sediment, and reducing contaminant transport downstream.

2. To determine whether the water parameters: pH, electrical conductivity (EC) and metal concentrations meet target water quality criteria.

3. To establish a baseline against which to assess future changes in water and sediment quality, and to serve as a periodic evaluation of the reed beds and sediment in containing AMD contaminants. This will assist AGA in determining whether investment in reed beds for AMD treatment is cost-effective and justified in the long term.

1.4 Research questions

The key questions in this study are:

1. Is there a spatial variation in the water parameters (pH, EC, Eh or ORP) and concentrations of ions in solution across the reed beds?

2. Is there a seasonal or temporal variation (April – end of wet season, versus July – mid dry-season) in the water quality (water samples) and surface sediments (0-2 cm) within the engineered reed beds?

1.5 The null hypothesis for this study

There is no difference in the contaminant concentrations in the water nor in the sediment (0-2 cm depth profile) between the reed beds.

1.6 Study sections

This study comprises six chapters. **Chapter 1** provides an introductory background to the study area and research. **Chapter 2** provides some review on AMD, its effects and remediation techniques. In **Chapter 3** the study area is described in detail, also the material and methods employed are explained. **Chapter 4** presents the results and data analysis of the different statistical tests done for the variables in the water and sediment samples. **Chapter 5** presents the discussion surrounding the key findings in the study. **Chapter 6** presents a summary of the research findings discussed in the previous chapter, with conclusions and recommendations.

Chapter 2: Literature review

This chapter describes the study area (the upper Varkenslaagte canal and stream), gold mining in South Africa, acid mine drainage, its effects and remediation techniques.

2.1 The gold mining sector in South Africa

The Witwatersrand gold basin has been mined for more than 100 years (Morrison, 2004). The main gold producing area in South Africa was concentrated on the Archaean Witwatersrand Basin. Witwatersrand gold occurs in layers of conglomerate rock forming part of the nearly 7000 metres thick sequence of sedimentary rocks of the Witwatersrand Super group (McCarthy, 2011). The gold-bearing Ventersdorp Super group and the Witwatersrand Super group are situated underneath the karst aquifers, made up of the dolomites of the younger Transvaal Super group which continuously flood the mines (Durand, 2012).

The gold mining industry in South Africa specifically the Witwatersrand goldfield is in decline but the post-closure decant of AMD poses serious environmental threats. The acid mine water started to decant from the defunct flooded underground mine workings near Krugersdorp Nature Reserve on the West Rand in August, 2002, leading to polluted surface waters (CSIR, 2009; Winde and Stoch, 2010). Tunnels of adjacent mines may eventually join up, creating a vast network of mine voids that are all inter connected extending kilometers underground. This feature of underground mines allowed AMD to spread within East Rand and West Rand (Durand, 2012).

The Witwatersrand conglomerates typically contain about 3% pyrite, most of which are deposited on tailings dumps. When pyrite minerals are exposed to water, air and bacterial activity (sulphur-utilizing bacteria), they undergo oxidation releasing sulphuric acid and thus becomes a source of AMD. Acid mine drainage formation brings about dissolution of other

metals. Subsequent leaching and decanting of these metals into the groundwater system occur, eventually seeping into surface drainage areas (McCarthy, 2011). Acid mine drainage formation usually occurs naturally, with very little environmental harm but mining, especially, gold mining has increased the exposure of the sulphide bearing rock on the earth's surface, thereby allowing for the production of AMD (Akcil and Koldas, 2006). Acid rock drainage will not occur upon the exposure of the sulphide bearing rock if the sulphide mineral is non-reactive. Acid mine drainage will also not be produced, if the rock contains adequate base potential to neutralize the acid, and also not, if effective AMD mitigating measures are implemented appropriately (Barton-Bridge and Robertson, 1989).

Gold mining sites can present several AMD sources broadly classified into primary and secondary sources (Akcil and Koldas, 2006). Some of the primary sources of AMD on a gold mine site include underground workings, waste rock dumps and TSFs. The secondary sources of AMD may include ore stockpiles and TSF footprints. Footprints refer to areas previously occupied by contaminated soils which are left behind after re-mining of the original TSF to reprocess and recover residual gold (Akcil and Koldas, 2006; Barton-Bridge and Robertson, 1989). Gold tailings dumps have been a feature of the landscape around large gold mining towns since the era of mining and have been discharging polluted seepage for decades (McCarthy, 2011). Tailings storage facilities and areas of contaminated soil where tailings have been previously removed cover 400-500 km^2 of the Witwatersrand basin gold fields and in total comes to around 6 billion tons of material (AGA, 2009). Streams draining these gold tailings dumps are therefore typically acidic and have high and potentially toxic metal concentrations causing serious environmental degradation in the region. The issue that South Africa is currently facing is that many of the gold mines were abandoned, before the full socio-economic and environmental impacts caused by these mines, became obvious. Thus, the previous mine authorities cannot be legally compelled to remediate the fall-out negative environmental impacts (Makgae, 2012). These abandoned mines are presently the State's responsibilities, because of their impact to the environment and the public and the cost of tackling these challenges is enormous (Naicker *et al*., 2003; Makgae, 2012).

2.1.1 Legislation

The early mining economy in South Africa was simply an extractive industry with little consideration given to possible adverse long term effects. It was only in 1996, that South Africa incorporated the objectives of sustainability and social justice into its constitution. The country then developed and implemented a comprehensive legislation to regulate environmental management and mine closure processes (Swart, 2003). In South Africa in the constitution, under Section 24, it is stated that,

> *"everyone has the right; (a) to an environment that is not harmful to their health or well-being; and (b) to have the environment protected, for the benefit of present and future generations, through reasonable legislative and other measures that – (i) prevent pollution and ecological degradation; (ii) promote conservation; and (iii) secure ecologically sustainable development and use of natural resources while promoting justify able economic and social development"*.

The subsequent environment and water acts give effect to the principles in the constitution (Constitution of the Republic of South Africa, Act 108 of 1996: p8).

In spite of the progress being made in South Africa in shifting policy frameworks to address mine closure and mine water management, and the mining industry changing practices to conform to new legislations and regulations, the present state of the environment still poses serious threats (Makgae, 2012). South Africa now has both the National Environmental Management Act (NEMA) (Act 107 of 1998) and the National Water Act (Act 36 of 1998) stipulating that a party has to take all reasonable measures to prevent pollution or degradation from occurring, continuing, or recurring as a result of mining operations for which it is responsible (Makgae, 2012; Swart, 2003). According to these Acts, investigations, training, ceasing or modification of activities or processes, containment and remediation have to be undertaken by the responsible party. There is now the 'polluters pay principle' which makes a party liable for whatever negative impacts its mining activities may cause. Another Act is the Mineral and Petroleum Resources Development (MPRDA) Act of 2002 which is definitely an achievement, in the revolution of the mining industry in all areas; it provides a wholesome cradle-to-grave strategy. Imbibed in the MPRDA Act, are the principles of sustainable

development. The environmental and socio-economic aspects are also integrated into the planning, implementation, closure and post-closure management of prospecting and mining operations (Swart, 2003).

2.2. Mining and the issue of acid mine drainage (AMD) in South Africa, the extent and the mitigating steps that have been employed

Vast mineral resources abound in South Africa and the income generated by the mining industry; specifically gold mining has fuelled the country's economy and funded its development. Mining has been in progress in South Africa since 1886, soon after gold was found and specifically in the Wonderfonteinspruit area for over 120 years. It later moved 30 kilometres to the west of Johannesburg in Gauteng province (Winde and Stoch, 2010). The Witwatersrand Super group where gold is found is geographically located in the southern part of the Gauteng province and in the North West province. Some gold was also found in some parts of the Free State in 1946 (Durand, 2012). Gold tailings dumps have been a feature of the South African landscape around large gold mining towns, since mining began and these tailings dumps have been discharging polluted mine water for decades (Tutu *et al*., 2008). Gold was initially extracted using a mercury (Hg) amalgam method (Tutu *et al*., 2008). The cyanide extraction method was introduced in 1915. Later, issues included the very deep underground mines being too hot for the miners and how to pump water which flooded the mine shafts (Tutu *et al*., 2008). Mining companies in a bid to keep the water table low to allow for deep underground mining had to resort to pumping large volumes of water from their underground workings during mining operations (Durand, 2012). The cyanide extraction method was highly effective for gold dissolution but it required finer milling. The resultant tailings were piped in aqueous slurry to disposal sites known as slimes dumps or tailings storage facilities. These mine dumps today are sources and major causes of AMD formation and potentially toxic salt and metal pollution (Makgae, 2012).

Acid mine drainage is one of the most serious environmental problems that the coal and metal mining industry is currently facing (Saria et al., 2006). Acid mine drainage is formed as a result of the accelerated oxidation of the primary sulphide mineral pyrite FeS_2 and other sulphidic

minerals resulting from the exposure of these minerals to both oxygen and water, as an outcome of the mining and processing of metal ores and coals (Johnson and Hallberg, 2005). The generation of acid mine drainage is a natural process that becomes accelerated and intensified by mining (Metesh *et al.*, 1998). The position of mine wastes, the groundwater table height, and the hydrology of the mine site have a great influence on whether or not AMD occurs (Kimball *et al*., 1994). The AMD generated differs with respect to the mine, depending on the type of sulphide mineral that abound, the TSFs, the permeability of the waste rock piles, the kinetic rates of dissolution of the waste rock and the innate ability of the host rock to neutralize acidity (Akcil and Koldas, 2006). The AMD produced in these waste rock piles, is either stored or flushed out immediately into either groundwater and/or surface water (Berger *et al*., 2000). Chemical reactions that bring about mine water pollution commence when the mine is still in operation. Water in the mine is controlled by pumping, to keep the mine dry. When the mines close, pumping ceases, this causes the ground water level to rise until it reaches the surface or discharges into overlying aquifers (Johnston *et al*., 2008). The simultaneous flooding of the mines and the dissolution of metals (from the submerged mine metal workings) cause formation of sulphuric acid and ultimately, AMD is generated (Figure 3). Remediation of mine water pollution includes attenuation processes such as sorption of ions, precipitation of metal ions and alkalinity from weathering of calcites (Figure 3).

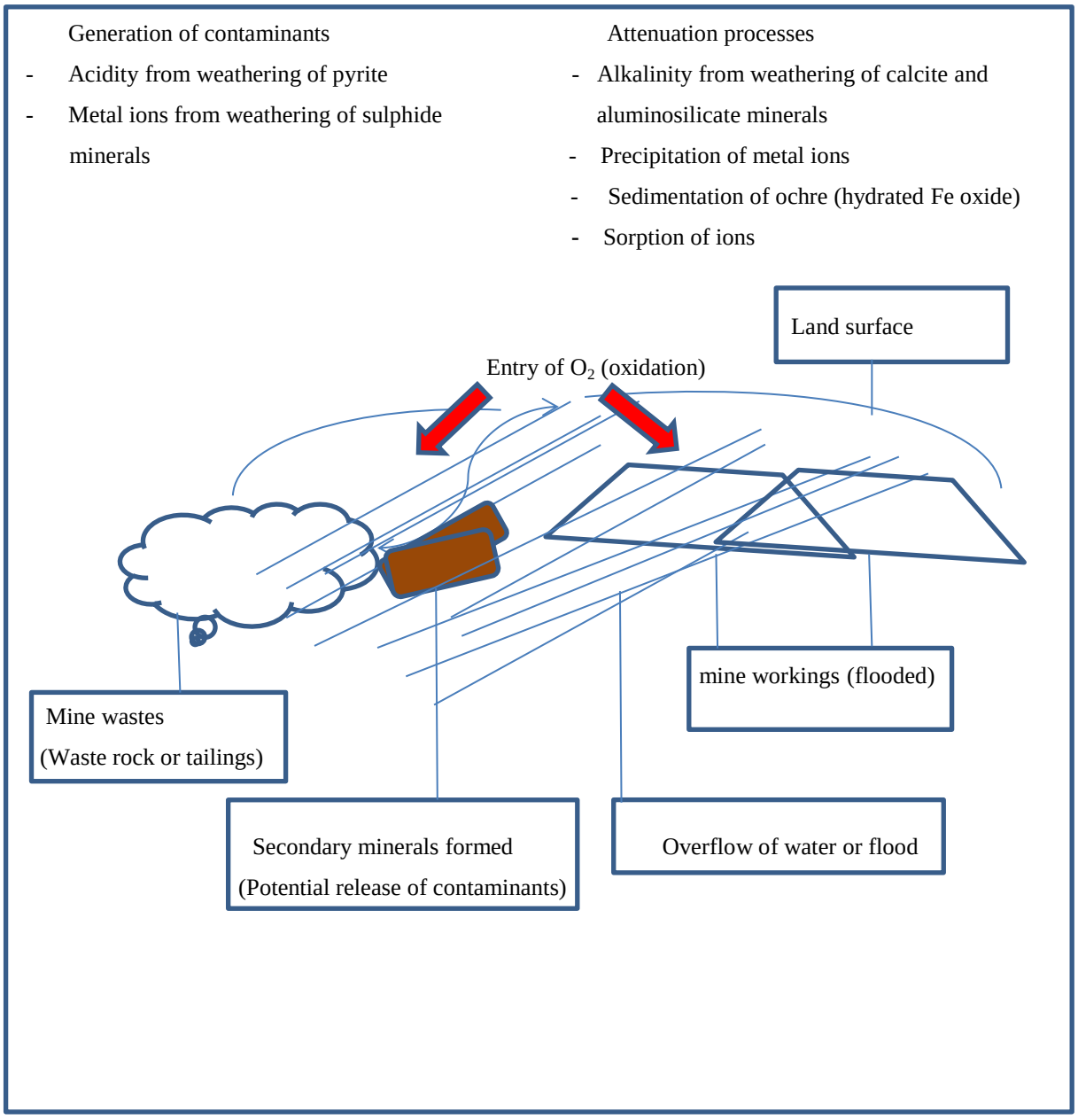

Figure 3: Some sources and processes of mine pollution (modified from Younger *et al.*, 2002).

Acid mine drainage has occurred in the Witwatersrand Basin, as a result of the exposure of pyrites and the filling in of the mining void by groundwater, following cessation of mining and pumping activities (McCarthy, 2011). In West Wits, there exists subsurface mining of coal and gold, and this often progresses below the water table, hence water must be constantly pumped out of the mines to prevent flooding. The West Rand in Witwatersrand, Johannesburg, South Africa is one of the most notable acid mine drainage sites in the world. Gold and coal deposits in South Africa are afflicted by acid production but according to McCarthy (2011), the diamond, vanadium, manganese and chrome mines do not generate acid-producing wastes.

After the decommissioning of mining activities many lands become infertile and unproductive (Ngigi, 2009). Mining activities have left a legacy of environmental degradation and nearby communities are struggling to cope with the environmental burdens associated with abandoned mining structures left behind (Robins, 2004). Acid mine drainage due to mining activities has greatly affected the Gauteng, Mpumalanga, North West and the Free State provinces of South Africa. The issue of AMD has resulted in the discharging of polluted mine water into the Vaal and Olifants River systems. The Vaal is the most important river in South Africa because it supplies water to the economic heartland of the country, not only in the Gauteng region but as far as the mining districts of Welkom, Sishen and Postmasburg (McCarthy, 2011). The discharging of polluted mine water has also affected Blesbokspruit in Springs and the Klip River (which drains the Southern portion of the Witwatersrand escarpment) (Tutu *et al*., 2008; McCarthy, 2011). According to a research report from the Council for Geoscience (CGS) for the Department of Mineral Resources (DMR), South Africa, AMD "hotspots" were found around the Witwatersrand gold fields' area, and the Witbank and Ermelo coal fields' area. In these areas, the effluent water quality has been found to have a pH of about 3-4, with EC of about 5000 ms/cm and high levels of sulphate, chloride, Fe, aluminum, Ni, copper, Cr, Mn, Co, lead and uranium (Makgae, 2012; Tutu *et al*., 2008). Factors that worsen the issue of AMD are inherent in mining facilities in South Africa. For instance, most mining operations are situated in or close to watersheds or on drainage lines. In South Africa, rainfall is relatively low, erratic and seasonal, with strong showers, and in the dry season with high evaporation rates and a low ratio of runoff to precipitation (Coetzee, 2004). These factors – topography, precipitation and evaporation - are directly related to the flow of pollutants.

The major sources of AMD in South Africa include underground mine shafts, runoff and discharge from open pit and mine waste dumps, tailings and ore stock piles (CSIR, 2009). Acid mine drainage contaminated waters will have a very low pH (possibly < 3), higher ionic strength due to their high sulphate and dissolved metal concentrations (in addition to iron) as a result of the associated ore-mineral elements with pyrite being released during the weathering process. Some of the ore-mineral elements include Cu in chalcopyrite, Zn in sphalerite and Ni in pentlandite (Neal *et al*., 2005; Chapman *et al*., 2013; Johnston *et al*., 2008).

South Africa has tried to mitigate and/ control the issue of AMD through a number of methods: i). The eMalahleni Water Reclamation Plant case study; where attempts were made to install treatment plants in the heavily polluted Brugspruit area near Witbank, Johannesburg, South Africa. These were of limited efficacy. The main aim was to address the pH issue in the area but there was no improvement on the salinity of the water in the area (McCarthy, 2011). Eventually, a water treatment plant based on reverse osmosis was commissioned in the area, to desalinate polluted water from local mining areas (McCarthy, 2011). This project demonstrated that it was possible to treat badly polluted water to drinking water standards, though at a high cost (McCarthy, 2011); ii). The government introduced a pumping subsidy to assist existing surrounding mines with the cost of pumping additional quantities of water from closed mines (CSIR, 2009; Makgae, 2012; McCarthy, 2011); iii). The government has laid down strategic plans to tackle the issue of decanting water from the Witwatersrand gold mines by the establishment of pumping and basic treatment operations such as the addition of lime and removal of Fe in three gold fields in the area, that are heavily affected by the AMD issue (Tutu *et al*., 2008; McCarthy, 2011); iv). The South African government has put in place legislative measures and further strengthened environmental regulations guiding the mining sector through the introduction of the National Environmental Management Act, Mineral and Petroleum Resources Development Act and the National Water Act; v). Most mining companies in South Africa have embarked on individual ways of tackling the AMD issue by the implementation of different AMD remediation strategies, many of which are expensive; vi). Many civil society groups in the country have raised awareness and placed huge emphasis on the issue of AMD, they have continually demanded for action plans from the government.

2.3 Characteristics of AMD contamination

Acid mine drainage is characterized by low pH (highly acidic) and high electrical conductivities (EC). Metals and metalloids which are toxic may also be present in solution (Akcil and Koldas, 2006).

2.3.1 pH

The pH is a measure of the concentration of hydrogen ion (H^+) and thus the acidity or alkalinity of the water. pH varies between 0 and 14 where lower numbers indicate more acidity, pH 7.0 is neutral and higher numbers more alkalinity (Hounslow, 1995). The generation of low pH causes the dissolution of metals from rocks and sediments (Saria *et al*., 2006). A decrease in pH under aerobic conditions increases bioavailability of many metals and the rate of metal uptake by aquatic organisms can be directly proportional to the levels of metal bioavailability in the environment if they do not have metal exclusion or mitigatory mechanisms (WRC, 2014a). When environments become severely acidic (less than 5) it causes a drastic decline in biodiversity (Hounslow, 1995). Low pH levels give rise to an increase in the concentration of dissolved aluminum and other major and trace metals which are carried into the surface water and ground water (Jung *et al*., 2001). The relationship between the oxidation-reduction potential (ORP) and pH influence the pathways and partitioning of trace metals, playing a major role in the bioavailability and toxicity of metals and metalloids (Sarmiento *et al*., 2009).

2.3.2 Oxidation –Reduction Potential (ORP or Eh)

There is a relationship between the pH and Eh in solution, and this can determine the species of metal present. A method of interpreting metal concentrations in relation to Eh-pH data relevant to the geochemist is the construction of the Eh-pH diagram also known as the Pourbaix diagram. The Eh-pH diagram is a plot of the metal in solution's oxidation state with variable Eh and pH conditions (Vance, 1996). The mineral phase (form of the precipitate) can be predicted knowing the ambient Eh and pH at a given temperature, and concentration. Oxidation-reduction refers to the oxidation (loss of electrons) and reduction (gain of electrons) reactions, which play an important role in the geochemical processes that occur in surface and groundwater, and are particularly useful in modeling pH-Eh speciation diagrams in order to understand the mobility of

metals in AMD (Vance, 1996). The transport, fate and bioavailability of trace metals in an aquatic environment are influenced by factors such as pH, precipitation, sorption, hardness, complexation, presence of carbonates, oxidation-reduction processes and biological factors (Ritter et al., 2002). The influence of pH and Eh and hence form of a solute in an aquatic system can be explained using the example of iron. For instance, soluble Fe^{2+} occurs in highly acidic, but well oxidized waters such as AMD streams and also waters of neutral pH and reducing conditions. At neutral pH and oxidizing conditions, soluble Fe^{2+} is converted to the insoluble Fe^{3+} in the form of Fe hydroxide (Fe $(OH)_3$) which now precipitates out of the solution (Chapman *et al*., 2013). As the Eh decreases, the solution is more reduced (i.e. has more electrons to give) and as the redox potential increases, the solution is more oxidized (i.e. will accept more electrons) (Chapman *et al*., 2013). Oxidation-reduction processes influence the environmental chemistry of trace metals which is in relation with the dissolved oxygen concentrations in water (Chapman *et al*., 2013; Ritter *et al*., 2002). Oxidation-reduction conditions of solutions bring about changes in trace metal concentrations by (i) altering a metal ion's oxidation state and by virtue of this influence the speciation of that metal, (ii) influencing the competition between complexing species and the bioavailability of some trace metal ions (Ritter *et al*., 2002; Chapman *et al*., 2013).

2.3.3 Electrical conductivity (EC)

High electrical conductivity (EC) is a feature of AMD contaminated substrata. The electrical conductivity of a solution is a measure of the ability of a solution to conduct a current. The conductivity value is directly proportional to the concentration of ions present (total dissolved solids or "salts" concentration in the water) (Hounslow, 1995). Water samples collected from zones of AMD seepage show elevated salt and metal concentrations and high EC values (Jung *et al*., 2001).

2.3.4 Major ions, trace and metal elements

Acid mine drainage contaminants include sulphate, Fe, metalloids such as Si and As and many metals such as Mg, Mn, Zn, Cu and Ca (Larsen and Mann, 2005). Anions such as chlorides and sulphates are considered contaminants in environmental waters. Increased concentrations of sulphate are usually the first indication of acid generation (Fadiran *et al*., 2014). When acid is generated, soil and rock become dissolved by the acid, with the dissolution of further salts and metals like Zn, Cu, Pb and Ni - these constitute some AMD contaminants. While sulphide oxidation generates acidity, dissolving carbonate in certain rock types such as dolomite buffers against pH reduction by providing alkalinity which neutralizes acidity (Zamzow, 2014). The ratio of the sulphides to a neutralizing agent like the carbonate rock determines the buffering capacity of a receiving environment and the overall acidity of mine drainage (Zamzow, 2014). The overall acidity and concentration of AMD contaminants in a drainage area may also be influenced by seasonal and temporal variations, for instance, dilution through the input of freshwater via rainfall and runoff may lower metal concentrations (Berger *et al*., 2000) though the pH of rainfall is typically acidic.

Trace and metal elements from AMD enter the surface water through groundwater, through runoff of precipitated salts and metals and also as dust dispersion by wind energy, as mining sites usually have high levels of erosion due to wind and water runoff (Navarro *et al*., 2008). Metal contaminants as a result of AMD generation are dissolved by water and enter into solution or they may remain adsorbed and/or be precipitated and then move with the soil particles. This means that the contaminants can occur in particulate or dissolved forms and may or may not be bioavailable for uptake by organisms (Ritter et al., 2002). Metals usually undergo complex biochemical and chemical reactions in water and sediments which affect their behavior and phase partitioning (Akcil and Koldas, 2006). Most trace elements only dissolve partially and most of the dissolved trace elements are bound to organic acids in soil solution while the rest are distributed as free ions and inorganic ion pairs (Carrillo-Gonzalez *et al*., 2006).

2.4 Processes, Mechanism and Chemistry of AMD

Mines that have been abandoned pose a greater problem than the ones still in operation. When mines are abandoned, dewatering or pumping stops and exposed mine workings get flooded (Figure 5) up to a point where the water table reaches the surface and the mine water now emerges as surface seepage. The activities of mining coal and minerals (especially gold) and the process of flooding of mines exposes the underground pyrite (FeS_2) bearing rock strata to oxygen and water, and acid formation begins through the oxidation of the pyrite (Chapman *et al*., 2013). Pyrite oxidation is a multistep process (Equations 1 – 4) where the primary oxidant is the ferric iron rather than the molecular oxygen (Evangelou, 1995). Acid formation begins when pyrite is oxidized to ferrous iron and sulphuric acid (Eq.1). Ferrous sulphate is further oxidized to ferric sulphate (Eq.2). The ferric sulphate reacts with water producing more acidity and ferric hydroxide (Eq.3). The summarized equation of AMD formation is given as equation 4. The oxidation of the reduced forms of iron and sulphur is very slow (Eq.2) but in the presence of acidophilic chemosynthetic bacteria the reactions are accelerated. Bacteria which flourish at low pH, such as *Thiobacillus ferroxidans*, *Thiobacillus thiooxidans* and *Metallogenium* oxidize Fe and sulphate (Kleinmann *et al*., 1981; Singer and Stumm, 1970).

Acid mine drainage formation is shown below as a series of steps (Johnson and Hallberg, 2005; Chapman *et al*., 2013; Evangelou, 1995):

1. Oxidation of pyrite into ferrous Fe and sulphuric acid:

$2FeS_2(s) + 7O_2(g) + 2H_2O(l) \rightarrow 2Fe^{2+}(aq) + 4SO_4^{2-}(aq) + 4H^+(aq)$ Equation 1

2. Oxidation of ferrous sulphate (ferrous Fe) into ferric sulphate (ferric Fe):

$4Fe^{2+}(aq) + 4H^+(aq) + O_2(g) \rightarrow 4Fe^{3+}(aq) + 2H_2O(l)$ Equation 2

3. Formation of ferric hydroxide:

$Fe^{3+}(aq) + 3H_2O(l) \rightarrow Fe(OH)_3(s) + 3H^+(aq)$ Equation 3

$Fe(OH)_3$ precipitates out of the solution as the red or yellow color of AMD.

The summarized equation of the multistep process of pyrite oxidation as given by Johnson and Hallberg (2005) is:

$$4FeS_2(s) + 15O_2(g) + 14H_2O(l) \rightarrow 4Fe(OH)_3(s) + 8SO_4^{2-}(aq) + 16H^+(aq) \quad \text{Equation 4}$$

Mine water discharges are usually acidic and laden with contaminants (major ions, trace and metal elements). However, in some cases, the discharges may be neutral or basic if the surrounding geology is high in carbonates and able to afford some neutralization (Kelly, 1988). The contaminants lead to an increase in acidity, turbidity, sedimentation and high toxic metal concentrations in the receiving water body (Chapman *et al*., 2013). The net acidity of AMD waters is derived both from "proton acidity" (i.e. hydrogen ion concentration) and "mineral acidity" (the combined concentration of soluble metals, notably Fe, aluminum and Mn, that produce protons when they hydrolyze) (Johnson and Hallberg, 2005). Net acidity in AMD needs to be offset against any alkalinity present. Alkalinity present is chiefly in the form of bicarbonate (HCO_3^-) deriving from the dissolution of basic minerals (e.g. calcium carbonate), though as noted above (Kelly, 1988), biological features and processes may also generate acidity or alkalinity in AMD streams (Johnson and Hallberg, 2005).

The form of a metal/metalloid element is greatly influenced by the host environment, which in turn largely determines the degree of trace metal toxicity, as the speciation of the element (i.e. the physical or chemical form of an element) stipulates whether it will have a range of positive or negative impacts on the environment (Ritter *et al*., 2002). Metal ions, especially transition metals with multiple oxidation states may undergo different processes such as oxidation-reduction reactions, ion exchange reactions and adsorption/desorption processes. These processes ultimately affect the mobility, bioavailability, bioaccessibility, environmental fate, distribution and the effect of metals and metalloids in aquatic systems (Carrillo-Gonzalez *et al*., 2006). Dissolved metals are more bioavailable than metals which are complexed to large organic molecules such as humic acids (Ritter *et al*., 2002). Complexation is whereby an ion or a molecule is linked to a metal. The pH has a direct influence on the toxicity and bioavailability of metal contaminants, as a small change in pH may have a large effect on the speciation of an element (Ritter *et al*., 2002; Carrillo-Gonzalez *et al*., 2006). Natural waters usually have a pH range from 4-5 to 9 due to the underlying geology and also may be as a result of acid neutralization by carbonates. Most metals form insoluble hydroxide precipitates under basic

conditions (Ritter *et al*., 2002; Nicholson *et al*., 1990). A major mechanism in sequestering trace elements and making them less bioavailable is the co-precipitation of trace elements which occurs easily within soil matrices that contain common components like clays, hydroxides, carbonates and metal oxides of Fe, Al and Mn (Carrillo-Gonzalez *et al*., 2006). Formation of coordination complexes or metal complexes is another important chemical process as a large proportion of soluble metals occur as complexes in association with dissolved natural organic matter (usually a mixture of fulvic and humic acids) (Carrillo-Gonzalez *et al*., 2006; Ritter *et al*., 2002). Coordination complexes also known as metal complexes consist of an atom or ion surrounded by bound molecules or anions of organic nature, these anions of organic nature are known as ligands or complexing agents. Metals may also complex with anions of inorganic nature such as chloride and sulphate altering their availability to organisms, and also, the hydrogen ion may be a competitor for metals in these metal complexes thus pH is important in determining the degree of formation of complexes (Ritter *et al*., 2002). As the pH increases, metal species in the aqueous form tend to precipitate to hydroxides, oxyhydroxides and hydroxysulphates (Berger *et al*., 2000). Metal complexes may also be formed between charged metal ions and oppositely charged complexing agents. Trace metals and metalloids such as mercury (Hg), arsenic (As) and lead (Pb) may form 'labile' (easily altered) organic complexes which may change their toxicity greatly. For example the methylation of Hg to methylmercury (CH_3Hg) or to dimethylmercury ($(CH_3)_2Hg$) generates more toxic forms than the elemental form (Hg) whereas the methylation of arsenic reduces its toxicity (Ritter *et al*., 2002). Methylated compounds are more easily bioaccumulated in the lipids of aquatic organisms and thus can pass through biological membranes into body fluids and organs (Ritter *et al*., 2002).

Other key processes include adsorption of metals onto particle surfaces, absorption of metals into particles, ion exchange and oxidation-reduction reactions. Physical and chemical properties of particles play a major role in the adsorption/absorption processes. For instance, trace metal ions tend to adsorb onto organic matter and clay minerals because of the negative charges found on the surface of both (Ritter *et al*., 2002). Ion exchange may occur when one element can replace another on charged exchange sites; this process is dependent on the environmental conditions and properties of the elements. For instance, Fe and Mn oxides may act as 'scavengers' sorbing (process of either adsorption or absorption or a combination of the two) trace metals onto and

into their particle surfaces (Ritter *et al*., 2002). Iron and Mn oxy-hydroxides are important compounds involved in metal retention in sediments from fluvial systems due to their high specific surface, tendency to form colloids and cation exchange capacity (Horowitz, 1991; Cravotta, 2008). Also, Fe and Mn are metals that are generally present in their reduced (Fe^{2+} and Mn^{2+}) ionic states in anoxic AMD and these forms of the metals are much more stable at higher pH than the fully oxidized (Fe^{3+} and Mn^{4+}) ions (Johnson and Hallberg, 2005).

Photosynthesis, respiration and decomposition are some of the processes that regulate dissolved oxygen concentrations in water and so invariably influence the trace metals concentrations (Chapman *et al*., 2013). Microorganisms such as micro-algae, bacteria and fungi affect the transformation processes of trace metals; this is an important feature in the attenuation of the concentrations of trace metals in contaminated waters, as are larger algae (Carrillo-Gonzalez *et al*., 2006).

2.5. Impacts of AMD

Acid mine drainage has a serious impact upon our waters. It affects the water quality, soils, plants and aquatic organisms such as macro-invertebrates. Acid mine drainage contaminated water has the potential to penetrate into the groundwater source and eventually leach into the surface water. The water source becomes degraded due to contamination with toxic metals up to a point that it becomes too toxic for use by humans and animals, e.g. for crop irrigation. Cancer and other health risks have been linked to the ingestion of AMD waters (Fadiran *et al.*, 2014).

2.5.1 Environmental impacts of AMD

The impact of AMD in benthic invertebrates has been widely reported with reduced abundances, species richness and diversity as key indicators. This is more evident in communities in benthic habitats than those in pool habitats (Van Damme *et al*., 2008). Mine pollution can inhibit microbial activity in the benthos, thereby reducing decomposition and nutrient cycling. This may lead to a decline of the invertebrates and plankton; that are an integral part of the food chain leading to the eventual shift in the community structure. Due to acid mine drainage, bacteria,

fungi and decomposing invertebrates can be inhibited from colonizing leaf litter and consequently reducing the rates of breakdown (Gray and Ward, 1983). Ferreira da Silva *et al*. (2009) reported that diatoms were rare at a location stressed by mine drainage with high levels of Cd, Pb and Zn. After acidification of a test area, the water column concentrations of Al, Ca, Mg and K increased, the downstream drift of immature insect larvae increased, emergence of mature stoneflies and mayflies decreased, periphyton (attached algae) biomass increased and trout migrated to areas of higher pH (WRC, 2014a). In Lynx Creek, Arizona, algal communities impacted by mine pollution exhibited reduced species richness compared to locations upstream and those in areas of substantial recovery downstream (Lampkin and Sommerfield, 1982). Koryak and Reilly (1984) observed reduced growth of the aquatic macrophyte American water willow, *Justicia americana* (L.) Vahl as a consequence of coal mine pollution in Ohio. Tremaine and Mills (1991) recorded that protozoans' abundance and grazing rates on bacteria were substantially reduced in a lake affected by AMD. Letterman and Mitsch (1978) noted that the standing crop of fish communities declined downstream of mine drainage on Ben's Creek, Pennsylvania from 228.2kg/ha to 11.2kg/ha. They also reported that the Sculpin, *Cottus bairdi* showed the greatest decline from 151.2kg/ha to 0.3kg/ha. Some amphibians are very sensitive to acidity especially during their reproductive periods. The fertilization stage is most noticeably affected by acidity because disintegration of the amphibian sperm occurs at low pH (WRC, 2014a). The embryonic stages of the leopard frog (*Rana pipens*) and the spotted salamander (*Ambystoma maculatum*) have suffered 100% mortality at pH of 4 – 5 (WRC, 2014a). Mine water pollution can result in fish mortalities, particularly the sensitive Salmonid species (Johnston *et al*., 2008). Acidity inputs due to mine water also causes loss of spawning gravels for fish reproduction and nursery streams (Johnston *et al*., 2008). The solubility and toxicity of metals such as Al, Cu, Pb, Zn and Cd brought about by mine water pollution can cause damage to the gills of fish (Johnston *et al*., 2008).

2.5.2 Health impacts of AMD

When sulphate is in excess it gives water an unpalatable taste and causes laxative effects. Also, excess Fe in the human body can cause toxemia in pregnancy, tumors and heart damage (Fadiran *et al*., 2014). Trace metals such as Pb and Cd may pose serious threats to human health by

interfering with essential nutrients needed by the body, i.e. essential nutrients of similar appearance like Ca^{2+} and Zn^{2+}. This is because lead has size and charge similarities with Ca and may replace the need for Ca in the bones. For instance, the skeletal systems of children require higher demands for Ca than adults and lead may take the place of Ca when ingested. Later when calcium is ingested, the lead already in the bone becomes mobilized in the body. This results in conditions like nephrotoxicity, neurotoxicity and hypertension (WRC, 2014b). Chromium exposure due to mine pollution may cause underdevelopment of roots in plants leading to poor plant growth; it may also cause respiratory and dermatological effects in humans (Fadiran *et al*., 2014; WRC, 2014b). Arsenic ingestion may cause cardiac abnormalities. Nickel is carcinogenic and long term exposure may result in the loss of body weight, skin irritation, heart and liver damage (Fadiran *et al*., 2014). Cadmium may interfere with the metallothionein's ability to regulate Zn and Cu concentrations in the body thereby disrupting the homeostatic levels (WRC, 2014b). Metallothionein is a protein that binds to excess essential nutrients in the body rendering them unavailable. Mercury contamination due to mine pollution poses great risk to humans especially in its methylated forms resulting in acute and chronic poisoning. Acute poisoning may cause symptoms like vomiting, pharyngitis, nephritis, gastroenteritis and circulatory collapse. Chronic poisoning may occur, when fish contaminated with mercury is ingested, which may cause liver damage, neural damage and teratogenesis (WRC, 2014b).

2.5.3 Social and economic impacts of AMD

Acid mine drainage causes reduced water availability for abstraction for public supply from both ground water and surface water sources (Chapman *et al*., 2013; Johnston *et al*., 2008). Rising mine water levels may bring about localized flooding in cellars and low lying land, and the re-emergence of long dormant springs (Johnston *et al*., 2008). Acid mine drainage can cause surface waters to be rendered unsuitable for irrigation and livestock watering (Chapman *et al*., 2013). Navigational rivers and canals may become contaminated due to mine drainage, thus affecting commercial and recreational use (Chapman *et al*., 2013; Johnston *et al*., 2008). Acid mine drainage brings about ecological damage in aquatic systems reducing the potential for commercial fishing and angling (Chapman *et al*., 2013). Highly colored ferruginous mine waters

affect the visual and aesthetic forms of water which in turn affect the recreational and amenity value of watercourses (Chapman *et al*., 2013; Johnston *et al*., 2008).

2.6 Prevention of AMD

It is preferable to prevent the formation of AMD in the first instance, given the axiom that "prevention is better than cure". Such preventive techniques are collectively known as "source control" measures (Johnson and Hallberg, 2005) (Figure 4).

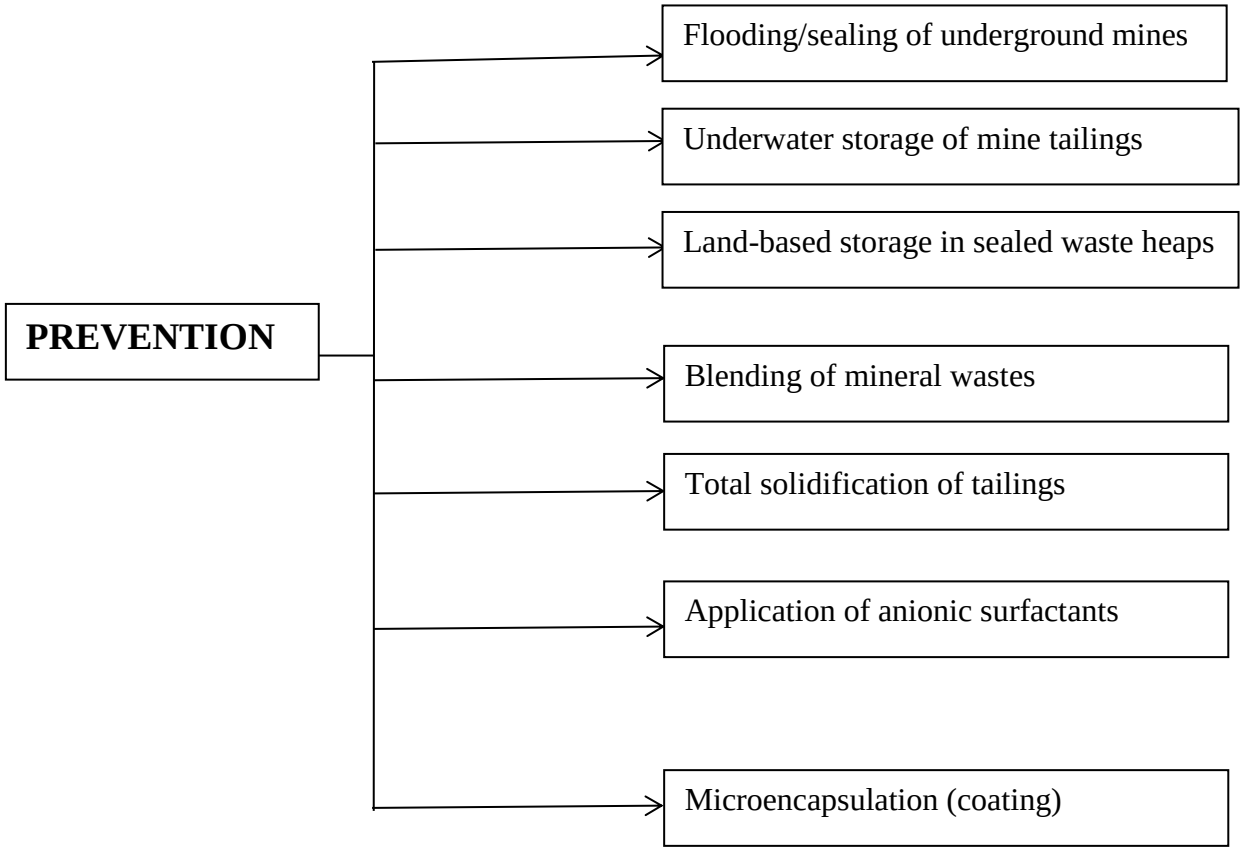

Figure 4: Various approaches that have been evaluated to prevent or minimize the generation of mine drainage waters (Johnson and Hallberg, 2005).

Some of the preventive techniques as shown in Figure 4 include:

1. Flooding/sealing of underground mines

This technique involves the exclusion of both oxygen and water. The dissolved oxygen present in the flooding waters (ca. 8-9 mg/l) will be consumed by mineral-oxidizing (and other) micro-organisms present and replenishment of dissolved oxygen by mass transfer and diffusion will be prevented by sealing of the mine (Johnson and Hallberg, 2005). However, this is only effective when the location of all the shafts and adits (seepage) are known and where influx of oxygen-containing water does not occur (Johnson and Hallberg, 2005).

2. Underwater storage of mine tailings

Underwater storage has been used for disposing and storing mine tailings that are potentially acid-producing (Li *et al*., 1997; Johnson and Hallberg, 2005). The objective is to prevent contact between the minerals and dissolved oxygen (Johnson and Hallberg, 2005). Shallow water covers may be used and their effectiveness may be improved by covering the tailings with a layer of sediment or organic material. This has a dual benefit of limiting oxygen ingress and affording some protection against re-suspension of the tailings due to the actions of wind and waves (Johnson and Hallberg, 2005).

3. Land-based storage in sealed waste heaps

Dry covers used for surface storage of reactive mineral spoils may also incorporate an organic layer. The "sealing layer" that covers the spoil is usually constructed from clay, although in areas of the world that experience acute wet and dry seasons, drying and cracking of the cover can render this technique less effective than in temperate zones (Swanson *et al*., 1997).

4. Blending of mineral wastes

Another technique for minimizing AMD production is to blend acid-generating and acid consuming materials, producing environmentally benign composites (Mehling *et al*., 1997; Johnson and Hallberg, 2005).

5. Total solidification of tailings

Solid-phase phosphates such as apatite can be added to pyritic mine waste in order to precipitate Fe (III) as ferric phosphate, thereby reducing its potential to act as an oxidant of sulphide minerals (Evangelou, 1998; Johnson and Hallberg, 2005). However inhibition of pyrite oxidation by employing this method may only be temporary, due to the process of "armoring" of the added phosphate minerals (Evangelou, 1998; Johnson and Hallberg, 2005).

6. Application of anionic surfactants

This involves the application of anionic surfactants such as sodium dodecyl sulphate (SDS) which are highly toxic to this group of microorganisms (Fe and sulphur-oxidizing bacteria) inhibiting their activities in minerals spoils and tailings (Johnson and Hallberg, 2005). However, this is a short-term control of the problem of mine drainage and it also requires repeated applications of the chemicals (Johnson and Hallberg, 2005).

7. Microencapsulation (coating)

This involves the use of coating technologies such as (i) the application of soluble phosphate together with hydrogen peroxide on pyrite surfaces (Evangelou, 1998). The peroxide oxidizes pyrite, producing ferric iron, which reacts with the phosphate to produce a surface protective coating of ferric phosphate and (ii) the application of silica coating on pyrite surfaces forming Fe oxide (Evangelou, 1998).

2.7. Mitigation of AMD

Techniques or methods applied in the mitigation of AMD are known as "migration control" measures. In locations where preventing the formation or the migration of AMD from its source is not feasible, it is necessary to collect, treat and discharge mine water (Johnson and Hallberg, 2005). The various options available for remediating AMD may be divided into those that use either physical, chemical or biological mechanisms to neutralize AMD and remove metals from solution. Both abiotic systems (physical and chemical mechanisms) and biological systems each include processes that are classified as "active" (i.e. require continuous inputs of resources to

sustain the process") and "passive" (i.e. require relatively little resource input once in operation) treatments (Johnson and Hallberg, 2005). A wide range of technologies are available for the remediation of AMD contaminated sites. Deciding on which passive treatment to use will depend on the severity of AMD and some site specific information namely; the water chemistry, the flow rate, the topography as well as the characteristics of the specific site (Ziemkiewicz *et al*., 2003). This is in line with Bell and Donnelly (2006) who also stated that the applicability of a particular method depends on the site conditions, the nature and extent of contamination, and the extent of remediation required. Efficient mitigating actions against AMD from abandoned mines include the neutralization of acid drainage by means of limestone, hydrated lime, ammonia and fly ash (Akcil and Koldas, 2006). In some instances, attenuation of acidity may occur naturally if carbonate rocks present in the local stratigraphic sequence interact with AMD (Barton-Bridge and Robertson, 1989). In general, active treatment of AMD mitigation refers to the continuous application of alkaline materials to neutralize acidic mine waters and precipitate minerals (Johnson and Hallberg, 2005). Passive treatment involves the use of natural and constructed wetland ecosystems. Passive treatment has the advantage of requiring relatively little maintenance (and recurring costs) compared with active systems (Johnson and Hallberg, 2005).

2.7.1. Abiotic mitigation strategies

This type of treatment involves the use of abiotic, expensive procedures and it has to deal with sludge disposal, which is a big concern in terms of environmental contamination (Smith, 1997). It is used in both physical and chemical systems as seen below:

2.7.1.1 Active abiotic strategies

Active abiotic strategies include both physical systems and chemical systems. Physical systems involve the process of water oxidation through impoundments and cascades, to facilitate the settlement of the contaminants into sludge. These systems are very expensive as they require capital investments for both construction costs and of the disposal of the resultant sludge (Diamond *et al*., 1993). In recent times, there have been more modern water treatment techniques that result in marketable chemicals from the resultant sludge.

A widespread chemical system that is used to mitigate acidic effluents involves the addition of an alkaline material to AMD to raise its pH, accelerate the rate of the chemical oxidation of ferrous Fe (for which active aeration or the addition of hydrogen peroxide is also necessary). This process causes many of the metals present in the solution to precipitate as hydroxides and carbonates, thereby resulting in an iron-rich sludge (Coulton *et al*., 2003; Chadwick *et al*., 1986; Johnson and Hallberg, 2005). The iron rich sludge may also contain various other metals depending on the chemistry of the mine water treated. Various neutralizing agents that may be added to the AMD include slaked lime, calcium carbonate, lime (calcium oxide) and sodium hydroxide. These agents vary in cost and effectiveness, for instance, sodium hydroxide is some 1.5 times as effective but is about nine times the cost of lime (Johnson and Hallberg, 2005). When calcium-containing neutralizing reagents are used, the removal of sulphate (as gypsum) is achieved. The down-sides to this mode of treatment include huge operating costs and problems with the disposal of the bulky sludge (Chadwick *et al*., 1986; Johnson and Hallberg, 2005). Modifications to this technique, involve the recycling of the sludge produced into lime-holding tanks that can produce a sludge that contains ca. 20% solids that can further be improved by dewatering to ca. 50% solids, a "high-density sludge". The major advantage of a "high-density sludge" process is that costs of disposal and storage of the final product are greatly reduced (Johnson and Hallberg, 2005).

2.7.1.2 Passive abiotic strategies

An alternative approach for addition of alkalinity to AMD is the use of anoxic limestone drains (ALD) (Kleinmann *et al*., 1998; Johnson and Hallberg, 2005). The objective is to add alkali to AMD while maintaining the Fe in its reduced form to avoid the oxidation of ferrous Fe and precipitation of ferric hydroxide on limestone ("armoring") which reduces the effectiveness of the neutralizing agent. Within the drain, the partial pressure of carbon dioxide is increased, accelerating the rate of limestone dissolution and consequently increasing the concentration of alkalinity (Kleinmann *et al*., 1998; Johnson and Hallberg, 2005). The concentration of alkalinity may reach up to 275mg/l compared to an open system which, in equilibrium, would produce only 50-60 mg/l alkalinity (Kleinmann *et al*., 1998). The use of ALDs is considered to be a passive approach to mine water treatment. Although the use of ALDs produces alkalinity at

lower costs, they are not suitable for all AMD waters (Johnson and Hallberg, 2005). Problems emanate when ALDs are used to treat aerated mine waters in which case a passage of AMD through an anoxic pond prior to the anoxic limestone drain is required to lower dissolved oxygen concentration to levels required to prevent iron oxidation (Johnson and Hallberg, 2005). Another potential drawback with using ALDs is the formation of ferrous carbonate and manganous carbonate gels within ALDs. This may cause the incongruent dissolution of the limestone gravel (Evangelou, 1998). Anoxic limestone drains are generally used as one component in a passive treatment system in association with aerobic and /or compost wetlands (Kleinmann *et al*., 1998). The addition of ALDs to constructed wetlands that have been performing poorly has been reported to cause dramatic improvements in the quality of waters draining these systems (Kleinmann *et al*., 1998).

2.7.2 Biological mitigation strategies

The biological mitigation strategies involve both the use of (i) active systems - this involves the use of off-line sulphidogenic bioreactors and (ii) passive systems, some of which include the use of aerobic wetlands, compost reactors/wetlands, permeable reactive barriers and packed bed Fe-oxidation bioreactors (Johnson and Hallberg, 2005). The significant biological processes applied in this mode of mine water treatment are derived on the basis of bioremediation and phytoremediation of AMD. The basis of bioremediation of AMD derives from the abilities of some microorganisms to generate alkalinity and immobilize metals, thereby essentially reversing the reactions responsible for the genesis of AMD (Johnson and Hallberg, 2005). Phytoremediation is applied in woodlands, to consume mine-waters and wetlands, constructed to treat AMD, whereby macrophytes such as *Typha* and *Phragmites* species are the obvious forms of life present, but their direct roles in improving water quality have been questioned (Johnson and Hallberg, 2005).

The biological systems for treating mine water are majorly dominated by the construction of semi natural or artificial habitats which facilitate bacterial activity to reduce contaminants through reed beds and wetlands (Chapman *et al*., 2013; Smith, 1997; Kalin, 2004). Natural

wetland ecosystems include swamps, marshes, fens, bogs and swampy lands. Wetlands enable flood control, shore line stability and help in water purification, since they act as bio filters, by removing toxic metals from the waters flowing through them. Wetlands can also be used naturally to attenuate dissolved toxic metals in the environment (O'Sullivan et al., 2005) and if the metals contained within the wetland are left undisturbed, they would be unavailable and non-polluting to the environment (Wildman *et al*., 1989). Wetland plants aid in the removal of pollutants from waste waters by the natural process of phytoremediation. The plants and associated organic matter adsorb contaminants such as Zn, Fe and copper, some of which are essential for plant growth (UNEP, 2010). Wetland plants thus have the ability to reduce the movement of contaminants in surface water systems (O'Sullivan et al., 2005). Natural wetlands have organic rich substrates which exchange dissolved metals. This exchange and other natural wetland processes have been found to remediate contaminants within AMD. The imitation of these natural wetland processes can work similarly in constructed wetlands such as reed bed systems (Smith, 1997). Some treatment technologies employ sulphate-reducing bacteria (SRB) mediated treatment of AMD. The SRBs serve to reduce sulphate to sulphide in sediments under anaerobic conditions.

Some processes that occur during wetland amelioration of AMD include the following (Perry and Kleinmann, 1991):

1. Adsorption
2. Ion exchange
3. Absorption and bioaccumulation
4. Bacterial and abiotic oxidation
5. Sedimentation
6. Neutralization
7. Reduction
8. Dissolution of carbonate minerals

Snyder and Aharrah (1985) verified *Typha* species as effective removers of Fe and Mn. Kleinmann (1985) recorded that iron concentrations dropped from 20-25 mg/l to 1mg/l and Mn concentrations dropped from 30-40 mg/l to 2mg/l in a constructed wetland system with *Typha*

species planted on it. According to Fennessy and Mitsch (1989), the most important design considerations in terms of wetland development and construction are these: biochemical processes, loading rate and retention time, slope, substrate, vegetation, sediment control, morphometric, seasonality and regulatory issues. Concerns have been raised about whether the wetland will able to sustain the continuous drainage emitted to it (Smith, 1997). The construction of the wetland system should include monitoring to ensure that it does not become saturated and begin to once again leak toxic substances back into the environment and thus will then require de-sludging (Smith, 1997). These wetland systems are relatively inexpensive to construct and run.

Their ecological principles suggest that biological systems may be a sustainable solution to mine drainage pollution (Kalin, 2004). However biological systems require the availability of suitable land areas close to the source of pollution and this is not always possible. Most treatment plants are a combination of aeration, settlement ponds and reed beds of *Typha* species and the common reed, *Phragmites australis* (Johnston *et al*., 2008). If there is enough alkalinity naturally present in the mine water, the pre-dissolved iron (during the dissolution of metal ions) now reacts with oxygen, the iron oxide (ochre) becomes insoluble (sedimentation of ochre) and is contained in the system, thereby no longer being available for contamination (Johnston *et al*., 2008 ; Younger *et al*., 2002). These chemical processes are enhanced by bacteria naturally present in the mine water and wetlands that utilize iron as an energy source (Johnston *et al*., 2008). The following case studies exhibit combinations and overlaps of different treatment processes.

A. The Wheal Jane Incident.

In January, 1992, one of UK's biggest pollution incidents took place when 45 million litres of heavily contaminated water burst from the recently closed tin mine at Wheal Jane in Cornwall. The mine water, loaded with Cd, As, Zn and Fe flooded into the River Carnon causing a vast plume of polluting orange water in the Falmouth Bay (Johnston *et al*., 2008; Chapman *et al.*, 2013). An emergency treatment plant was constructed. The treatment plant involved the addition of lime to the discharge and used the tailings dam at the mine to settle out most of the metals (Johnson and Hallberg, 2005; Neal *et al*., 2005). A passive approach was suggested and investigated at first and a pilot-scale treatment plant was built to test combinations of aerobic and

anaerobic wetlands (Johnston *et al*., 2008; Chapman *et al.*, 2013). The plant was ideal but would require the use of so much land to treat the whole discharge this was not feasible and so an active chemical treatment plant was then chosen (Johnston *et al*., 2008). The mine water is now pumped from the shaft and lime is added to raise the pH and cause the metals to form insoluble compounds such as oxyhydroxides and carbonates (Johnston *et al*., 2008). These insoluble compounds settle out with the aid of a chemical flocculant and the treated water overflows to the river in compliance with the conditions of a discharge standard set by the Environment Agency (Johnston *et al*., 2008; Chapman *et al.*, 2013). The resulting sludge is pumped into the mine's tailings dam where it is contained (Johnston *et al*., 2008).

B. The Bull House Mine water Project.

The mine water remediation treatment at Bull House on the River Don in Yorkshire involved the use of a physical settlement lagoon and a wetland area. This resulted in significant reductions in the loadings of metals with Fe being most effectively removed (Laine and Dudeney, 2000).

C. The River Pelenna Mine water Project.

From the 1960s to the late 1990s, the River Pelenna in South Wales was impacted for a distance of 7km by five significant discharges from abandoned coal mines. Elevated Fe and low pH caused conspicuous orange staining of the water. This had detrimental effects on the river's ecology (Wiseman *et al*., 2003). The River Pelenna Mine water Project involved the construction of a series of passive wetland systems to treat the discharges onto the river (Chapman *et al*., 2013; Wiseman *et al*., 2003). After a monitoring program on the project from between 1993-2001, performance data from the wetlands showed that on average, the treatment systems are removing 82-95% of the Fe loading from the mine water. Increase in pH downstream of the discharges was also observed (Wiseman *et al*., 2003). The brown trout (*Salmo trutta*) recovered quickly following the mine water treatment (Wiseman *et al*., 2003). Also, the return of sensitive invertebrate species e.g. the mayfly - *Empherella ignita* and birds such as dippers (*Cinclus cinclus*) were observed.

2.7.2.1 Phytoremediation

Phytoremediation is the direct use of living plants for *in situ* remediation of contaminated soil, sludge, sediments and groundwater through contaminant removal, degradation or containment (USEPA, 1999). This natural ability of plants can be applied in environmental remediation processes using soft engineering techniques. Apart from the reed beds (*Phragmites australis*) which have been planted on the Varkenslaagte stream, other tree species have been planted on AMD from AGA's TSFs by the University of the Witwatersrand as part of the Mine Woodlands Project for AngloGold Ashanti between the years 2003 and the present (AGA, 2013). The woodlands developing around the TSFs have the same function as riparian woodland (Dye *et al*., 2008; Dye and Weiersbye, 2013). Some of the ways plants bring about contaminants' removal are shown in Table 1 below.

Table 1: Various methods of phytoremediation

Phytoextraction	This is a process whereby plants absorb, translocate and store toxic contaminants from a sediment profile into their roots and shoot tissue. It also involves the plant's ability to intercept and accumulate metals in its harvestable biomass (USEPA, 1999; Lasat, 2002).
Rhizofiltration	This involves plant roots adsorbing or absorbing contaminants from an aqueous matrix flowing through their root system (UNEP, 2010).
Phytostabilization	This is a process whereby plants produce decaying organic matter and chemical compounds that immobilize metals in soils or roots thereby reducing metal mobility and bioavailability (Smit and Freeman, 2006; Miller, 1996).
Phytodegradation	This is process whereby plants take up, store and then degrade (break down) contaminants within their tissue by enzymatic metabolic processes (UNEP, 2010).
Phytovolatilization	This refers to a plant's ability to take up contaminants from its root and shoot tissues and subsequently volatilize the contaminants into the atmosphere (UNEP, 2010).

Advantages of phytoremediation include: (a) it can be used for various organic and inorganic waste compounds; (b) phytoremediation is energy efficient and it is an aesthetically pleasing method of remediating sites with low to moderate levels of contamination (Wuana and Okieimen, 2011; Pivetz, 2001); (c) phytoremediation allows for both *in situ/ex situ* applications (Wuana and Okieimen, 2011); (d) the phytoremediation technique is less disruptive to the environment as disposal sites for sludge are not needed as required in other remediation techniques (Wuana and Okieimen, 2011); (e) expensive equipment and highly specialized personnel are not required hence cost of operation is reduced (Pivetz, 2001); (f) phytoremediation can be used to treat sites polluted with more than one type of pollutant (Wuana and Okieimen, 2011). AngloGold Ashanti has reshaped the Varkenslaagte canal to re-establish the original drainage line on the wetland soils and planted remediation reed beds in a series of shallow depressions, consisting of common reeds (*Phragmites australis), Typha capensis* and sedge species (*Schoenoplectus* and *Cyperus* spp). The reed beds have been put in place to bring about AMD remediation by the aid of phyto-immobilisation and rhizofiltration.

Potential drawbacks of phytoremediation include:

- A significant drawback of phytoremediation is the depth limitation due to the generally shallow distribution of plant roots. Effective phytoremediation of soil or water generally requires that the contaminants should be within the zone of influence of the plants' roots. Selection of deep rooted plants and the use of techniques to induce deep rooting could help alleviate this challenge (Pivetz, 2001).
- A longer time period is required for phytoremediation to be effective, as this technology is dependent on plants' growth rates for the establishment of an extensive root system (Wuana and Okieimen, 2011; Pivetz, 2001).
- Plant matter that is contaminated will require proper disposal or an analysis of risk pathways. If the phytoremediation technique fails, an increased mass of material will need to be remediated (Pivetz, 2011).
- Phytoremediation might require the use of a greater land area than other remedial methods (Wuana and Okieimen, 2011).

- A phytoremediation system can lose its effectiveness during winter (when plant growth slows or stops) or when damage occurs to the vegetation from harsh weather, disease or pests. A back-up remedial technology might then be necessary (Pivetz, 2001).
- Large scale operations involving the use of phytoremediation technique may require access to agricultural equipment and knowledge (Wuana and Okieimen, 2011).
- Success of the phytoremediation technique is dependent on the tolerance of the plant to the pollutant (Wuana and Okieimen, 2011).
- Amendments and cultivation practices that take place during phytoremediation application might have unintended effects on metal mobility. For instance, the application of many common ammonium-containing fertilizers can affect the oxidation-reduction potential of the soil and invariably lower the soil pH. This might result in increased metal mobility and leaching of metals to groundwater (Pivetz, 2001).

2.8 Remediation options: factors in decision making

The choice of a remediation option is influenced by environmental and economic factors (cost implications) (Chapman *et al*., 2013; Johnson and Hallberg, 2005; Metesh *et al*., 1998). For instance, consideration will be given to the amount of fossil fuel energy needed to transport limiting materials which may be long distances from source to mine sites (Johnson and Hallberg, 2005; Neal *et al*., 2005).

The necessary and available land surface area and topographic problems may rule out the passive biological systems in some situations (Johnson and Hallberg, 2005; Metesh *et al*., 1998). Site specifics such as slope, water chemistry and available land for treatment may greatly influence the choice of a remediation option (Metesh *et al*., 1998).

None of the remediation/mitigation techniques are maintenance-free. Passive systems also require management and will eventually fill with (i) accumulated ochre in aerobic wetlands and (ii) sulphides in compost reactors (Johnson and Hallberg, 2005). The long-term stabilities of these materials (contaminants) stored in these treatments are uncertain, but since they may

contain toxic elements such as arsenic and cadmium, their storage or disposal requires careful consideration (Johnson and Hallberg, 2005).

The acid-generating condition of the potential source material is another factor that should be taken into consideration when selecting an AMD remediation technique. Once a source material can be remediated, the downstream impacts may be remediated naturally (Metesh *et al*., 1998).

A site's hydrology after mining, the geochemical analysis of over burden and the method of overburden placement in the backfill during reclamation can greatly influence the choice of a remediation option to employ (Ziemkiewicz and Skousen, 1996). The flow rate of the water to be treated, water residence time and the loading rates of metals are features that influence the option of a wetland remediation technique (Metesh *et al*., 1998).

The effectiveness and sustainability of any remediation system is becoming increasingly critical in decision making (Johnson and Hallberg, 2005). Legislation is likely to become the dominant factor in determining which remediation system can be used in any situation as it might become increasingly untenable to dispose of base metals in sludge and sediments when there are technologies available for recovery and recycling (Johnson and Hallberg, 2005). Also limits on the concentration of sulphate that can be discharged from processing plants may restrict the choice of a system to one that effectively removes sulphate as well as metals and acidity from mine waters (Johnson and Hallberg, 2005).

Factors that were taken into consideration when the choices for the Varkenslaagte remediation were made are possibly: i) safety and suitability for the type of chemical pollutants; ii) environmental and economic factors; iii) land surface area and; iv) the use of a system that does not involve sludge generation and disposal.

Chapter 3: Materials and methods

This chapter describes the study site. The chapter also explains the research methodology used. The processes involved in the collection and analysis of the various data are described.

3.1 Study site - Varkenslaagte canal and stream

The Varkenslaagte stream is geographically located about 75 km West of Johannesburg and about 8 km South of Carletonville, Gauteng province, South Africa, within AGA's West Wits mining facility. The Varkenslaagte sub catchment area occupies the north western portion of the West Wits operations and is bounded by the Gatsrand Ridge to the south east (AGA, 2009). The Varkenslaagte stream has been heavily contaminated by polluted effluents from the Old North Complex TSF and the Savuka TSFs/New North Slimes TSFs within the AGA West Wits mining area (AGA, 2013) (Figure 5). To curtail this AMD contamination on the Varkenslaagte stream, AGA, like many other South African mining companies, has been attempting to rehabilitate historically impacted land and associated water systems as one of the company's legal obligations. An example is the rehabilitation project initiated in the Varkenslaagte drainage area within the West Wits operations (AGA, 2013). The first phase of the rehabilitation project in 2011 to 2012 involved the progressive removal of the historic tailings spills. The next phase in 2011 to 2013 involved the progressive re-establishment of the Varkenslaagte drainage line and development of reed beds in collaboration with AGA's research partners the Ecological Engineering and Phytotechnology Programme (EEPP) Unit at the University of the Witwatersrand. The AGA sustainability report of 2013 reveals that some 76,000 m^3 of tailings spillage had been removed from the Varkenslaagte drainage line. The early (2003 to 2007) and current (2012 to 2014) phases also involve 65 ha of indigenous woodland species being planted to exert hydraulic control on AMD seepage from the western TSFs into groundwater, and into the Varkenslaagte stream and reed beds.

Phase 1 of the remediation reed beds (reed beds 1 – 7) (Figures 5, 6 and 7) were constructed from 1-12-2011 to 6-12-2011, followed by the planting of the *Phragmites australis*, *Typha capensis* and *Schoenoplectus sp*. (reed species *Phragmites australis*, being the dominant wetland plant) from 11-1-2012 to 19-1-2012. Reed beds 8-15 were constructed and the reeds were planted in phase 2 which ran from 12-9-2012 to 21-9-2012 (Joubert, 2013) (Figures 5, 6 and 7).

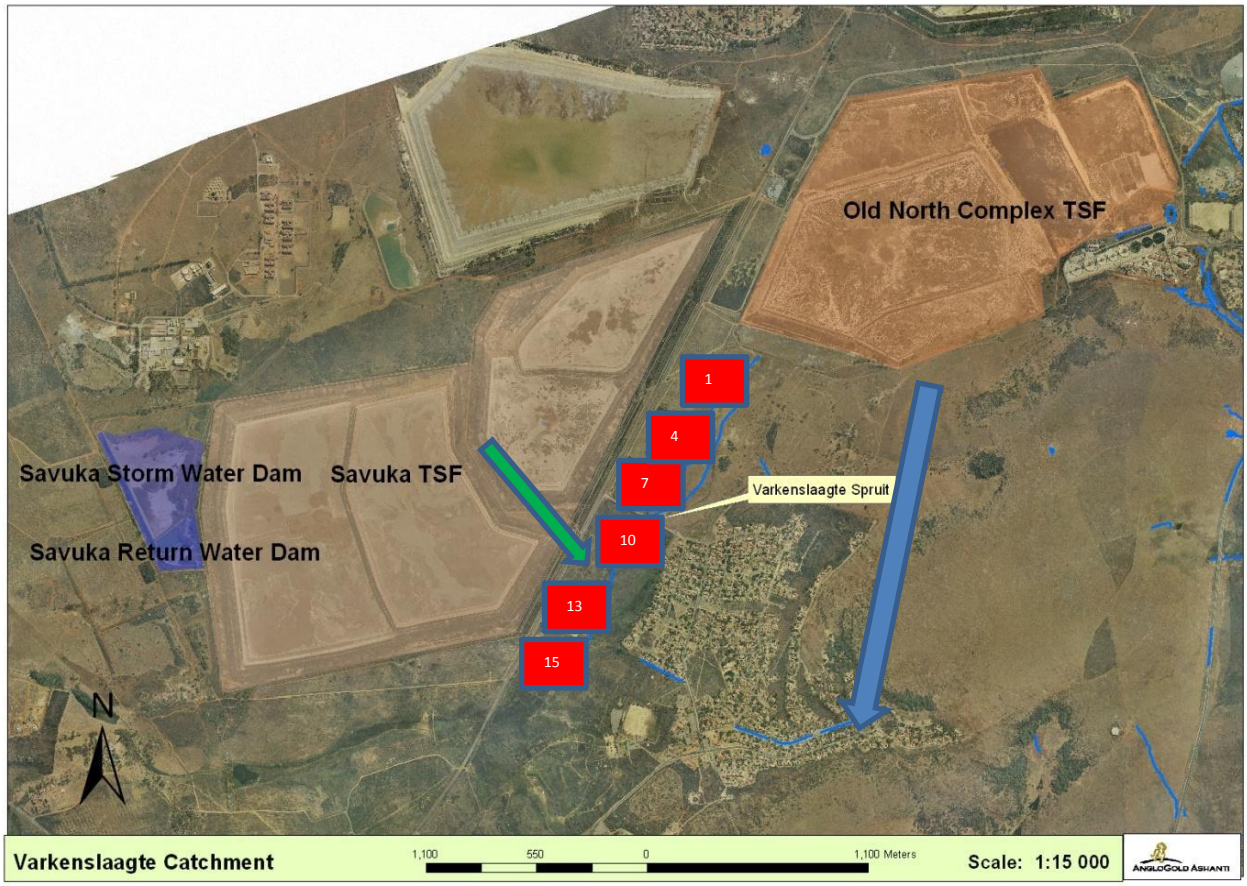

Figure 5: A map showing the Varkenslaagte spruit (stream) with remediation reed beds (RBs 1,4,7,10,13 and 15), in the context of the Old North Complex TSF and the Savuka TSFs (also known as the New North Slimes TSFs). The blue arrow represents direction of flow of water, a South-Westerly direction and the green arrow depicts a point of lateral seepage entry from the TSF into reed beds 13 and 15 (modified from De Waard, 2012).

Figure 6: A picture showing remediation reed beds (RBs) 1 and 4 (furthest upstream in the reed bed system), 7 and 10 (in the middle) and 13 and 15 (furthest downstream) along the Varkenslaagte stream in 2014 (see inset in Figure 1).

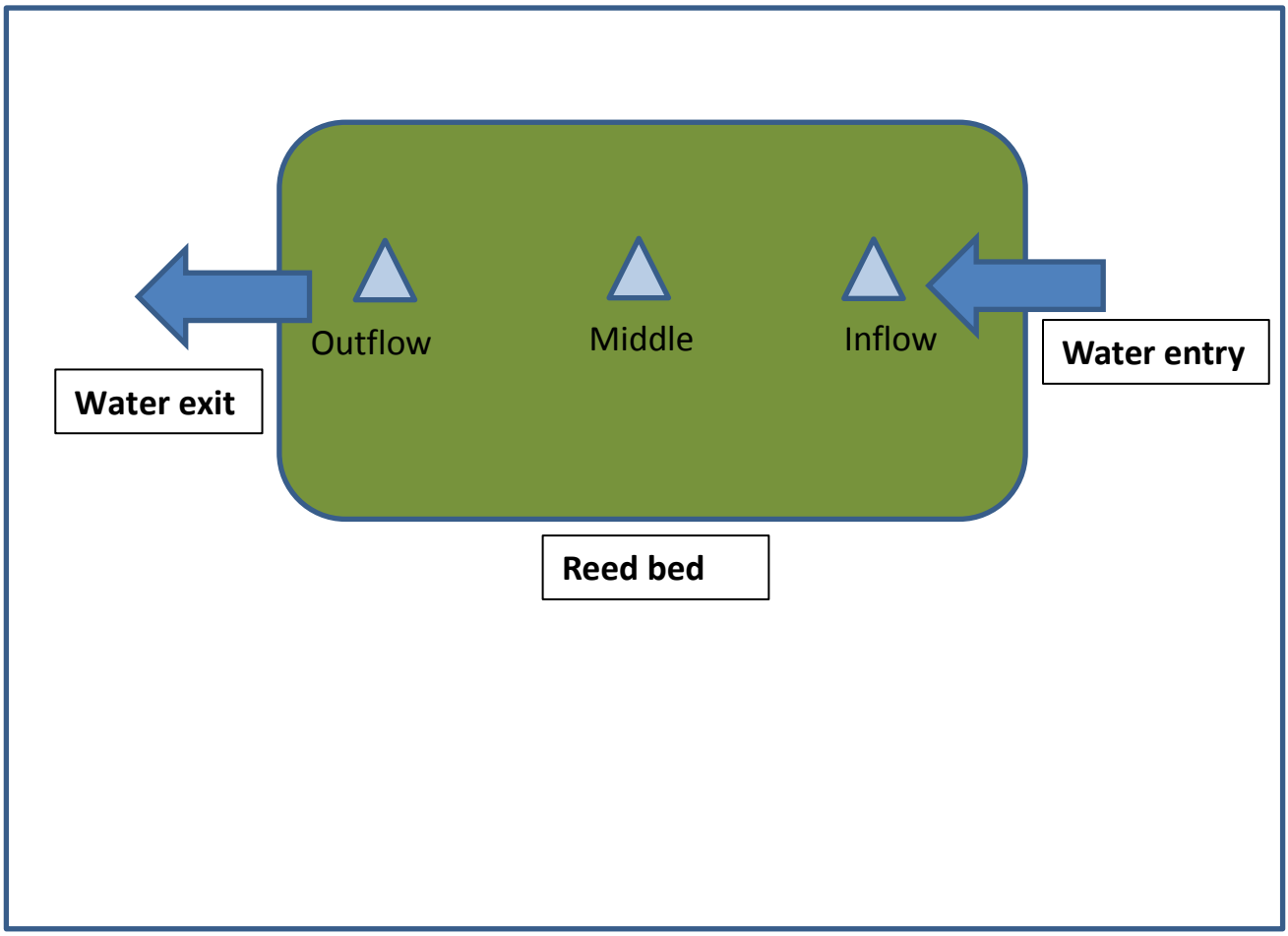

Figure 7: Schematic diagram of sampling locations within reed beds

During the course of this study, water and sediment samples (soil cores) from these reed beds along the heavily polluted Varkenslaagte stream were analyzed to ascertain the concentration of AMD contaminants therein with respect to seasonal variations. For both the first and second site visits, 18 water samples were collected from each of these six reed beds ((RBs) 1, 4, 7, 10, 13 and 15 (3 samples per reed bed, at the in-flow, mid-flow and out-flow points).

The upper Varkenslaagte runs in a south westerly direction from below the Old North Complex TSF until a point where the Varkenslaagte stream continues under the Mangaan Drive and where the lower weir is situated (Figure 5). Thereafter the stream continues WSW and under the main road, and West towards the Wonderfontein spruit. The Varkenslaagte stream is the main drainage path that drains the Varkenslaagte sub catchment from east to west (AGA, 2009; AGA; 2013). The Varkenslaagte drainage area runs off from the Old North TSF complex and the New North/ Savuka TSF complexes and the Storm and Return Water Dams (AGA, 2013). The Varkenslaagte stream acts as a drain/sink for both the Old North Complex TSF and the active New North TSFs (these are unlined slimes dams). Previously, the Varkenslaagte was a tributary to the Wonderfonteinspruit, which feeds into the Mooi River and eventually into the Vaal River System – supplying Potchefstroom and Johannesburg with drinking water but presently, it is thought to flow into the dewatered Turffontein Dolomite Compartment (De Waard, 2012). The Varkenslaagte stream is located within the Vaal catchment (AGA, 2013).

The main topographical characteristics of the area are slight undulating plains with small rock peaks. A north-east south-westerly spread of shale and quartzite of the Timeball Hill formation of the Pretoria Group of the Transvaal Super group underlies the study site (AGA, 2009). The Varkenslaagte drainage area experiences a temperate climate with rainfall (mean annual precipitation (MAP) ranges from 650 – 1200 mm annually) occurring in summer during which moderately high temperatures may occur, whereas in winter, aridity is experienced (AGA, 2009). The dry season is well defined between May and September when severe frosts may occur (AGA, 2009). Vegetation is grassy with reed beds and wetlands. 60% of the grassland biome, primarily in the mining area, has been transformed, i.e. there has been reduction in grassland due to land clearing (AGA, 2009).

Effective remediation of the Varkenslaagte drainage area is critical in ensuring compliance with the quality requirements for discharge water and AGA recently stated that they were confident that the seepage and downstream water quality will significantly improve over the next few years as a result of the rehabilitation project (AGA, 2013). The target river quality classes (RQC) at the point where the main road crosses the Varkenslaagte is 400 mg/l sulphates, and this has been achieved since late 2012 (AGA, 2015).

3.2 Experimental design, sampling and chemical analyses

3.2.1 Experimental design

For this study, two experimental designs were incorporated, (a) Factorial: year (1:2014) × season (2: summer, winter) × media (water, surface sediment (0-2 cm) and (b) Linear distance from source for the 6 reed beds (1, 4, 7, 10, 13 and 15) – change in water and sediment quality (surface sediment).

3.2.2 Sampling

Four sampling visits were conducted in April/May and July, 2013 and 2014. For all four visits, water samples were collected from each of these six reed beds ((RBs) 1, 4, 7, 10, 13 and 15. Reed beds 1 and 4 are at the top of the drainage line, RBs 7 and 10 are at the middle and RBs 13 and 15 are towards the downstream end of the reed bed system (Figures 5 and 6). Acid mine drainage influx occurs on two aspects; North, down the drainage line and West, on a broad parallel front to the drainage line. The sampling was carried out on the same points in May and July 2013 by a previous researcher (Joubert, 2013). The water samples were collected from the inflow, mid- point and out flow at each reed bed. *In situ* measurements of pH, dissolved oxygen (DO), EC, ORP, nitrate and temperature were taken at all 15 reed beds. The *in situ* measurements were carried out with a portable kit (WTW multiparameter instrument pH/Cond 340i and ORP, Germany) equipped with a pH electrode, an integrated temperature probe, a standard conductivity cell and an oxidation-reduction potential probe. The metres were calibrated and

tested prior to sampling using standard buffer solutions according to the manufacturer's instructions. Oxidation-reduction potential was obtained from platinum electrode versus Ag/AgCl and all reported potentials were corrected relative to standard hydrogen electrode (SHE).

The soil cores (sediment depth profile samples) were taken from an upstream, middle and downstream location (3 points) within each of 3 reed beds (RBs 1, 10 and 15; Figures 5, 6 and 7) making a total of 9 soil cores. Samples were extracted using 1 m long polyvinylchloride (PVC) pipes of 12 cm diameter, with a sharpened end, that were hammered about 30 cm into the sediment. The pipes were then extracted and sealed, stored in a cold room at the University, and cut into two longitudinal halves in the laboratory for slicing and measurement of sediment samples at depth intervals of 0-2 cm, 2-5 cm, 5-10 cm, 10-20 cm and 20-30 cm. Ten grams of each of the soil depth intervals was mixed in 20 ml of deionized distilled water (1:2 mass/volume), and stirred vigorously to homogenize to a liquid paste consistency then laboratory measurements of pH, EC and Eh/ORP were taken. Approximately 20 g of each of the remaining soil samples was freeze-dried at -40º C for a period of three days using the Labconco freeze drier (Vacutec, South Africa). After freeze drying, the samples were sieved using a 2 mm plastic sieve (to remove gravel, stones and coarse sand and coarse roots. The dried samples were then crushed and ground in an acid-washed and rinsed agate pestle and mortar to homogenized powder and then stored at 4º C in plastic specimen bottles for further preparation. Approximately 5 g samples were placed in plastic cups covered with a Formvar film, and then quantitative X-ray Fluorescence Spectroscopy (XRF) using Certified Reference Materials (CRMs) was conducted with the aid of the XRF machine, i.e. XRF Spectroscout Geo+ (1), in the Ecological Engineering and Phtytotechnology Programme (EEPP) laboratory in the School of Animal, Plant and Environmental Sciences, University of the Witwatersrand.

3.2.3 Chemical analyses

X-ray fluorescence analysis was conducted using the XRF Spectroscout (Geo + (1)) with twin tubes for detection of light to heavy elements, to determine the major and trace elements present. In order to establish the system performance and conduct quantitative XRF analysis, the samples

were measured along with the appropriate CRM (Stream Sediment NCS DC 73312a – NCS DC 73315a) issued in 2010 by China National Analysis Centre for Fe and Steel, Beijing, China. For the analysis of cations and anions, each water sample was filtered soon after sampling through a cellulose acetate Millipore 0.45 µm filter membrane and then divided into two aliquots. The aliquot for anion analysis by ion chromatography was not stabilized and the aliquot for cation analysis was stabilized with suprapure nitric acid (HNO_3) (Merck) (1% v/v). Both were kept at 4^o C in nitric-acid cleaned and distilled water rinsed plastic bottles until analysis.

The Ion Chromatography (IC), Inductively Coupled Plasma Mass Spectrometry (ICPMS) and Inductively Coupled Plasma Optical Emission Spectroscopy (ICP-OES) analyses were conducted in the School of Chemistry i.e. the Environmental Analytical Chemistry laboratory, University of the Witwatersrand. Inductively Coupled Plasma Mass Spectrometry analysis was conducted to determine minor and trace elements; V, As, Co, Sn and U. Here, a sample solution was aspirated into high temperature plasma to generate ions by means of a Perkin Elmer ICP-MS. Sample duplicates were used, resulting in relative standard deviations (RSDs) lower than 10 %. Blanks (deionized water filtered through a 0.45 µm membrane filter) were also prepared in order to take into account possible impurity of reagents and membranes. In this case, the concentrations of all analytes were close to or below the detection limits of the methods. During the ICP-MS, the ions pass through a magnetic quadrapole that deflects their flight path with the degree of deflection related to the mass of each ion. A sampler measures the number of atoms detected under a given magnetic field specific to a certain element to determine concentration. The linear range is six to seven orders of magnitude with detection limits in the ppb to ppt level (Downing *et al*., 1998). The ICP-MS parameters such as ion optics voltage, mass scan, time scan, pump speed and argon flow were optimized for a better resolution and analyte-background intensity ratio. The software used for data analysis was Smart Analyzer provided by SPECTRO (Downing *et al*., 1998; Lusilao, 2012).

Inductively Coupled Plasma Optical Emission Spectroscopy was conducted on the acidified water samples using an ICP-OES instrument (Spectro Genesis, Germany) to determine major elements; Al, Ca, Fe, Mg, Ni, P, S and Zn. The instrumental conditions were optimized (Table 2) to obtain sufficient sensitivity and precision and the concentration of each element was

determined at various wavelengths. The stock solutions supplied at a concentration of 10 mg/l in 1% HNO_3 (De Bruyn Spectroscopic Solutions, SA) were diluted to make daily working standards of 0.1 to 1mg/l for instrument calibration (Downing *et al*., 1998; Lusilao, 2012; Perkins *et al*., 1995). Calibration curves were constructed after the analysis of these standards. The instrument limit of detection (LOD) was calculated for each analyte using results for standard calibrations.

Table 2: Optimized parameters of the ICP-OES

Parameter	Value
Coolant flow	14 mL min^{-1}
Plasma power	1400 W
Auxillary flow	1 mL min^{-1}
Nebulizer flow	1 mL min^{-1}
Type of nebulizer	Cross-flow
Injector tube diameter	0.889 mm

Filtered water samples that were non-acidified were analyzed by Ion Chromatography (IC) for sulphate and chloride. The water samples were manually injected into the Metrohm, 861 Advanced Compact Ion Chromatography (Metrohm, Switzerland) using a 5 ml syringe equipped with a male pressure fitting. The IC is equipped with a separation center (733 IC), a detector (732 IC), an interface (762 IC), a suppressor module (753 IC) and a pump (709 IC) (Fadiran *et al*., 2014; Lusilao, 2012; Perkins *et al*., 1995). The IC was set at 17 minutes analysis time for each sample. Analyses were performed using the parameters in Table 3. The IC offers high sensitivity and multiple analyte determination in a single run. The eluent was a solution of 1.0 mM $NaHCO_3$ and 3.2 mM Na_2CO_3. The solution was sonicated and filtrated under vacuum through a 0.45 µm filter. A 50 mM solution of H_2SO_4 was used as a conductivity suppressor regenerant solution (Downing *et al*., 1998; Lusilao, 2012; Perkins *et al*., 1995). A 1000 mg/l multi-standard stock solution of sulphate and chloride was prepared by diluting an accurately weighed amount of their corresponding salts, namely NaCl (Merck) and Na_2SO_4 (Merck)

respectively in 1 L of deionized water (Millipore, USA). The stock solution was then filtered with a 0.45 µm filter and kept at 4 ^{0}C. Working standards of 1, 5, 10 and 20 mg/l were freshly prepared daily from the stock solution and used for calibrating the instrument (Fadiran *et al*., 2014; Lusilao, 2012; Downing *et al*., 1998). Water samples were first filtered as for the stock solution to avoid the clogging of the working column and diluted before analysis in order to fit them in the calibration curve and to avoid detector saturation. The results were recorded electronically as the instrument was connected to a computer.

Table 3: IC parameters for anion determination

Parameter	Value
Guard column	Metrosep A supp A/5 (6 1006 500) (Metrohm)
Analytical column	Metrosep A supp 5 (6 1006 520) 150/4.0 mm (Metrohm)
Flow rate	0.7 ml min^{-1}
Temperature	± 25 $^{\circ}$C
Injection volume	± 50 µl
System back pressure	12 MPa
Run time	17 minutes

3.2.3.1 Minimum detection limit (MDL)

Minimum detection limits were based upon seven replicate measurements of a series of spiked calibration blanks. Each blank solution was spiked with analytes at concentrations between 2 and 5 times the estimated instrument detection limit (IDL). The minimum detection limits calculated were generally in the low µg/l (ppb) range for most of the trace elements detected by ICP-MS. The limit of detection (LOD) is the lowest analyte concentration that can be detected by the machine used. This was calculated using the following formula (Hutter, 2011):

LOD = 3 x standard deviation of a blank sample (Equation 5)

3.3 Statistical procedure

The commercial statistics software package SAS Enterprise 7.1 for Windows was used for statistical analyses in this study. Descriptive statistics (mean, median, standard error, minimum and maximum) were done for each dependent variable on each reed bed with N = 3. A stratification technique was employed by categorizing each reed bed into 3 i.e. inflow, middle and outflow. For instance, RB 1 was categorized as 1.1(inflow), 1.2 (middle) and (1.3) outflow (as shown in Figure 7). Box plots were constructed to allow graphical examination of the data and it is also a check for whether the data in question followed a normal distribution. The target water quality ranges for aquatic ecosystems (DWAF, 1996) were used as criteria for comparing with the mean concentrations of major ions, trace and major elements. Statistical analyses were performed in this study to test:

1) Differences between the reed beds within a sampling period (April or July) by constructing box plots and using the One Way Analysis of Variance (ANOVA).

2) Differences in spatial patterns between seasons i.e. between April and July and relationships/associations between indicative AMD pollutants. This was evaluated by performing the Pearson correlation analysis and constructing the correlation matrices.

3) Principal component analysis (PCA), a multivariate technique, was performed to investigate relationships between pollutants along the major axes of variation between reed beds. Inter-annual differences in these relationships were also explored with PCAs.

For the pH calculation, the geometric mean was calculated i.e. the measured pH was converted back to [H+] concentration

$pH = - \log [H+]$

then the arithmetic mean was calculated and converted back to pH (WRC, 2014a).

According to Makgae (2012) and Tutu *et al*. (2008), there are high concentrations of sulphates, Mg, Mn, Al, Co, Ni, Fe, Ca and Cu in the waters and sediments of the Witwatersrand basin, specifically West Wits. This informed the decision on which elements to perform statistical analyses on. The Kruskal-Wallis non-parametric test and the one way ANOVA parametric test

are tests conducted on 3 groups or more (Galpin and Krommenhoek, 2014). In this study, there are 6 groups (6 reed beds). A non-parametric test (Kruskal-Wallis) is more appropriate when any of the assumptions of the one way ANOVA parametric test have not been met (Galpin and Krommenhoek, 2014). The multicomparison tests were carried out only when the P value (Pr > F) of the ANOVA parametric test is significant (i.e. when the P-value is less than 0.05/ ANOVA is significant) (Galpin and Krommenhoek, 2014). The multicomparison tests take into account the multiple testing, each pair-wise test is conducted at a more stringent level than the original test thereby showing where the differences lie amongst the groups (Galpin and Krommenhoek, 2014). Each particular statistical test has its own pair of hypotheses (the null hypothesis (H_0) and the alternative hypothesis (H_A)). The significance level or error or alpha (α) used was 5% (0.05).

For the analysis of differences between reed beds, the statistical tests in this study were performed in this order:

(a) Test for Normality
(b) Test for Equality of Variances
(c) ANOVA parametric test , if not applicable then the;
(d) Kruskal-Wallis non-parametric test
(e) Tukey multicomparison test

Chapter 4: Results

The box plots, correlation matrices, principal component analyses (PCAs) and other results obtained from this study are presented in this chapter.

4.1. Physico-chemical parameters in water samples

4.1.1. pH

The pH of the water collected from three data points i.e. inflow (1.1), middle (1.2) and outflow (1.3) (Figure 7) of each of the reed beds (RBs) 1, 4, 7, 10, 13 and 15 in April and July is shown below by way of box plots for pH in April and July (Figures 8 and 9). On each box plot, the maximum, mean, median and minimum values of the three data points for each reed bed (e.g. 1.1, 1.2 and 1.3 of RB 1) can be viewed. The diamond shape on the box plots represents the mean value.

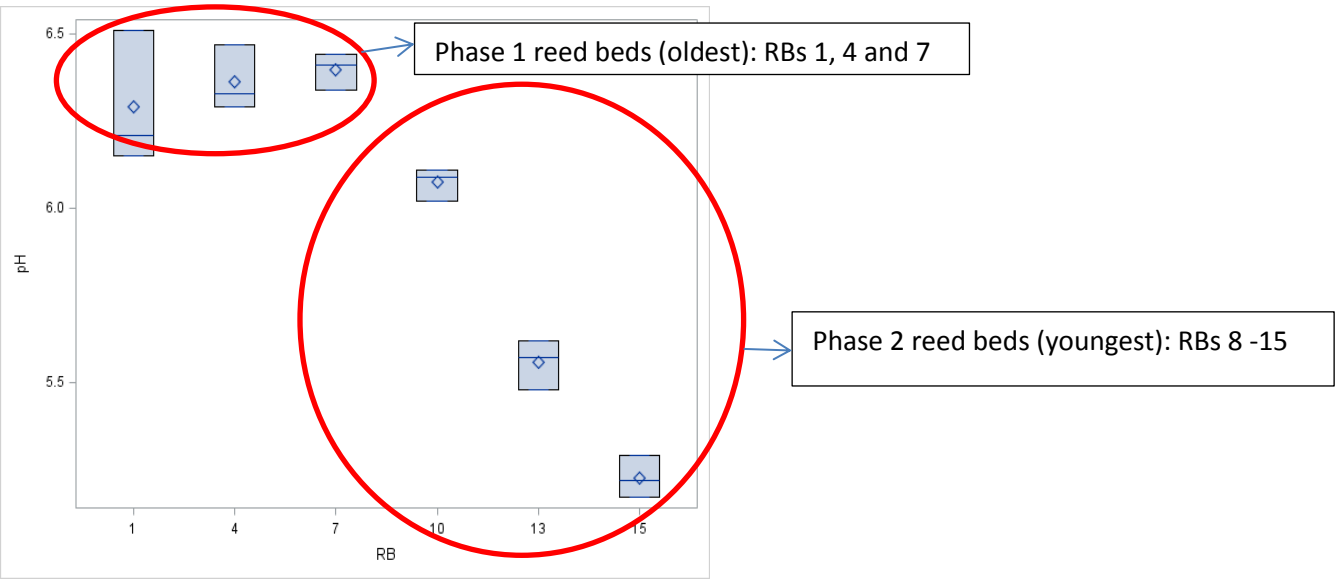

Figure 8: Box plot for pH in water in April, 2014.

A slight increase in pH is observed from RBs 1 to 4 to 7 (Phase 1), which suggests an attenuation pattern of AMD while a progressive decrease in pH is observed in the water flowing across RBs 8 to 15 (Phase 2) in April (wet season).

Circles have been used to illustrate the differences between RBs 1, 4, 7 and RBs 8-15. The two phases were implemented over a 2 year - period, the reed beds upstream (RBs 1- 7) are older (were constructed first) than the reed beds downstream (RBs 8 – 15). Hence, there are less likely to be conspicuous improving trends in RBs 8-15, and in fact, there seems to be a trend of deteriorating water quality, because they were so young at the time of this study. Furthermore, it is likely that the lower reed beds were also receiving secondary sources of seepage from the western TSFs since lateral inputs were visible in the field at the time of sampling.

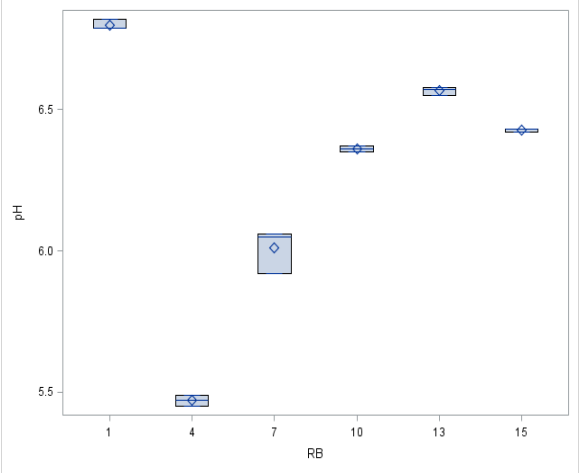

Figure 9: Box plot for pH in water in July, 2014.

An initial sharp decline in pH from RB1 to RB4 is observed, followed by a progressive increase from RB4 to RB13, with only minor differences between the three lower reed beds. This dry season pattern in pH is the reverse of the pattern seen in April. There are similar ranges of 5.5 - 6.5 for most sites in both seasons, but the spatial pattern differs. The pH in the water for both seasons was in the 3 – 6 pH range in the 2013 survey (Joubert, 2013).

The Test for Normality (R-Square), the Test for Equality of Variances (Bartlett and Levene tests) and the One way ANOVA parametric test (if applicable) were performed. The Kruskal-Wallis non-parametric test was performed for the pH in April and July respectively (Table 4).

Table 4: Statistical tests and the P-values for pH in April and July, 2014

Month	pH range	R-Square	Bartlett test	Levene test	ANOVA	Kruskal-Wallis
April	5.17 - 6.51	0.9671	P(x) 0.3555	P(F) 0.0596	P(F) 0.0001	N/A
July	5.45 – 6.82	0.9957	P(x) 0.0138	P(F) 0.0293	N/A	P(x) 0.0053

Table 4 above shows R-Square values that are high. In April, the test for Equality of variances / homogeneity of variances (Bartlett and Levene tests) had P-values that were greater than 0.05 therefore the null hypothesis was upheld i.e. variances were equal, so based on this, ANOVA was performed. The ANOVA was significant ($P < 0.05$) therefore the Tukey test (multicomparison test) was carried out for the pH in April. The reverse was the case for the test of equality of variances in July, where the variances were unequal. Subsequently ANOVA and Tukey tests were not performed. Instead, the Kruskal-Wallis test was performed and it was significant ($P < 0.05$). The result for the Tukey test for pH in April is shown below (Table 5).

Table 5: Tukey test for pH

Month	Parameter	RB 1	RB 4	RB 7	RB 10	RB 13	RB 15
April	pH	AB	AB	A	B	C	D
July	pH	N/A	N/A	N/A	N/A	N/A	N/A

For pH in April:

There are no significant differences in pH between reed beds 1, 4 and 7 (Phase 1, oldest reed beds). Downstream from RB 8 onwards (Phase 2, youngest reed beds), each reed bed has significantly lower pH than the previous one.

The Tukey test was not applicable for pH in July since ANOVA was not applicable either.

4.1.2 EC

The EC values in April are generally high and they fall within the 3500- 4600 µs/cm range (Figure 10).

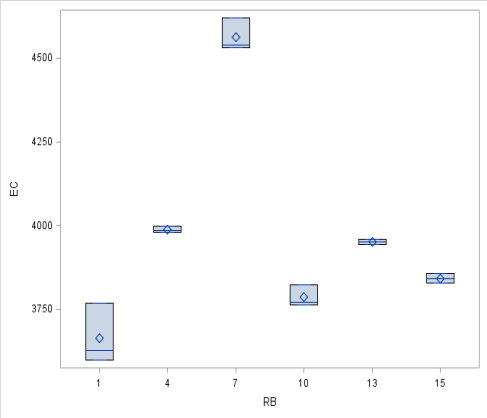

Figure 10: Box plot for electrical conductivity (µs/cm) in water in April, 2014.

Electrical conductivity is very similar between sites, between 3500 and 4000 µs/cm, except for a higher value of 4600 at RB7. In May 2013, the EC range was 2500 – 4550 µs/cm (Joubert, 2013), indicating similar ranges in both years for this season.

In July, the EC values of the reed beds fall within the 2600-5500 µs/cm range as shown below (Figure 11).

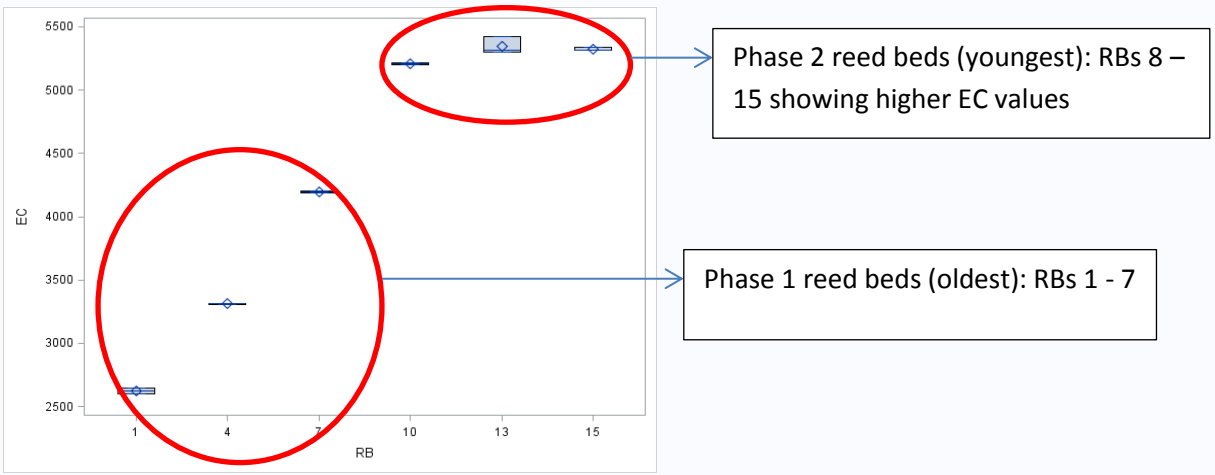

Figure 11: Box plot for electrical conductivity (µs/cm) in water in July, 2014.

Unlike the April samples where there was no clear pattern, in July the EC increased progressively down the reed bed series (downstream) from RBs 1 – 15, reaching much higher values (>5000 µs/cm) in the three downstream reed beds (RBs 10, 13 and 15) than observed at any site in April. The EC range in the water in July, 2013 was 3000 – 4600 µs/cm (Joubert, 2013), indicating somewhat higher EC values for the lower reed beds in 2014.

Results of the statistical tests performed on the EC data for July are presented below (Table 6).

Table 6: Statistical tests and P-values for electrical conductivity in April and July, 2014.

Month	EC range (µs/cm)	R-Square	Bartlett test	Levene test	ANOVA	Kruskal-Wallis
April	3550-4550	0.9838	P(x) 0.0195	P(F) 0.0443	N/A	P(x) 0.0058
July	2600-5500	0.9995	P(x) 0.0030	P(F) 0.0297	N/A	P(x) 0.0065

Table 6 shows that in April and July, the test for equality of variances / homogeneity of variances (Bartlett and Levene tests) had P-values that were less than 0.05 ($P < 0.05$) therefore the null hypothesis was not upheld i.e. variances were unequal. Hence neither ANOVA nor the Tukey test was performed. Instead, the Kruskal-Wallis non parametric test was performed. The Kruskal-Wallis test showed that there was a significant difference in the EC across the reed beds ($P < 0.05$) in April and July.

4.1.3 Eh/ORP

Box plots of Eh for the two 2014 sampling visits are shown in Figures 12-13.

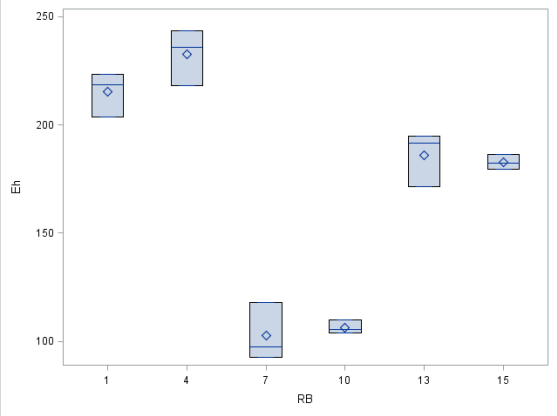

Figure 12: Box plot for oxidation-reduction potential in water in April, 2014.

It is observed from Figure 12 that the furthest upstream reed beds (RBs 1 and 4) have high Eh values, whereas much lower Eh is observed around the middle reed beds (RBs 7 and 10) and intermediate values are observed further downstream (RBs 13 and 15).

Figure 13 shows that similar Eh values in RB 1 and RB 4 are followed by sharp increase, which levels off in the 3 downstream reed beds at more than double the values observed in the two uppermost sites.

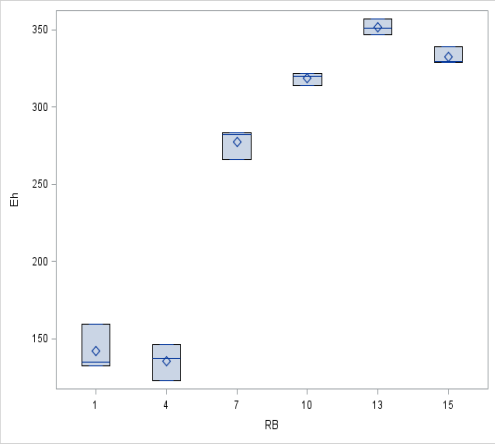

Figure 13: Box plot for oxidation-reduction potential in water in July, 2014.

The results of the statistical tests for Eh in April are shown below (Table 7).

Table 7: Statistical tests and P-values for oxidation-reduction potential in April and July, 2014

Month	Eh range (mV)	R-Square	Bartlett test	Levene test	ANOVA
April	92.50 - 243.40	0.9724	P(x) 0.3802	P(F) 0.2624	P(F) 0.0001
July	122. 70 - 357.20	0.9926	P(x) 0.5317	P(F) 0.1572	P(F) 0.0001

Table 7 above shows R-Square values that are high. In April and July, the test for equality of variances / homogeneity of variances (Bartlett and Levene tests) had P-values that were greater than 0.05, so the null hypothesis was upheld i.e. variances were equal, and therefore ANOVA was performed. The ANOVA was significant ($P < 0.05$) therefore the Tukey test (multicomparison test) was carried out for the Eh in April and July (Table 8).

Table 8: Tukey multicomparison test for oxidation-reduction potential in April and July, 2014

Month	Parameter	RB 1	RB 4	RB 7	RB 10	RB 13	RB 15
April	Eh	A	A	C	C	B	B
July	Eh	D	D	C	B	A	AB

In April, the Tukey test shows that (i) RBs 1 and 4 (upstream reed beds) are not significantly different, (ii) RBs 7 and 10 (middle reed beds) are not significantly different and (iii) RBs 13 and 15 (downstream reed beds) are not significantly different. However, each pair is significantly different from the other pairs. This is also observed in the Eh box plots.

For Eh in July, it was observed that (i) RBs 1 and 4 were not significantly different from each other but the pair was different from the other RBs, (ii) RB 7 was significantly different from the rest of the other reed beds, (iii) RB 10 was not significantly different from RB 15 but was different from the rest, (iv) RBs 13 and 15 were not significantly different from each other but the pair was different from RBs 1and 4, and RB 7. This was also observed in the Eh box plot in Figure 13, which shows the sharp increase in Eh from the uppermost 2 reed beds to the lowest 3 reed beds.

4.2. Physico-chemical parameters in sediment samples.

4.2.1 pH

The pH of three data points (upstream, middle and downstream (surface sediment (0-2 cm)), in each reed bed of each soil core of RBs 1, 10 and 15, in April and July, 2014, is shown below (Figures 14 -15). Only the 0-2 cm soil depth profile has been selected for statistical analysis; this is for the purpose of uniformity and the avoidance of ambiguity, since, for the water data, only three data points (upstream, middle and downstream) have been equally utilized for statistical analysis. Additional data from other sediment depth profiles measured are included in the Appendices.

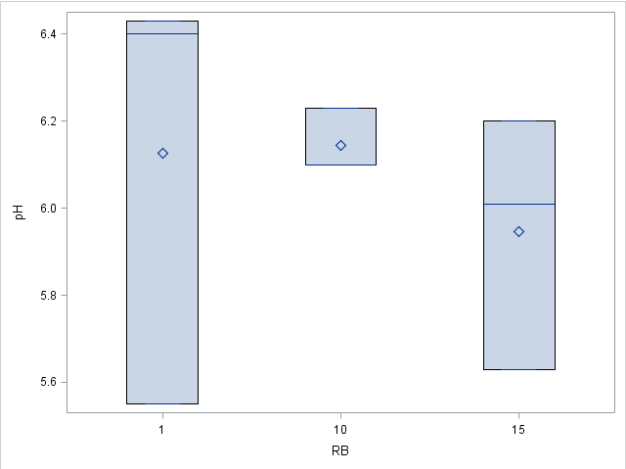

Figure 14: Box plot for pH in surface sediment (0-2 cm) in April, 2014.

It can be observed from Figure 14 above, that the pH values from the three reed beds are not very low as would be expected of typical AMD contaminated sediment. The pH in the sediment profile across the reed beds in April lies in the 5.6 - 6.4 range with no obvious differences between sites.

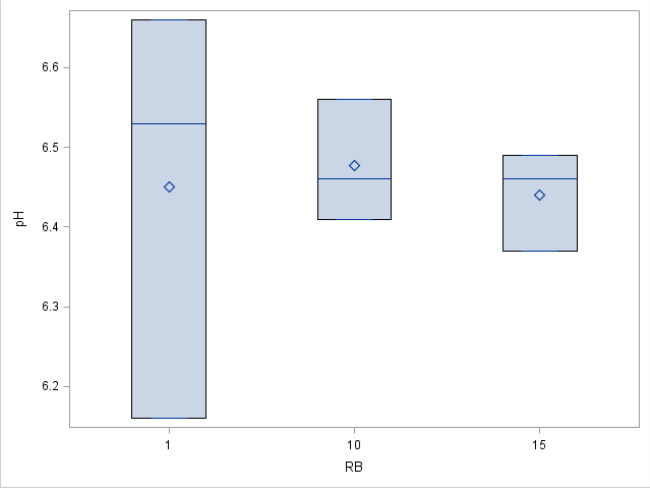

Figure 15: Box plot for pH in surface sediment (0 -2 cm) in July, 2014.

The pH pattern observed in Figure 15 above is similar to the pH-pattern in April (Figure 14), with no major differences between sites, but a slightly higher pH range (6.2 - 6.6) than in April.

The pH regimes in both April and July are not as low as the typical pH of AMD contaminated areas.

The result of the statistical tests performed for pH in the sediment in April and July (Table 9).

Table 9: Statistical tests and P-values for pH in surface sediment in April and July, 2014

Month	pH range	R-Square	Bartlett test	Levene test	ANOVA
April	5.55 – 6.43	0.095	P(x) 0.1289	P(F) 0.1473	P(F) 0.7410
July	6.16 – 6.66	0.014	P(x) 0.1400	P(F) 0.1026	P(F) 0.959

In April and July, the test for equality of variances / homogeneity of variances (Bartlett and Levene tests) had P-values that were greater than 0.05 therefore the null hypothesis was upheld i.e. variances were equal, based on this ANOVA was performed (Table 9). Differences between sites were not significant in either season (P > 0.05).

4.2.2 Electrical Conductivity

The box plots for EC in sediment in April and July, 2014 are shown below (Figures 16 and 17).

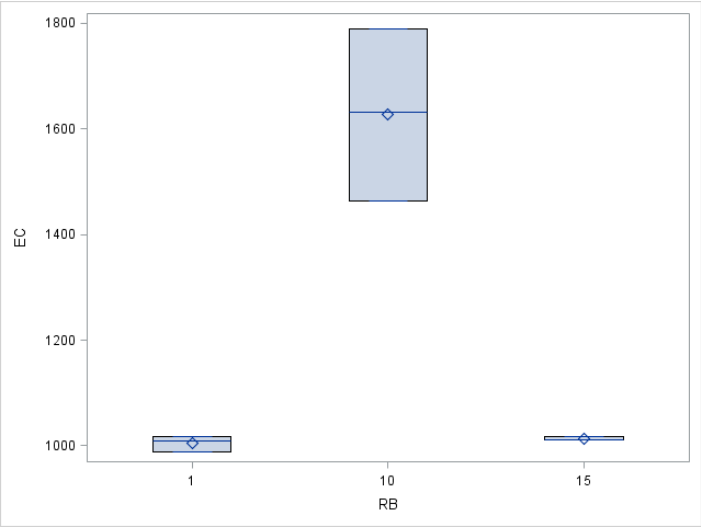

Figure 16: Box plot for electrical conductivity in surface sediment (0 – 2 cm) in April, 2014.

In April, EC in the surface sediment of RB 10 (middle reed bed) reaches 1800 µs/cm, while the EC in RBs 1 and 15 are much lower at around 1000 µs/cm.

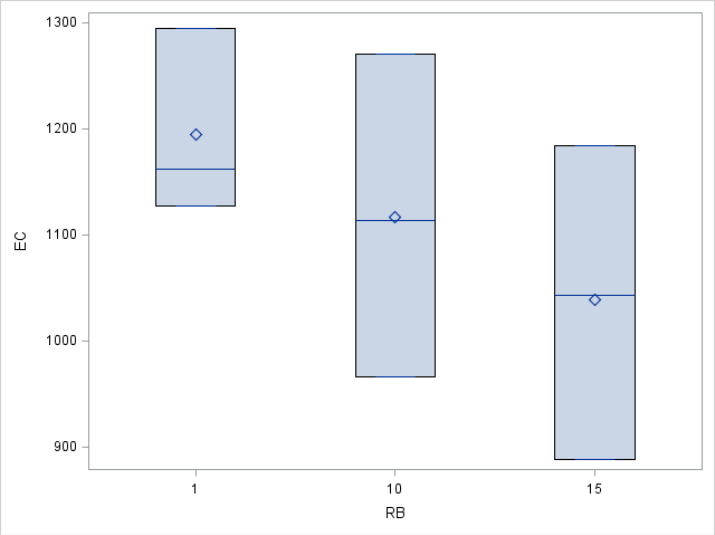

Figure 17: Box plot for electrical conductivity in surface sediment (0 -2 cm) in July, 2014.

In July the differences between sediment pH are much smaller. In Figure 17, a slight decline in EC range from RB1 (point of water entry) to RB 10 (middle reed bed) to RB 15 (furthest downstream) is observed, but with large overlaps between sites. The main difference in sediment EC between seasons is the presence of elevated EC in RB10 sediments in April but not in July.

The result of the statistical tests and P-values for EC in sediment in both April and July are shown below (Table 10 -11).

Table 10: Statistical tests and P-values for electrical conductivity in surface sediment in April and July, 2014

Month	EC range (µs/cm)	R-Square	Bartlett test	Levene test	ANOVA
April	988 – 1790	0.935	P(x) 0.0006	P(F) 0.0800	P(F) 0.0003
July	888 – 1295	0.258	P(x) 0.7699	P(F) 0.4911	P(F) 0.4095

ANOVA was performed on both seasons of EC data and this confirmed that the only significant difference between reed beds was the elevated EC in the sediment of RB10 in July.

Table 11: Tukey test for electrical conductivity in surface sediment in July, 2014

Month	Parameter	RB 1	RB 10	RB 15
April	EC	B	A	B
July	EC	N/A	N/A	N/A

4.2.3 Eh/ORP

The Box plots for Eh in the sediment profile for April and July are shown below (Figures 18 - 19).

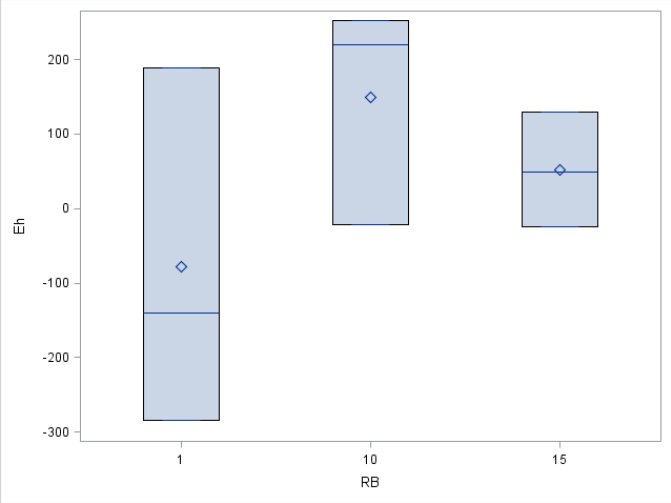

Figure 18: Box plot for oxidation-reduction potential in sediment (0 -2 cm) in April, 2014.

Figure 18 shows that RB1 presents a reducing condition, which changes to oxidizing conditions down the reed beds (at the middle and downstream). The large spread of values in RB1 indicates spatial variability within the plot.

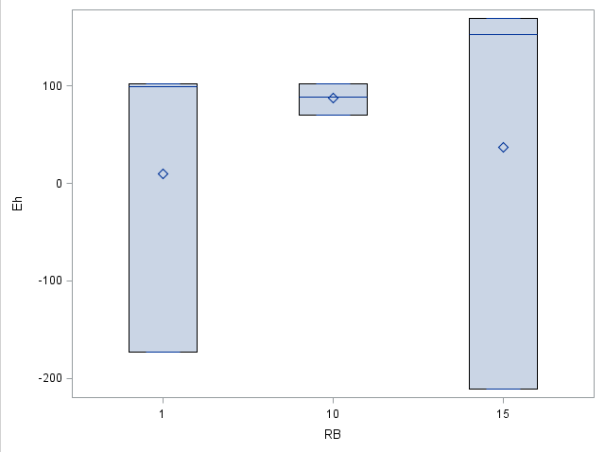

Figure 19: Box plot for oxidation-reduction potential in sediment (0 – 2 cm) in July, 2014.

For July, 2014, it was observed that Eh increased slightly from RB 1 to RB 10 to RB 15, though their mean values all fall within the 0 – 100 range (Figure 19).

The result of the statistical tests and P-values for Eh in sediment in both April and July are shown below (Table 12).

Table 12: Statistical tests and P-values for oxidation-reduction potential in sediment in April and July, 2014

Month	Eh Range (mV)	R-Square	Bartlett test	Levene test	ANOVA
April	-284.30 – 252.50	0.3113	P(x) 0.3902	P(F) 0.1916	P(F) 0.3266
July	-211.20 – 169.30	0.0610	P(x) 0.0459	P(F) 0.1815	P(F) 0.8280

ANOVA showed no significant differences between reed bed sediments in either season, in terms of the Eh.

4.3. Selected ions, trace and major elements in water samples

4.3.1 Anions

(a) Chloride (Cl^-)

Figures 20 and 21 below show the box plots for chloride in water in April and July, 2014 respectively.

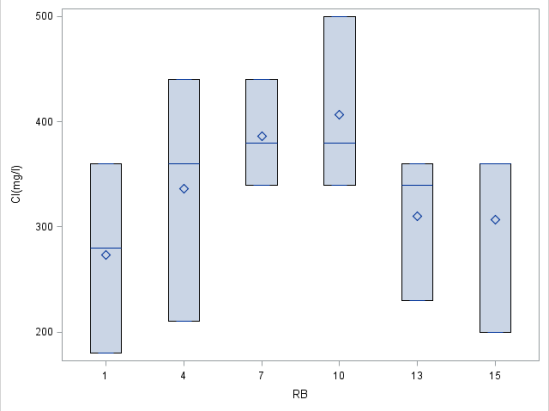

Figure 20: Box plot for chloride in water in April, 2014

Figure 20 show that there was a progressive increase in chloride concentration from RBs 1 to 10 and then a decline occurred at RBs 13 and 15. The highest mean concentration of chloride in the water was 500mg/l at RB 10 in April. The range (180 – 500 mg/l) as seen above is higher than the TWQR (90 – 100 mg/l) for chloride in aquatic ecosystems in South Africa (DWAF, 1996). The chloride range in the water flowing through the reed beds in both sampling periods in 2013 was 170 – 400 mg/l (Joubert, 2013) similar to that observed in the present study.

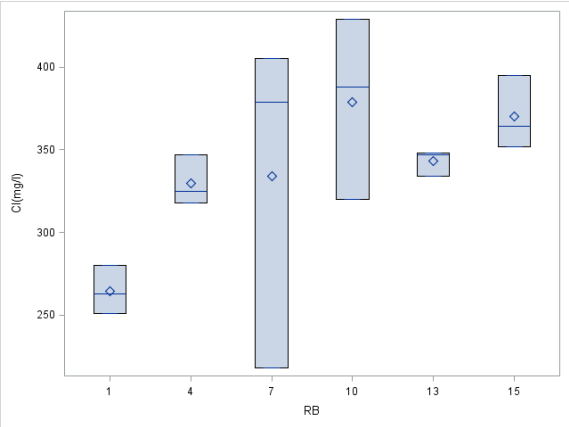

Figure 21: Box plot for chloride in water in July

Figure 21 also shows a progressive increase in chloride concentration from RBs 1 to 10, and again, a decline occurred at RB 13 but increased slightly at RB 15. The highest mean concentration of chloride in the water was also at RB 10 in July, 2014. Chloride concentration in

the water in July was also above the TWQR for aquatic ecosystems (90 – 100 mg/l) (DWAF, 1996). Overall, chloride concentration in the water was high in both April and July, 2014.

(b) Sulphate (SO_4^{2-})

Figures 22 and 23 show box plots for sulphate in water in April and July, 2014.

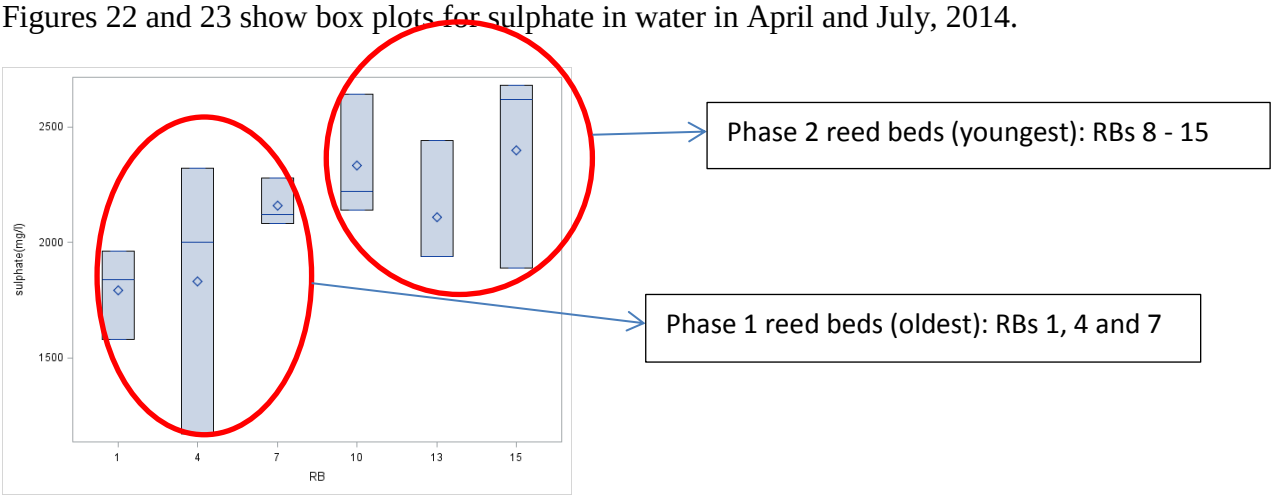

Figure 22: Box plot for sulphate in water in April, 2014

Figure 22 show a progressive increase in sulphate concentration from RBs 1 to 10, with a leveling off thereafter. Sulphate in April, 2014 shows a similar pattern to chloride concentration across the reed beds. The highest mean concentration of sulphate in the water was at RB 15 in April, 2014. Since the reed beds were constructed in phases at different periods, there is a difference in the age of the two sets of reed beds – Phase 1 reed beds were almost 2 years old whereas phase 2 reed beds were about 6-10 months old only, at the time of sampling.

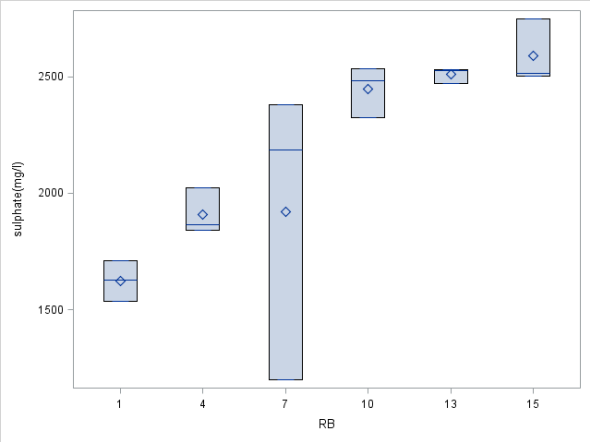

Figure 23: Box plot for sulphate in water in July, 2014

A similar but more obvious general increase in sulphate is seen across the reed beds in July with the highest mean concentration at RB 15. The sulphate concentrations in the water in both April and July are an order of magnitude above the TWQR of 0 – 200 mg/l for aquatic ecosystems in South Africa (DWAF, 1996) and the target RQC for the point of release from AGA property of <400 mg/l sulphate. The sulphate concentrations were also far above the same TWQRs in both seasons in 2013 and the concentrations were also higher at the reed beds downstream (Phase 2 reed beds) (Joubert, 2013).

4.3.2 Alkali and Alkaline Earth Metals

(a) Potassium (K)

Figures 24 and 25 show the box plots for potassium in water in April and July, 2014.

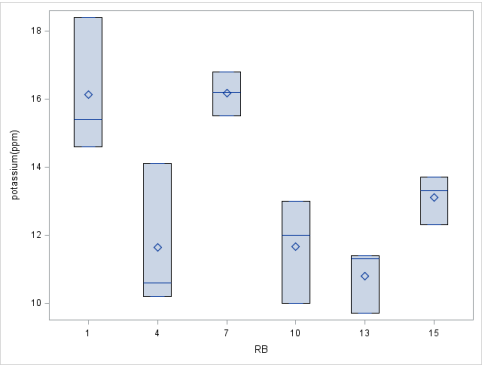

Figure 24: Box plot for potassium in April, 2014

Potassium concentrations varied between 10-20 mg/l in April, with no clear pattern but within the acceptable limit of 50 mg/l (DWAF, 1996).

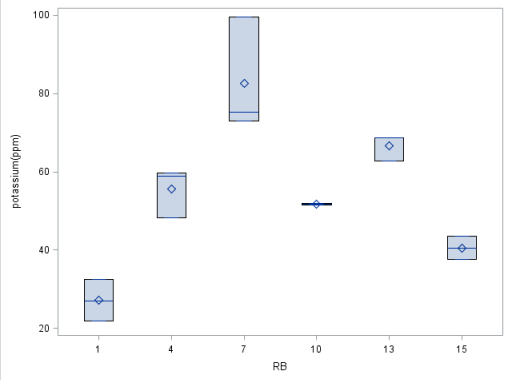

Figure 25: Box plot for potassium in July, 2014

Potassium concentrations were generally much higher in the water in July than in April, 2014. An increase in potassium occurred from RBs 1-7, followed by a general decline downstream. In July, 2014, potassium concentration in several reed beds was higher than the TWQR of (50mg/l) for aquatic ecosystems in South Africa (DWAF, 1996).

(b) Magnesium (Mg)

Box plots for Mg in waters in April and July 2014 are shown in Figures 26 - 27 below.

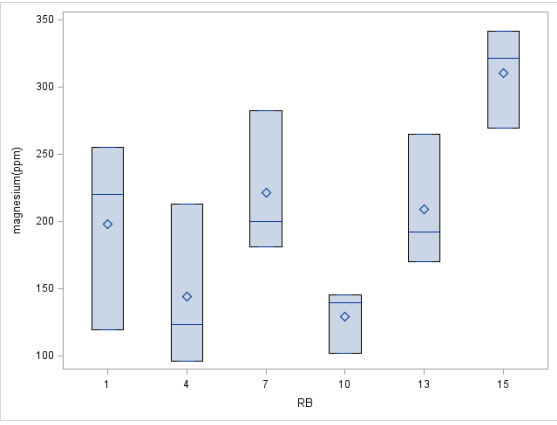

Figure 26: Box plot for magnesium in April, 2014

For Mg in April, 2014, no clear pattern was seen from RBs 1 – 10, but a rapid increase occurred in the reed beds downstream (RBs 13 and 15). The concentration of Mg in each reed bed was up to an order of magnitude higher than the TWQR (30mg/l) for aquatic ecosystems (DWAF, 1996).

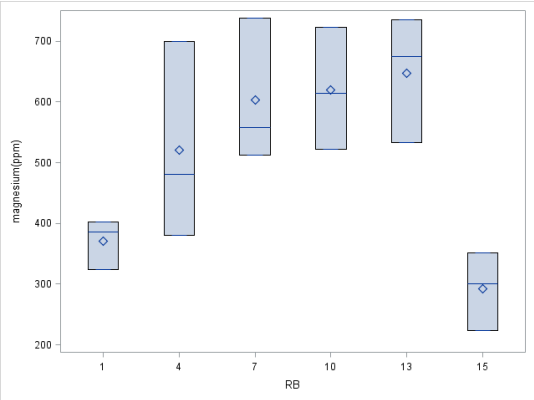

Figure 27: Box plot for magnesium in July, 2014

There was a steady increase in Mg concentration in the water flowing through the reed beds in July, 2014, but the concentration abruptly decreased at RB 15. Magnesium concentrations in the water in July are mostly much higher than in April, exceeding 700mg/l in several reed beds. The Mg concentrations in the water in July, 2014 are generally 10-20 times greater than the TWQR of 30mg/l for aquatic ecosystems (DWAF, 1996).

4.3.3 Base Metals

(a) Iron (Fe)

Figures 28 and 29 below show box plots for Fe in April and in July, 2014.

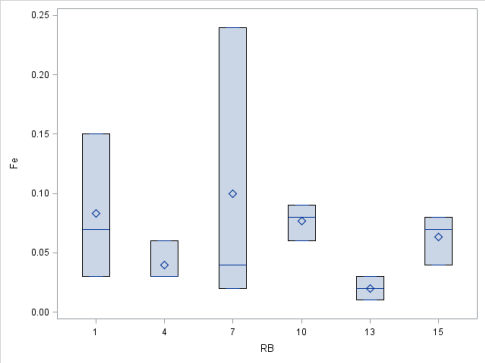

Figure 28: Box plot for iron in April, 2014

No clear pattern was observed in the Fe conentration across the reed beds in April, 2014 (Figure 28). The Fe concentration at RBs 1 and 7 exceed the TWQR of 0 – 0.1 mg/l for Fe for aquatic ecosystems (DWAF, 1996). The rest of the reed beds have Fe concentrations that are within acceptable limits.

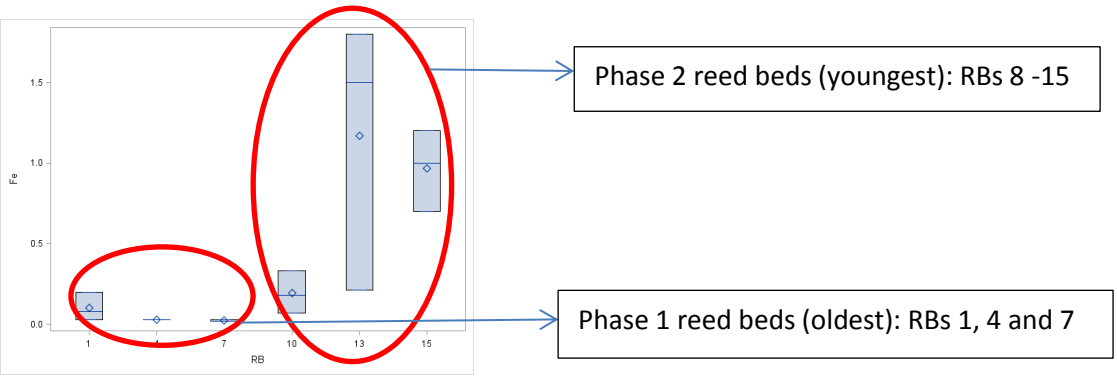

Figure 29: Box plot for iron in July, 2014

In July, 2014, RBs 10, 13 and 15 have much higher Fe concentrations than in April, in some cases more than ten times the TWQR of 0 – 0.1 mg/l for Fe.

(b) Manganese (Mn)

The box plots for Mn in April and July in 2014 are shown below (Figures 30 – 31).

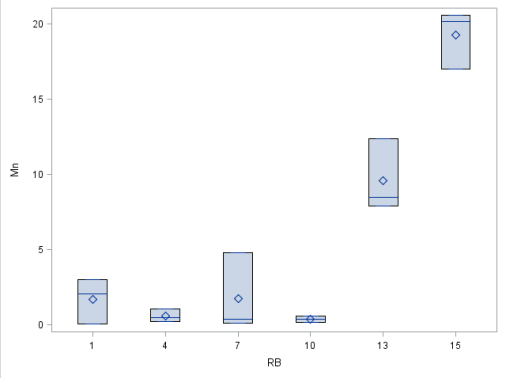

Figure 30: Box plot for manganese in April, 2014

In April, 2014, the Mn concentration sharply increased at RBs 13 and 15, exceeding 20 mg/l at RB 15, more than 400 times higher than the TWQR of 0 – 0.05 mg/l for aquatic ecosystems (DWAF, 1996).

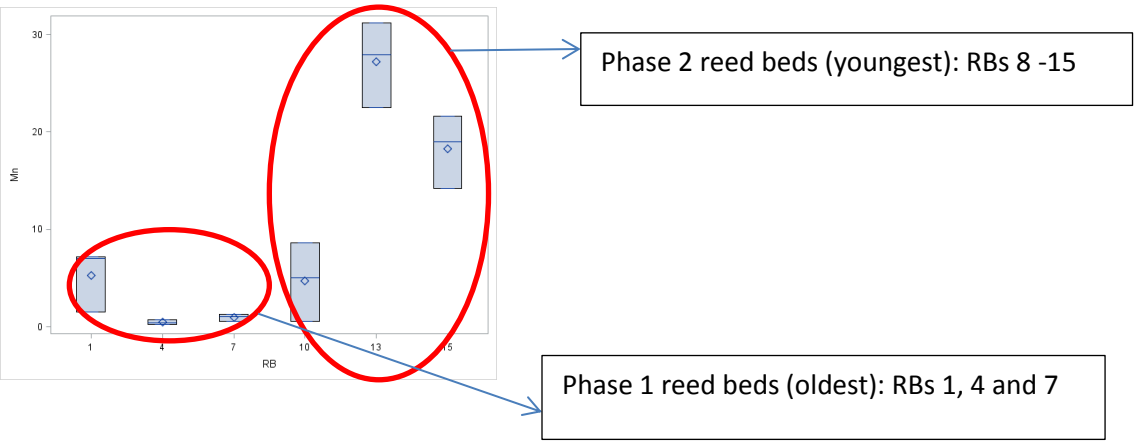

Figure 31: Box plot for manganese in July, 2014

Figure 31 shows a similar pattern for Mn to the Fe concentrations observed across the reed beds in July. The Mn concentrations across the reed beds in July were even higher than April, reaching a concentration of over 30 mg/l at RB 13, which is > 600 times higher than the TWQR. The box plots for both Fe and Mn in the water in July show similar trends in terms of increase of concentrations in the lower reed beds (Figures 29 and 31). The concentration of Mn in the water showed similar patterns in 2013, decreasing slightly from RBs 1 – 7 (phase 1 reed beds) and then increasing dramatically thereafter (phase 2 reed beds) in both May and July (Joubert, 2013).

4.4. Selected elements in sediment samples (surface sediments)

Box plots were constructed for Mg, Fe, Zn, Co, Ni and Cu. These are some of the metals known to be associated with the Witwatersrand conglomerates and are known to become mobile under acidic conditions (Makgae, 2012; Tutu et al., 2008).

Table 13: Some measured certified reference material (CRMs) of selected sediment parameters using XRF Spectroscout Geo+ (1)

Parameters	Measured CRMs - April 2014 (S 1)	Absolute Error (S 1)	Measured CRMs - July 2014 (S 2)	Absolute Error (S 2)	Actual CRMs - Stream sediment NCS DC 73315a
Mg	1.381 %	0.032 %	1.425 %	0.034 %	1.290 ± 0.030 (%)
Mn	1042 µg/g	8 µg/g	1060 µg/g	8 µg/g	-
Fe	4.551 %	0.005 %	4.547 %	0.005 %	5.270 ± 0.070 (%)
Cr	<5.1 µg/g	0 µg/g	<5.1 µg/g	0 µg/g	-
Co	21.5 µg/g	2.5 µg/g	17.7 µg/g	2.3 µg/g	-
Ni	35.9 µg/g	0.8 µg/g	35.3 µg/g	0.8 µg/g	-
Cu	111.1 µg/g	1.1 µg/g	107.4 µg/g	1.1 µg/g	-
Zn	245.4 µg/g	1.2 µg/g	242.1 µg/g	1.2 µg/g	263 ± 5 (µg/g)

N.B: Certified values of stream sediment reference materials (Issued 2010, approved by China National Analysis Centre for Iron and Steel, Beijing, China) is shown on Appendix 11.

4.4.1 Cobalt (Co) in sediments

The box plots for Co concentration in the surface sediment (0 – 2 cm) in April and July, 2014 are shown below (Figures 32 and 33).

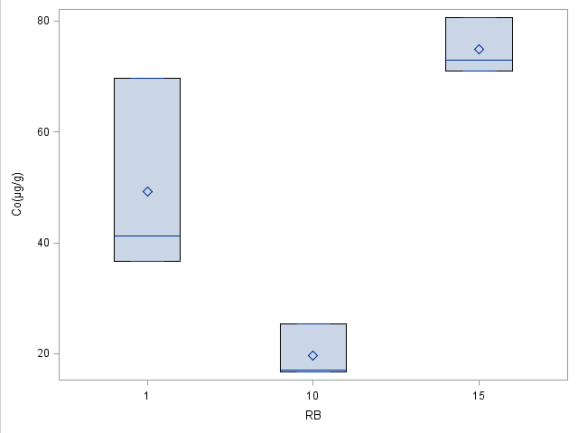

Figure 32: Box plot for cobalt in surface sediment (0 -2 cm) in April, 2014

From the Figure 32 above, it was observed that the Co concentration decreased from the uppermost (RB1) to the middle reed bed (RB 10) and an increase occurred at the reed bed downstream (RB 15), reaching 80 µg/g in the surface sediment in April (wet season).

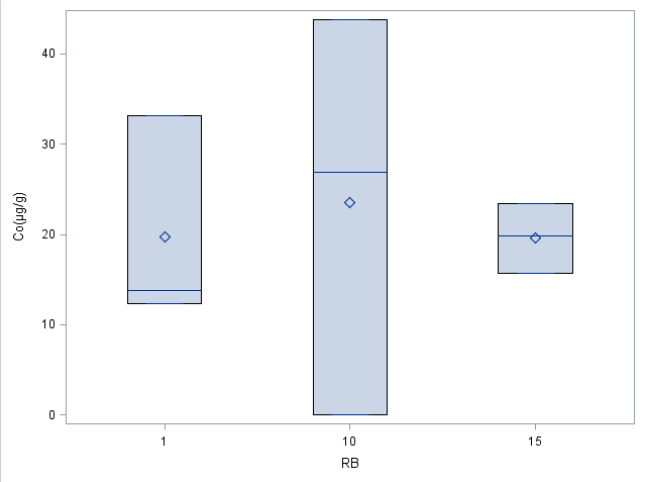

Figure 33: Box plot for cobalt in surface sediment (0 – 2 cm) in July, 2014

It was observed from Figure 33, that there were no clear differences amongst the reed beds in July, but compared with the April samples the sediment concentrations of Co in July are much lower in RBs 1 and 15.

4.4.2 Nickel (Ni) in sediments

The box plots for Ni concentration in the surface sediment (0 – 2 cm) in April and July, 2014 are shown below (Figures 34 and 35).

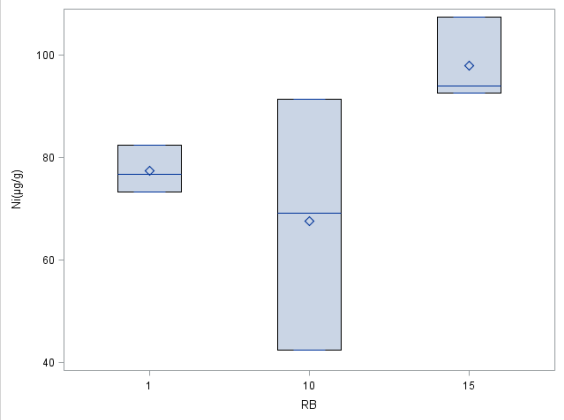

Figure 34: Box plot for nickel in surface sediment (0 – 2 cm) in April, 2014

It was observed from Figure 34 that the surface sediment of the last reed bed, RB 15 (where the water exits) had a higher Ni concentration than the first reed bed, RB 1 where polluted water enters the stream. The highest concentration of Ni was at RB 15 in April, where a concentration of 100 µg/g was observed.

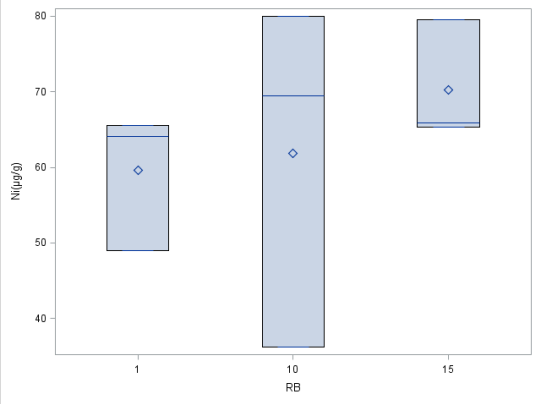

Figure 35: Box plot for nickel in surface sediment (0 – 2 cm) in July, 2014

Figure 35 show that in July, the pattern of the Ni concentrations across the reed beds is similar to that in April, but with slightly lower concentrations than in April sediment samples.

4.4.3 Copper (Cu) in sediments

The box plots for Cu concentration in the surface sediment (0 -2 cm) in April and July, 2014 are shown below (Figures 36 and 37).

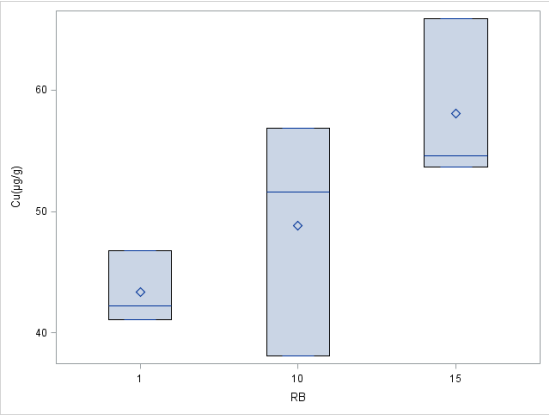

Figure 36: Box plot for copper in surface sediment (0 -2 cm) in April, 2014

Figure 36 above shows that there was a progressive increase in Cu within the surface sediment profile in April across the reed beds. The highest concentration of Cu at about 65 µg/g was observed at RB 15 in the sediment in April, 2014.

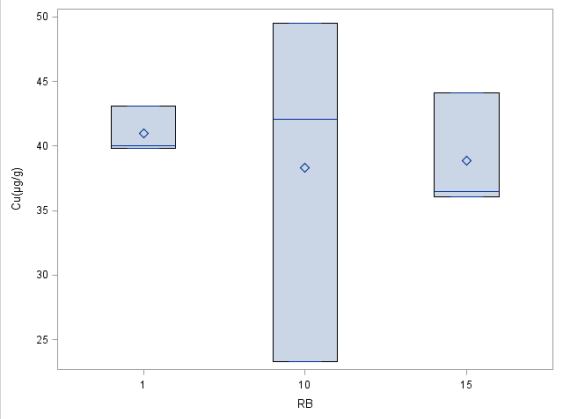

Figure 37: Box plot for copper in surface sediment (0 - 2cm) in July, 2014

The Cu concentration in the sediment in July is lower than the Cu concentration in the sediment in April, with no obvious differences between reed beds in July but a bigger range and maximum concentration of 50 µg/g in RB10.

4.4.4 Magnesium in sediments

The box plots for Mg, measured as MgO, in the surface sediment (0 – 2 cm) in April and July, 2014 are shown below (Figures 38 – 39).

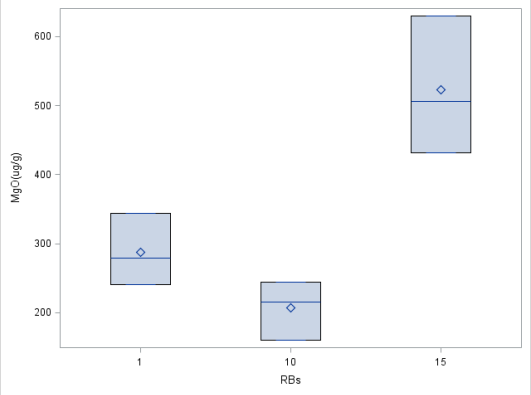

Figure 38: Box plot for magnesium (measured as MgO) in surface sediment (0 – 2 cm) in April, 2014

Figure 38 shows that the highest concentration of Mg (over 600 µg/g, as MgO) in the surface sediment in April, 2014 was at RB 15.

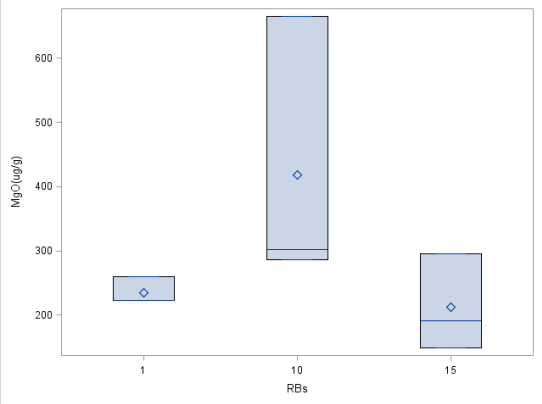

Figure 39: Box plot for magnesium (measured as MgO) in surface sediment (0 – 2 cm) in July, 2014

A rather different pattern was observed in July (Figure 39), with the highest concentration of Mg (over 600 µg/g as MgO) at RB 10.

4.4.5 Manganese in sediments

The box plots for Mn, measured as MnO, in the surface sediment (0 – 2 cm) in April and July are shown below (Figures 40 – 41).

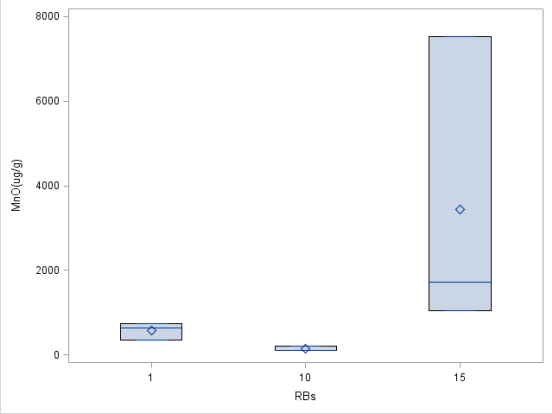

Figure 40: Box plot for manganese (measured as MnO) in surface sediment (0 – 2 cm) in April, 2014

The concentrations of Mn were an order of magnitude higher at RB15 than at RB1 or RB10 in April (Figure 40), reaching about 7500 µg/g as MnO. However, in July the highest concentration of Mn at about 900 µg/g as MnO, was observed at RB 10 (Figure 41), with sediment concentrations in RB15 being much lower than the April samples.

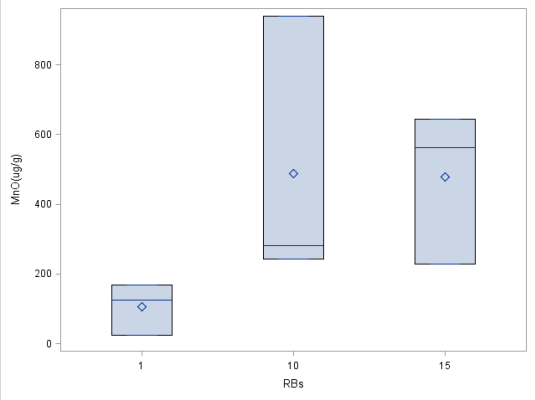

Figure 41: Box plot for manganese (measured as MnO) in surface sediment (0 – 2 cm) in July, 2014

4.4.6 Iron (Fe) in sediments

The box plots for Fe, measured as FeO, in the surface sediment (0 – 2 cm) in April and July, 2014 are shown below (Figures 42 – 43).

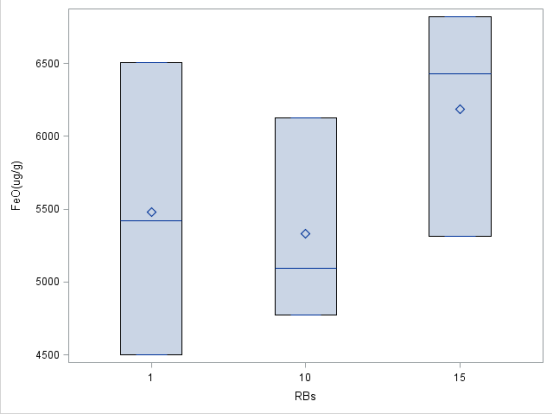

Figure 42: Box plot for iron (measured as FeO) in surface sediment (0 – 2 cm) in April, 2014

The highest concentrations of Fe in the surface sediment in April were found in RB 15 (≈ 7000 µg/g as FeO) but there were large overlaps between sites (Figure 42).

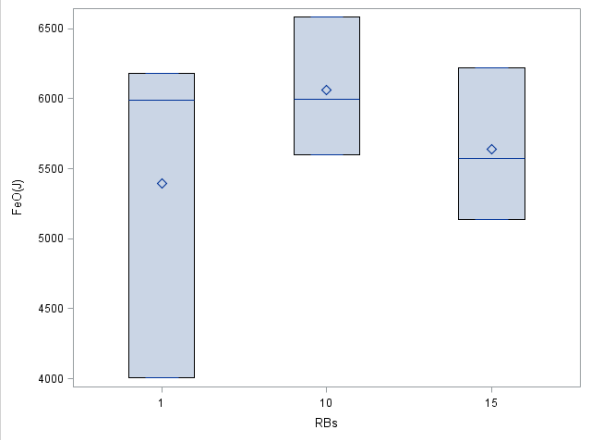

Figure 43: Box plot for iron (measured as FeO) in surface sediment (0 – 2 cm) in July, 2014

Figure 43 shows that in the surface sediment profiles in July, across the reed beds, the highest concentration of Fe was about 6500 µg/g as FeO at RB 10. Concentrations were generally very similar to the April samples.

4.5. Correlations of water quality chemical parameters

4.5.1 Correlations showing comparisons within a season in water

The Pearson's product-moment correlation analysis was performed on water chemistry data and correlation matrices were constructed. Investigating the correlations between contaminants from the correlation matrices is expected to enable the identification of the differences in spatial patterns between seasons i.e. between April and July, 2014 and relationships/associations between indicative AMD pollutants. The Pearson's correlation coefficients (r - values) were interpreted using Dancey and Reidy's categorization. When the rank coefficient 'r' falls between ± (0.1 – 0.3) this could be termed as a weak correlation, ± (0.4 – 0.6) as a moderate correlation and ± (0.7 – 0.9) as a strong correlation (Dancey and Reidy, 2004). The results of the correlations between the physico-chemical and ionic parameters in water in April and in July are shown in Table 13 below (The upper section represents the April values while the lower section represents the July values).

Table 14: Correlation coefficients of the correlations between water parameters in April (upper section) & July (lower section) 2014 (upper boxes = r, lower boxes = p; significant correlation in bold where p<0.05)

Pearson Correlation Coefficients, N = 18 Prob > |r| under H0: Rho=0									
	pH	**EC**	**Eh**	**Fe**	**K**	**Mg**	**Mn**	**chloride**	**sulphate**
pH	1.0000	0.3020	-0.0841	0.1324	0.3442	**-0.6325**	**-0.9120**	0.1897	-0.3526
		0.2233	0.7401	0.6004	0.1619	0.0048	<.0001	0.4510	0.1512
EC	0.1754	1.0000	**-0.4889**	0.2330	0.2720	0.1316	-0.1676	0.3046	0.0804
	0.4865		0.0395	0.3521	0.2749	0.6026	0.5062	0.2191	0.7512
Eh	0.3379	**0.9607**	1.0000	-0.3101	-0.1352	0.0537	0.1611	-0.4217	-0.3638
	0.1702	<.0001		0.2105	0.5927	0.8324	0.5230	0.0814	0.1378
Fe	0.3702	**0.5942**	**0.5883**	1.0000	0.3938	0.3547	-0.0745	0.1876	0.0565
	0.1305	0.0093	0.0102		0.1059	0.1487	0.7689	0.4560	0.8239
K	-0.4358	0.3209	0.3515	0.0269	1.0000	0.3691	-0.1234	-0.1405	-0.1411
	0.0706	0.1941	0.1526	0.9157		0.1317	0.6257	0.5780	0.5765
Mg	-0.2083	0.2284	0.2510	-0.0696	**0.6473**	1.0000	**0.7594**	-0.2299	0.1596
	0.4069	0.3619	0.3150	0.7838	0.0037		0.0003	0.3588	0.5271
Mn	**0.5052**	**0.6140**	**0.6326**	**0.8181**	-0.0099	0.0572	1.0000	-0.2969	0.2886
	0.0325	0.0067	0.0048	<.0001	0.9690	0.8218		0.2316	0.2455
Chloride	-0.1148	**0.6002**	**0.5249**	0.2539	0.3184	0.1541	0.1582	1.0000	**0.7528**
	0.6502	0.0085	0.0253	0.3093	0.1978	0.5417	0.5308		0.0003
Sulphate	0.1853	**0.8226**	**0.7618**	**0.5757**	0.1803	0.1306	**0.5896**	**0.8642**	1.0000
	0.4618	<.0001	0.0002	0.0124	0.4741	0.6054	0.0100	<.0001	

Strong inverse correlations were observed between pH and both Mg and especially Mn in April. The values in April in the upper section show a moderate inverse correlation between EC and Eh. Strong positive correlations between both Mg and Mn, and between chloride and sulphate, were also observed.

In July, as observed in the lower section of Table 14, there were a greater number of positive correlations. There was a moderate positive relationship between pH and Mn. There were positive correlations between EC and all of the following; Eh, Fe, Mn, chloride and sulphate. There were also positive correlations between Eh and all of the following; EC, Fe, Mn, chloride and sulphate, i.e. the same general correlations observed for EC were also observed for Eh, given the very strong relationship between these two in the July samples. For Fe, there was a strong

positive correlation with Mn and a moderate positive correlation with sulphate. Other correlations include moderate positive correlations between K and Mg and between Mn and sulphate, while a strong positive correlation between chloride and sulphate was also observed, as seen in the April samples.

4.5.2 Correlations showing comparisons between seasons (April versus July) in water

To investigate whether various water quality parameters showed the same spatial patterns between reed beds on both sampling occasions, analysis of Pearson spatial correlations between seasons was performed (Table 15). The correlation coefficients (r - values) with asterisks are significant at $p<0.05$.

Table 15: Correlation coefficients for selected water quality parameters across reed beds between seasons (April & July water samples)

Parameter	Correlation coefficients
pH	-0.42*
EC	0.06
Eh	-0.58*
Fe	-0.26
K	-0.12
Mg	-0.46
Mn	0.70*
Chloride	0.45*
Sulphate	0.48*

Table 15 shows a moderate inverse relationship between April and July samples for pH (r = -0.42) and Eh (r = -0.58). Moderate positive relationships were found between seasons only for chloride (r = 0.45), sulphate (r = 0.48) and a strong positive correlation for Mn (r = 0.70). Hence there are few spatial similarities in water quality parameters between seasons, with only Mn showing strong relationships between seasons.

4.6. Correlations of sediment chemical parameters

4.6.1 Correlations showing comparisons within a season in sediment

Pearson correlation analysis was performed between the physico-chemical parameters and selected elemental compositions within the surface sediments for both April and July 2014 samples. The results are shown in Table 16 below (the upper section represents the April values while the lower section represents the July values).

Table 16: Correlation coefficients of the correlations between sediment parameters in April (upper section) & July (lower section) 2014 (upper boxes = r, lower boxes = p; significant correlation in bold where p<0.05)

Pearson Correlation Coefficients, N = 9 Prob > |r| under H0: Rho=0											
	pH	**EC**	**Eh**	**Co**	**Ni**	**Cu**	**Cr**	**Zn**	**Mg**	**Mn**	**Fe**
pH	1.000	0.180	-0.575	-0.123	-0.111	0.038	0.394	-0.238	-0.096	0.327	-0.627
		0.644	0.105	0.752	0.777	0.923	0.294	0.537	0.807	0.390	0.071
EC	0.257	1.000	0.472	**-0.818**	-0.592	-0.135	0.462	-0.655	-0.629	-0.407	-0.207
	0.505		0.199	0.007	0.093	0.730	0.210	0.056	0.070	0.277	0.593
Eh	-0.172	-0.573	1.000	-0.395	0.093	0.297	0.175	-0.068	-0.117	**-0.677**	0.663
	0.658	0.107		0.293	0.811	0.437	0.652	0.862	0.764	0.045	0.052
Co	-0.276	0.070	0.426	1.000	**0.734**	0.475	-0.348	**0.887**	**0.853**	0.357	0.052
	0.472	0.858	0.253		0.024	0.196	0.359	0.001	0.003	0.346	0.894
Ni	-0.289	-0.463	-0.038	-0.088	1.000	**0.846**	0.046	**0.825**	**0.845**	0.061	0.534
	0.450	0.210	0.922	0.823		0.004	0.906	0.006	0.007	0.876	0.139
Cu	-0.159	-0.257	-0.041	-0.189	**0.849**	1.000	0.188	**0.722**	**0.761**	-0.200	0.431
	0.684	0.504	0.917	0.626	0.004		0.629	0.028	0.017	0.607	0.247
Cr	0.237	0.377	0.081	**0.762**	-0.476	-0.485	1.000	-0.366	-0.341	0.288	-0.025
	0.539	0.318	0.836	0.017	0.195	0.186		0.332	0.369	0.453	0.949
Zn	0.051	0.176	0.151	**0.842**	-0.282	-0.322	**0.897**	1.000	**0.977**	-0.003	0.324
	0.896	0.651	0.698	0.004	0.462	0.398	0.001		<.0001	0.995	0.394
Mg	-0.131	0.070	0.210	**0.695**	0.377	0.465	0.493	0.563	1.000	0.033	0.269
	0.737	0.857	0.588	0.038	0.318	0.208	0.177	0.115		0.934	0.484
Mn	-0.122	-0.575	-0.109	-0.030	0.262	-0.036	-0.030	0.234	-0.133	1.000	-0.429
	0.754	0.105	0.779	0.940	0.497	0.926	0.938	0.545	0.734		0.249
Fe	0.028	0.243	0.002	0.397	-0.242	-0.539	0.295	0.371	-0.164	0.069	1.000
	0.944	0.528	0.995	0.290	0.530	0.134	0.441	0.326	0.673	0.861	

Table 16 shows a moderate inverse relationship in April samples between Eh and Mn and a strong inverse correlation between EC and Co. Strong positive correlations existed in April between; (i) Co with Ni, Zn, and Mg (ii) Ni with Cu and Zn, (iii) Cu with Zn. Each of Co, Ni, Cu and Zn had strong positive correlations with Mg in April.

In July, shown in the lower section of Table 16, Co shows strong positive correlations with several other metals (Cr, Zn and Mg) while Ni is strongly correlated with Cu and Cr is strongly correlated with Zn.

4.6.2 Correlations showing comparisons between seasons (sediments)

The results of the Pearson correlation analysis performed for similar parameters in the sediment samples between April and July 2014 are shown below in Table 17.

Table 17: Correlation coefficients of correlations between seasons (April & July sediment samples)

Parameter	Correlation coefficients
pH	0.75*
EC	0.06
Eh	0.54
Co	-0.74*
Ni	-0.62*
Cu	-0.32
Cr	0.11
Zn	-0.71*
Mg	-0.49
Mn	-0.39
Fe	0.04

Table 17 shows a strong positive correlation between pH in April and July (r = 0.75) but all other significant correlations were negative, including Co (r = -0.74) Ni (r = -0.62) and Zn (r = -0.71).

4.6.3 Summary of the water and sediment chemistry data

Common trends in the chemistry data include the following:

(i) Chloride, sulphate and Mn concentrations in the water across the reed beds in April and also in July were above freshwater TWQRs (DWAF, 1996) and the RQC for sulphate of 400 mg/L. This can be viewed from the box plots (Figures 20, 21, 22, 23, 30 and 31);

(ii) Inverse correlations were observed between the pH in both seasons and also for the Eh in both seasons (Table 15), showing spatial changes between seasons for both parameters;

(iii) In the sediments, pH was lowest at the downstream reed bed RB 1) in both April (Figure 14) and July (Figure 15) with a positive correlation (r = 0.75) in spatial pattern between seasons (Table 17). The inverse correlations observed in the surface sediment profiles between the seasons for Co, Ni and Zn (Table 17) may be due to differences in the mobility of these metals – some leaching more readily to deeper sediments and some precipitating out.

Table 18: World Health Organization (WHO) Guidelines for Water Quality, (WHO, 2004)

Metal	Threshold value (mg/l or µg/ml)
Cu	2.00
Co	0.02
Zn	0.01
Ni	0.003
Mn	0.03
Fe	0.07

Table 19: Stream pH categories for southern Africa (Dallas and Day, 1994)

Category	pH
Natural	6.5 – 8.0
Good	5.75 - 6.46 and 8.05 - 9.00
Fair	5.00 - 5.70 and 9.05 - 10.00
Poor	<5.00 or >10.00

4.7. Inter-annual differences between survey years, 2013 and 2014

Principal component analysis is a multivariate technique, that illustrates the loadings of selected variables on each axis (how strongly one contaminant drives that component and also the closeness to the axis) i.e. how much of the variance is explained by that axis alone (Galpin and Krommenhoek, 2014). Therefore, the PCAs served to investigate relationships between pollutants along the major axes of variation between reed beds. Inter-annual differences between the survey years, in these relationships, were also explored with PCAs.

4.7.1 Principal component analyses

Principal component analyses (PCAs) of water chemical parameters in May 2013 (0513), July 2013 (0713), April 2014 (0414) and July 2014 (0714) were performed using covariance matrices for multivariate data. The mean concentrations of each parameter or variable at each of the 6 reed beds were used.

4.7.1.1 PCA for May 2013

Below are the PCA for May 2013, the Eigen values of the covariance matrix (Table 20), the Scree Plot and Variance Explained (Figure 44) and the Pattern Plot (Figure 45).

Table 20: PCA for May, 2013

Principal component analysis for May, 2013 (0513) Observations: 6 Variables: 15 Total variance: 229731.68 Eigenvalues of the Covariance Matrix				
	Eigenvalue	Difference	Proportion	Cumulative
1	170764.29	112571.78	0.74	0.74
2	58192.51	57570.26	0.25	0.99
3	622.24	511.77	0.01	1.00
4	110.47	68.30	0.00	1.00
5	42.18	42.18	0.00	1.00

From the Eigenvalues of the covariance matrix on Table 20:

i. Difference – this column gives the difference between the successive eigenvalues e.g. 170764.29 - 58192.51 = 112571.78 and 58192.51 - 622.24 = 57570.26 etc.

ii. Proportion – this is the proportion of the total variance 229731.68 that each factor accounts for, e.g. 170764.29/ 229731.68 = 0.74 and 58192.51/ 229731.68 = 0.25 etc.

iii. Cumulative – this column represents the sum of the proportion column and shows the cumulative variance explained, e.g. 0.74 + 0.25 = 0.99

From the eigenvalues of the covariance matrix table, it can be noted that the cumulative variance explained of the first PCA axes with proportions (0.74 + 0.25) gives 0.99 i.e. ≈100 %. This means that most of the information from the data set is explained by the 2 eigenvalues of the first two principal components, so only two principal components out of the 15 are retained.

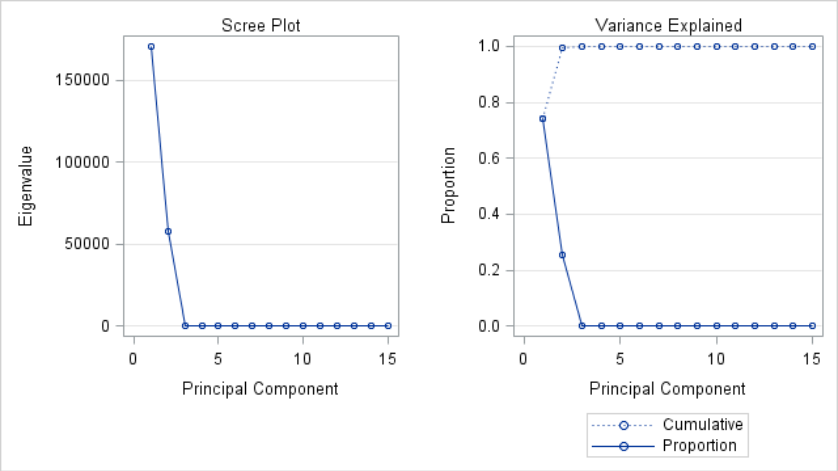

Figure 44: Scree Plot and Variance Explained for May, 2013

The Scree Plot graphs the eigenvalue against the principal component number. The variance explained plot on Figure 44 graphs the proportion and cumulative proportion against the principal component number. From the graph, it can be observed that component one explains 0.74 i.e. 74 % (most of the variation in the data). Component 2 explains 0.25 (25 %, the rest of the variation in the data).

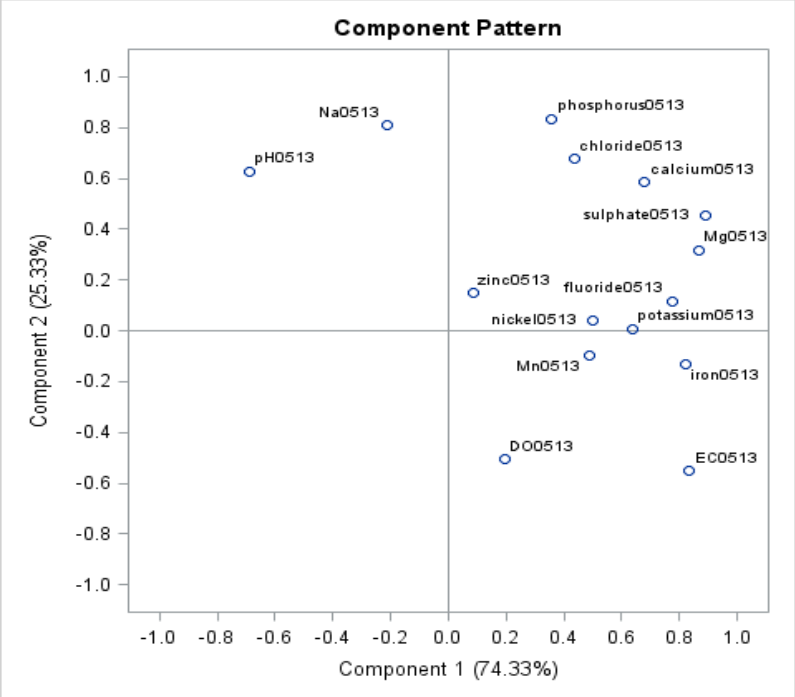

Figure 45: Pattern plot of component 2 by component 1 for May, 2013

The loading values ≥ 0.75 signifies 'strong', the loading with values between 0.50 and 0.75 indicates 'moderate' while loading values between 0.30 and 0.50 are denoted as weak (Liu *et al*., 2003).

Figure 45 shows that almost all the variables load more positively on principal component 1 than on principal component 2. Sulphate had the highest loading on component 1, followed by EC and Mg (Figure 45) and it can be observed that component 1 is contributing as much as 74.33 % of the information from the data set in May, 2013. On component 1, pH had a high negative score (a component where EC had a high positive score, pH is usually inverse to EC (Fadiran *et al*., 2014). On component 2, pH had a high positive score (a component where EC had a high negative score, evidencing coupled effects of processes involving acid drainage and pH), though component 2 is responsible for 25.33 %. The variables with the highest loadings on the component (component 1) that is contributing the highest cumulative percentage of variation (74.33 %) are EC, Mg and sulphate. They are responsible for the most of the variation in the water quality data from May, 2013.

4.7.1.2 PCA for July, 2013

Below are the PCA for July, 2013, the Eigen values of the covariance matrix (Table 21), the Scree Plot and Variance Explained (Figure 46) and the Pattern Plot (Figure 47).

Table 21: PCA for July, 2013

Principal component analysis for July, 2013 (0713) Observations: 6 Variables: 15 Total variance: 280895.97 Eigenvalues of the Covariance Matrix				
	Eigenvalue	Difference	Proportion	Cumulative
1	266150.57	252934.99	0.95	0.95
2	13215.567	11938.61	0.05	1.00
3	1276.95	1062.24	0.00	1.00
4	214.71	176.54	0.00	1.00
5	38.17	38.17	0.00	1.00

From the eigenvalues of the covariance matrix on Table 21, it can be noted that the cumulative variance explained by the first two principal components is almost 100% (0.95 + 0.05). This means that most of the information from the data set is explained by the 2 eigenvalues of the first two components, so only two principal components are retained.

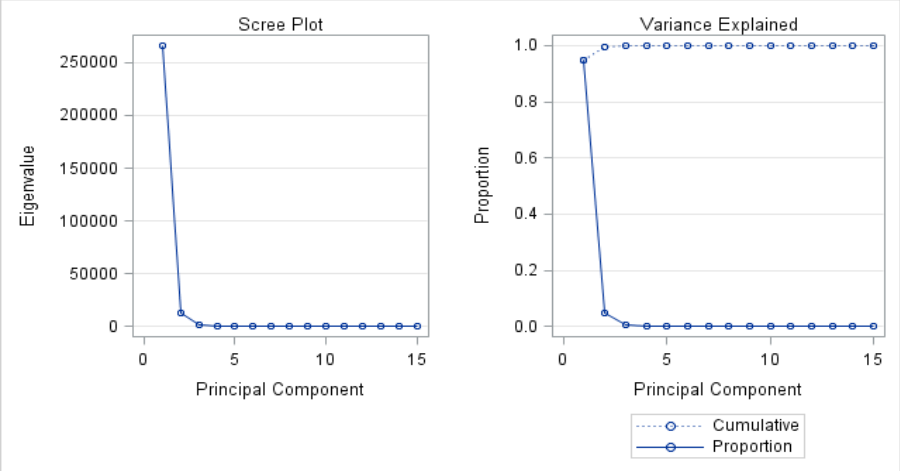

Figure 46: Scree Plot and Variance Explained for July, 2013

The variance explained plot on Figure 46 graphs the proportion and cumulative proportion against the principal component number. The graph shows that component one explains 0.95 i.e. 95 % (most of the variation in the data). Component 2 explains 0.05 (5 %), the rest of the variation in the data). Again, this means that only two principal components (components 1 and 2) are retained.

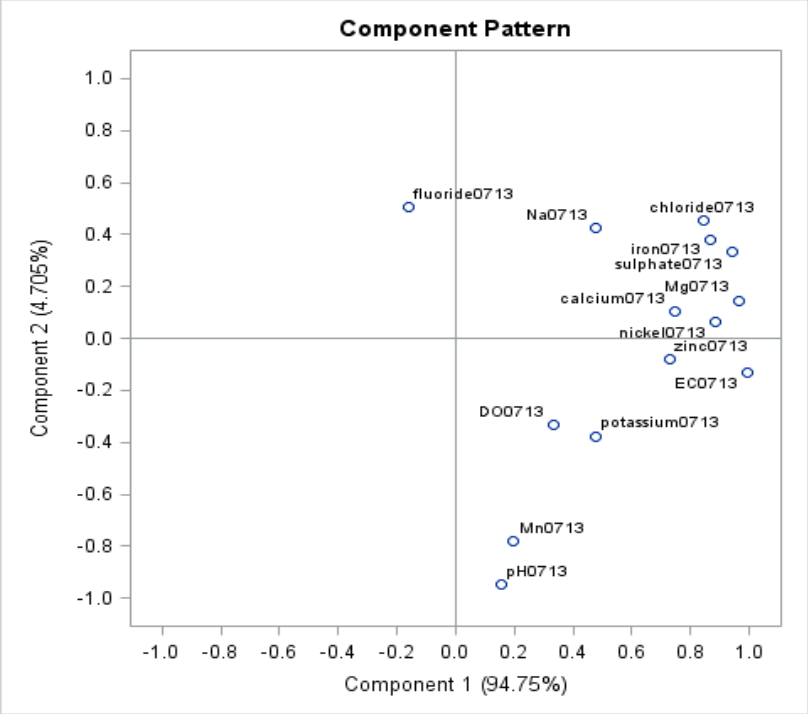

Figure 47: Pattern plot of component 2 by component 1 for July, 2013

Figure 47 shows that all the variables except fluoride, load more positively on principal component 1 than on principal component 2. Electrical conductivity had the highest loading on component 1, followed by sulphate and Mg (Figure 47) and it can be observed that component 1 is contributing as much as 94.75 % of the information from the data set in July, 2013. On component 2, pH had a high negative score though component 2 is responsible for only 4.71 % therefore EC and sulphate are responsible for the most of the variation in the data from July, 2013. The observation that most contaminants load more positively on the first principal component suggests the strong influence of a common factor which increases all concentrations together, i.e. probably an evaporation/concentration signal. On principal component 2, pH and Mn had a high negative score while fluoride had a positive score, suggesting stronger influences on their concentrations than evaporation - though component 2 is responsible for only 4.71 % of variance explained.

4.7.1.3 PCA for April, 2014

Below are the PCA for April, 2014, the Eigen values of the covariance matrix (Table 22), the Scree Plot and Variance Explained (Figure 48) and the Pattern Plot (Figure 49).

Table 22: PCA for April, 2014

Principal component analysis for April, 2014 (0414)
Observations: 6
Variables: 14
Total variance: 173149.19

Eigenvalues of the Covariance Matrix

	Eigenvalue	Difference	Proportion	Cumulative
1	103649.28	41253.72	0.60	0.60
2	62395.56	56135.63	0.36	0.96
3	6259.93	5537.03	0.04	1.00
4	722.90	601.38	0.00	1.00
5	121.52	121.52	0.00	1.00

Table 22 shows that three principal components will be retained.

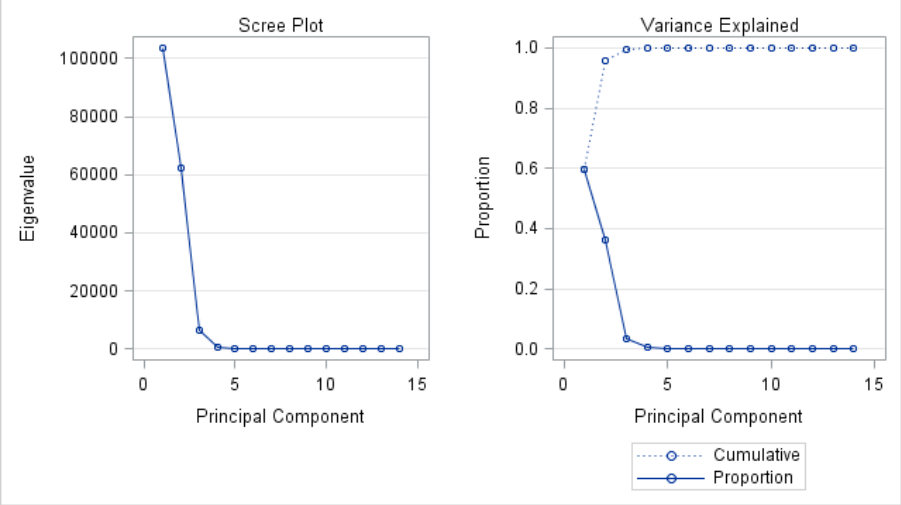

Figure 48: Scree Plot and Variance Explained for April, 2014

The Variance Explained graph on Figure 48 shows that 0.60 % of the variation in the data set is due to component 1 while 0.36 % is due to component 2 and 0.04 % is due to component 3 (Figure 48 and Table 21). Hence, three principal components were retained.

a).

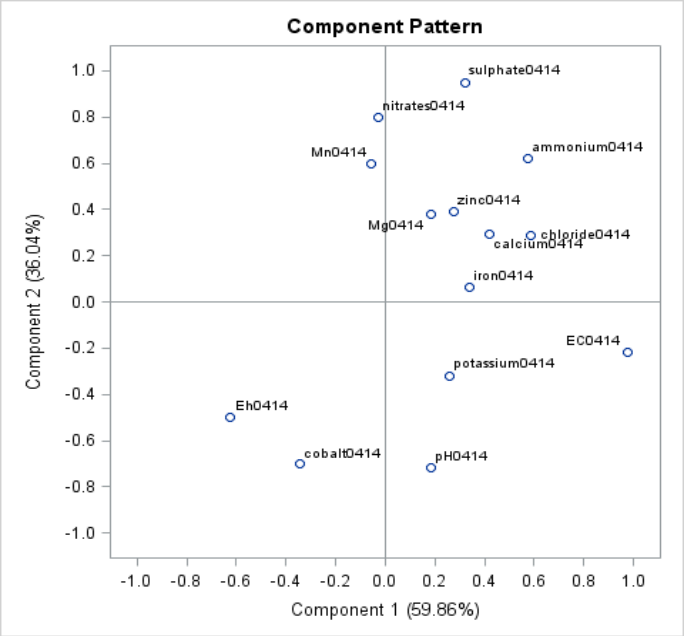

b).

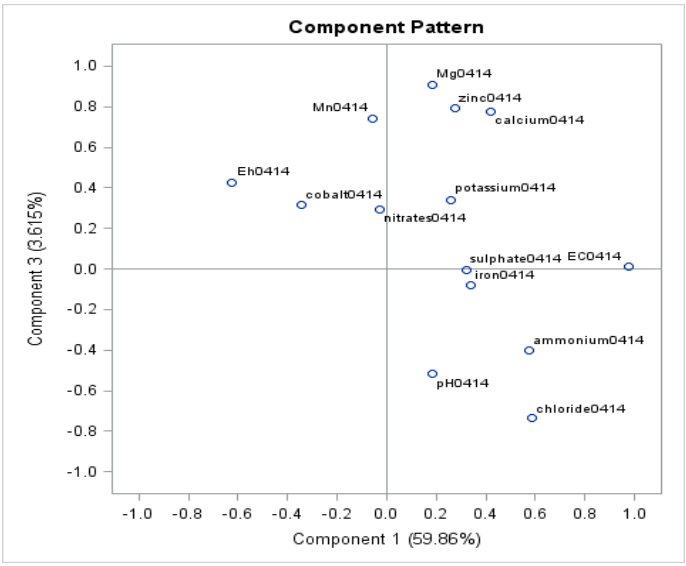

Figure 49: a). Pattern plot of component 2 by component 1; b). Pattern plot of component 3 by component 1 for April, 2014.

All but four variables (Eh, Mn, Co, nitrate) load positively on component 1 (Figures 49 a & b), which is strongly associated with EC, chloride and ammonium, while Eh has the strongest negative loading. Component 1 contributes almost 60% of the cumulative percentage variation from the dataset from April 2014. There is very little association between nitrate, pH and Mn with the first principal component indicating that these are largely associated with other factors.

Component 2 explains 36% of variance in the April data (Figure 49a) and sulphate, nitrate, ammonium and Mn have the highest positive loadings on this component, while pH, Co and Eh have the greatest negative loadings. Magnesium, Mn, Zn and Ca all had high loadings on component 3, but component 3 explains only 3.6 % of variance in the dataset.

4.7.1.4 PCA for July, 2014

Below are the PCA for July, 2014 and the Eigen values of the covariance matrix on Table 23, the Scree Plot and Variance Explained (Figure 50) and the Pattern Plot (Figure 51).

Table 23: PCA for July, 2014

Principal component analysis for July, 2014 (0714)
Observations: 6
Variables: 14
Total variance: 1551322.75

Eigenvalues of the Covariance Matrix

	Eigenvalue	Difference	Proportion	Cumulative
1	1512105.28	1479925.48	0.97	0.97
2	32179.80	25993.41	0.02	0.99
3	6186.39	5436.21	0.01	1.00
4	750.18	649.08	0.00	1.00
5	101.10	101.10	0.00	1.00

From the eigenvalues of the covariance matrix on Table 23, it can be noted that only two principal components will be retained.

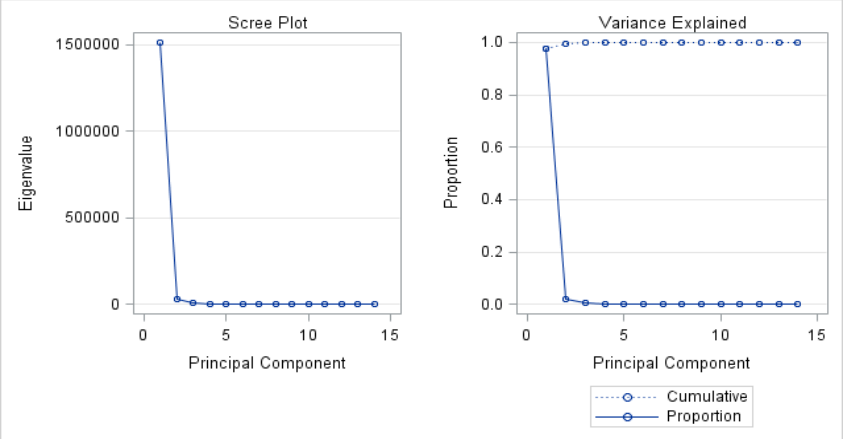

Figure 50: Scree Plot and Variance Explained for July, 2014

The Scree Plot and Variance Explained graphs on Figure 50 shows that 0.97 % of the variation in the data set was explained just by component 1 and only 2 % by component 2, i.e. about 99 % of the information from the dataset was explained by these two components.

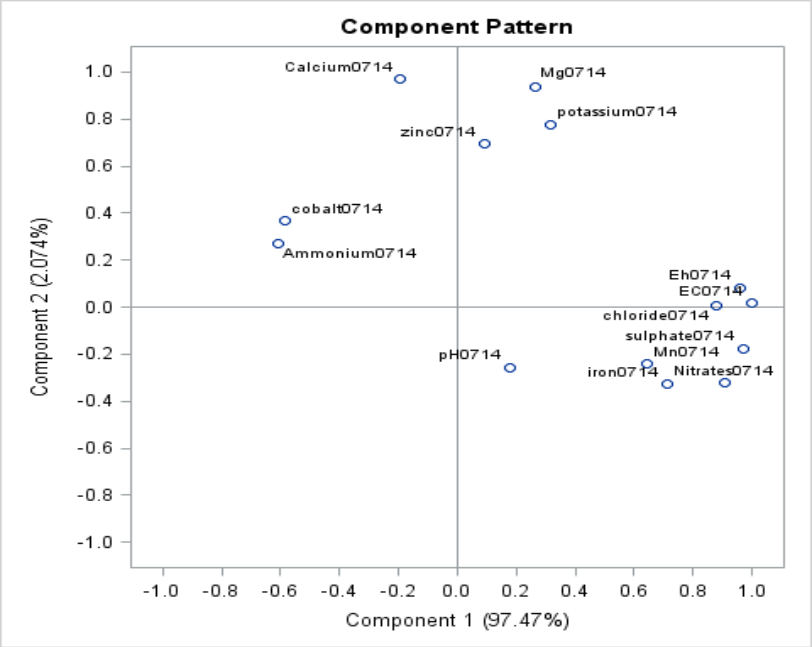

Figure 51: Pattern plot of component 2 by component 1 for July, 2014

It can be observed from Figure 51, that component 1 was responsible for 97.47 %. On component 1, pH had a weak loading, while EC, Eh, sulphate, nitrate, chloride, Fe and Mn all had strong positive loadings. These variables contributed the most to the variability of the

dataset, with EC being the most responsible, as it has the highest positive loading value on component 1 (the component with the highest cumulative percentage of variation). On the other hand, on component 2 (contributing 2.07 %), the major and trace elements were the sources of variation, as Ca, Zn, Mg and K all had moderate to strong positive loadings.

Compared with July 2013, while many contaminants show strong positive loadings along principal component 1, there are some contaminants (ammonium, Co, Ca) that show negative loadings. Hence while evaporation/concentration may explain elevated levels of many contaminants, some other processes are linked to ammonium, Co and Ca concentrations.

Summarily, EC and sulphate, alongside trace and major elements like Mg, Mn and Zn were the variables responsible for most of the variation from the 4 datasets, with EC being the most responsible in most cases. EC had the highest positive loading(s) on most of the significant (larger variance percentage) components.

4.8. Comparison of seasonal mean water chemical parameters within reed beds between 2013 and 2014

Similarities and differences in the data from the two survey years were sought by constructing bar charts (Figures 52 - 61) of the data for some of the contaminants (pH, EC, sulphate, Fe and Mg) that were responsible for most of the variation in the datasets, according to the PCAs (Figures 45 – 51) that were performed.

The bar charts below (Figures 52 – 61) were constructed with RBs along the x-axis and paired May 2013 (0513)/April 2014 (0414) and separate charts for the July 2013 (0713)/July 2014 (0714) data - to inspect whether similar spatial patterns were observed between years.

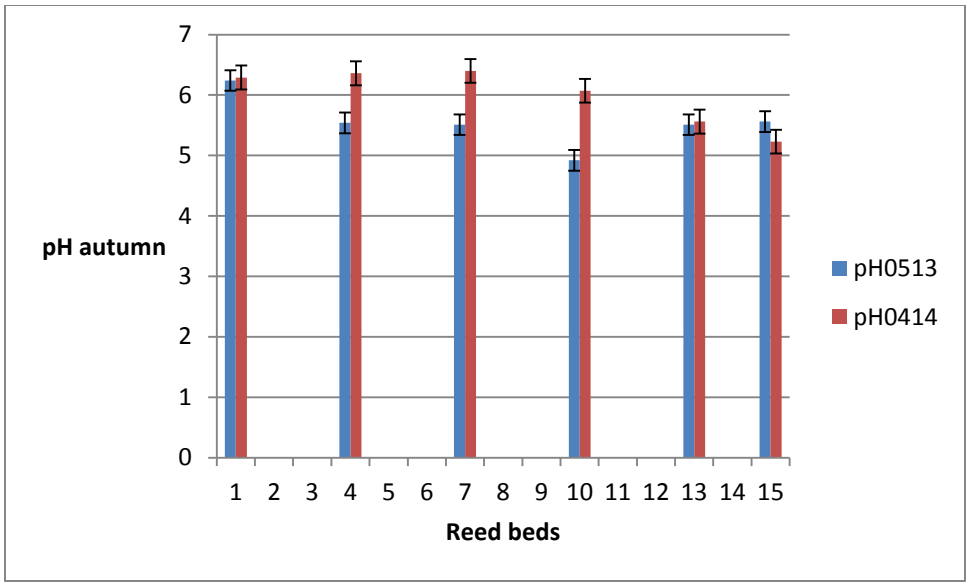

Figure 52: Bar chart (±SE) for pH in autumn for May, 2013 and April, 2014

Figure 52 shows that the pH in the autumn sampling period in 2013 and 2014 were somewhat similar, though the pH values in 2014 across the RBs were slight higher (in the range of 5.5 – ≥ 6) than the previous year. The pH values recorded at the reed beds downstream (RBs 10, 13 and 15), i.e. the phase 2 reed beds and where lateral seepage was observed, were slightly lower than the pH values recorded in the reed beds upstream (RBs 1, 4 and 7, i.e. phase 1 reed beds) in April, 2014, but the differences were less apparent in May, 2013.

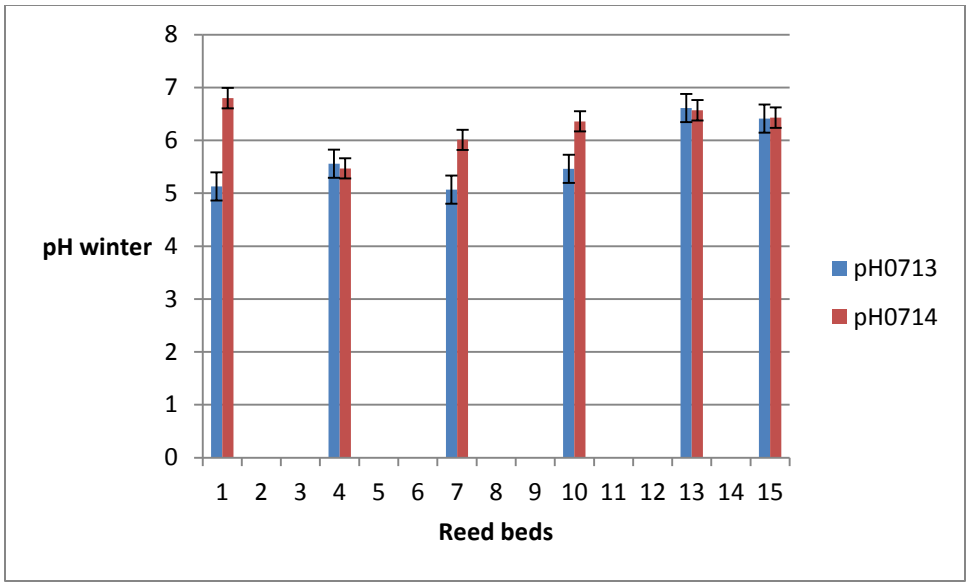

Figure 53: Bar chart (±SE) for pH in winter for July, 2013 and July, 2014

A seasonal difference (autumn versus winter) was observed in both years, i.e. between the pH in winter in 2013 and 2014 (Figure 53) and the pH in autumn in both survey years (Figure 52). The main difference between years is the presence of slightly higher pH values in many of the reed beds in 2014, relative to 2013.

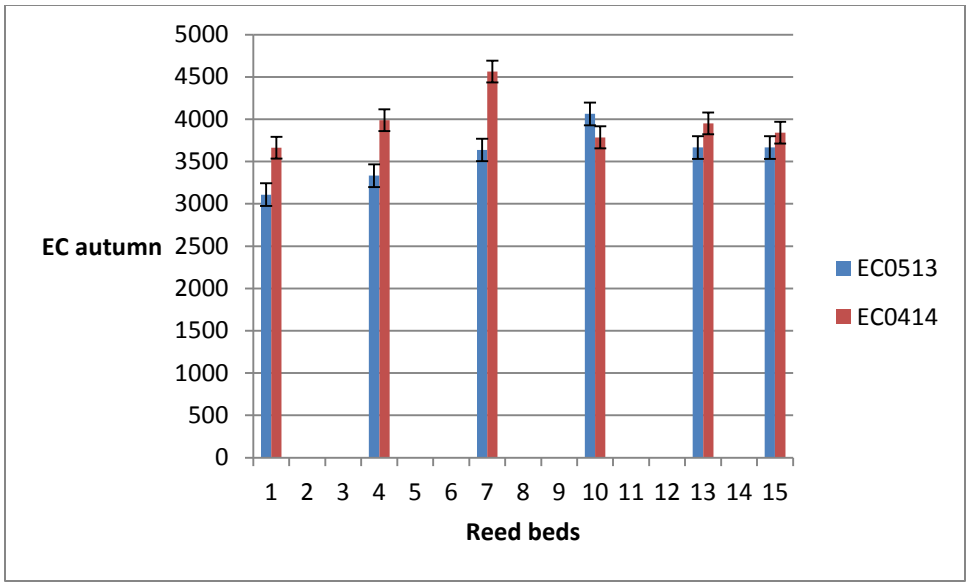

Figure 54: Bar chart (±SE) for EC in autumn for May, 2013 and April, 2014

Figure 54 shows that in April, 2014, RB 1 actually has lowest EC. The similarity trend observed was that, both years showed increases in EC towards central reed beds, which declines again in lower reed beds, whereas, the difference is that there was higher EC in most reed beds in 2014, relative to 2013.

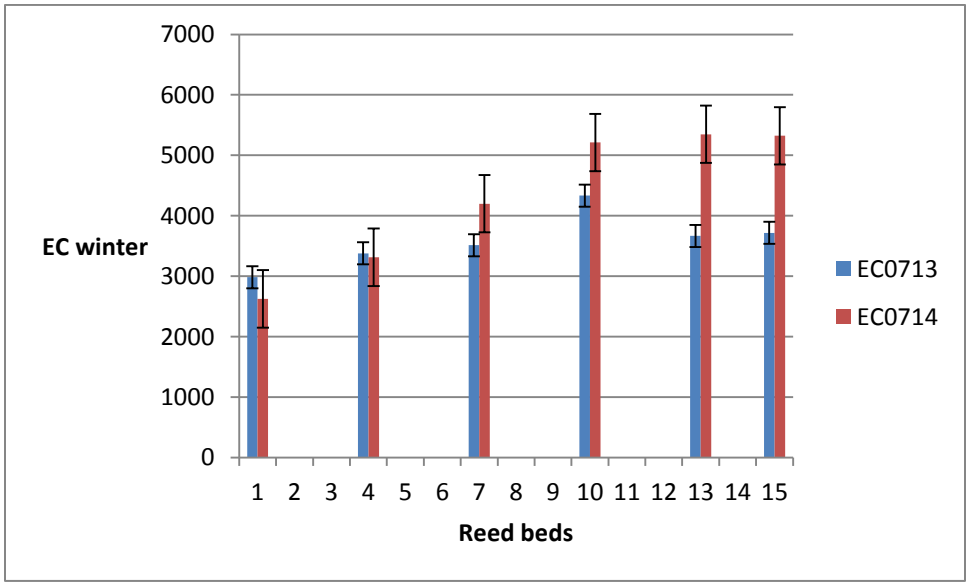

Figure 55: Bar chart (±SE) for EC in winter for July, 2013 and July, 2014

Figure 55 shows that in July, 2013, there was a progressive increase in EC across the upper-middle reed beds linearly (RBs 1 -10) and then decreased slightly at RBs 13 and 15, which is

similar to the trend observed in the autumn period of the same year (May, 2013) (Figure 54). A more distinct progressive increase in EC across all the reed beds, downstream, was observed in July, 2014, with the highest EC values (≥ 5000 µs/cm) were recorded in July, 2014 at the reed beds downstream (RBs 10, 13 and 15) where lateral seepage might be occurring. The main difference between years is the higher EC in the middle and especially downstream reed beds.

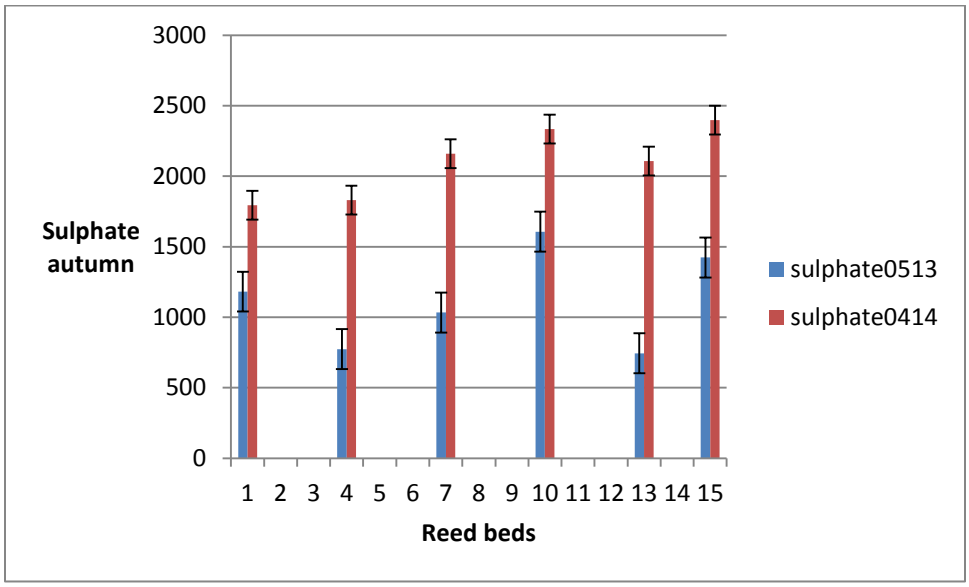

Figure 56: Bar chart (±SE) for sulphate in autumn for May, 2013 and April, 2014

Figure 56 shows no distinct pattern of increase/decrease in the sulphate concentrations across the reed beds in May, 2013 whereas, a more distinct pattern of a progressive increase in sulphate across the reed beds was observed in the autumn period of the following year (April, 2014). The main difference is that much higher sulphate concentrations were recorded in autumn of 2014 than in autumn of 2013, i.e. a year after.

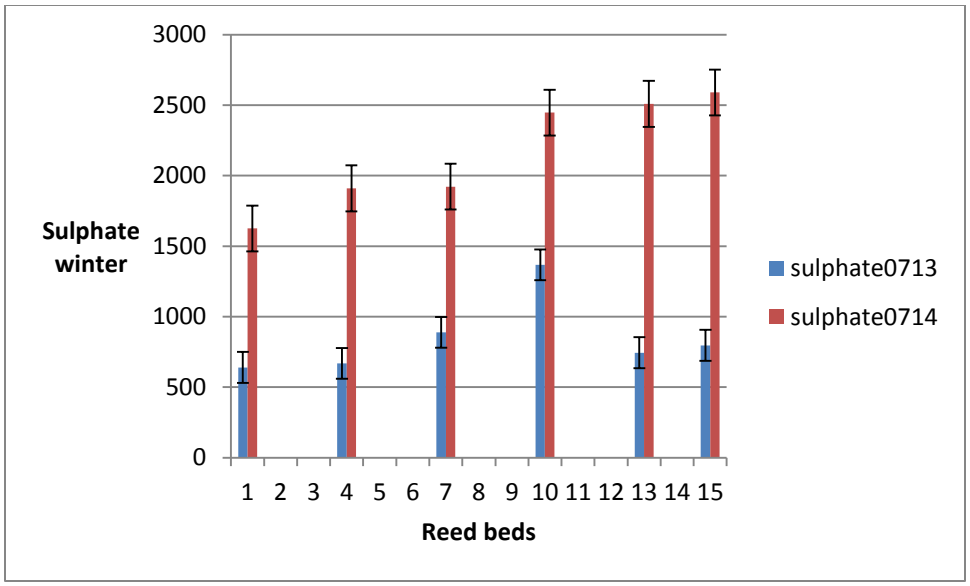

Figure 57: Bar chart (±SE) for sulphate in winter for July, 2013 and July, 2014

Figure 57 shows similar difference between years, in that, the sulphate concentrations of the water flowing across the reed beds in the winter of 2014, by far exceeded (doubled) the sulphate concentrations in the winter of 2013,

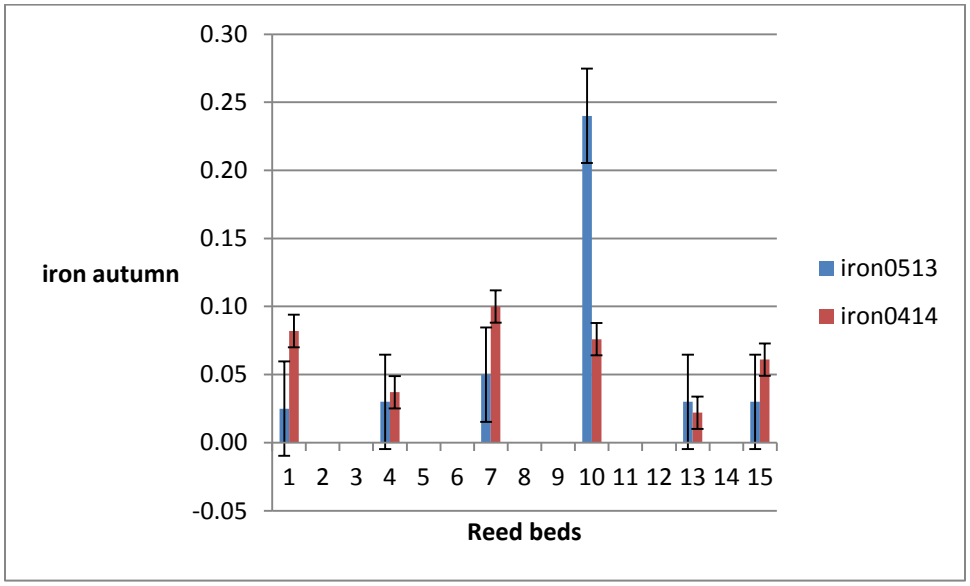

Figure 58: Bar chart (±SE) for iron in autumn for May, 2013 and April, 2014

Figure 58 shows that in autumn for both years (May, 2013 and also April, 2014), the iron levels were generally within acceptable limits, relative to the TWQR (0 - 0.1 mg/l) (DWAF, 1996) for

aquatic ecosystems, with the exception of RB 10, in May, 2013. The 2014 levels were otherwise generally higher than the iron levels in 2013.

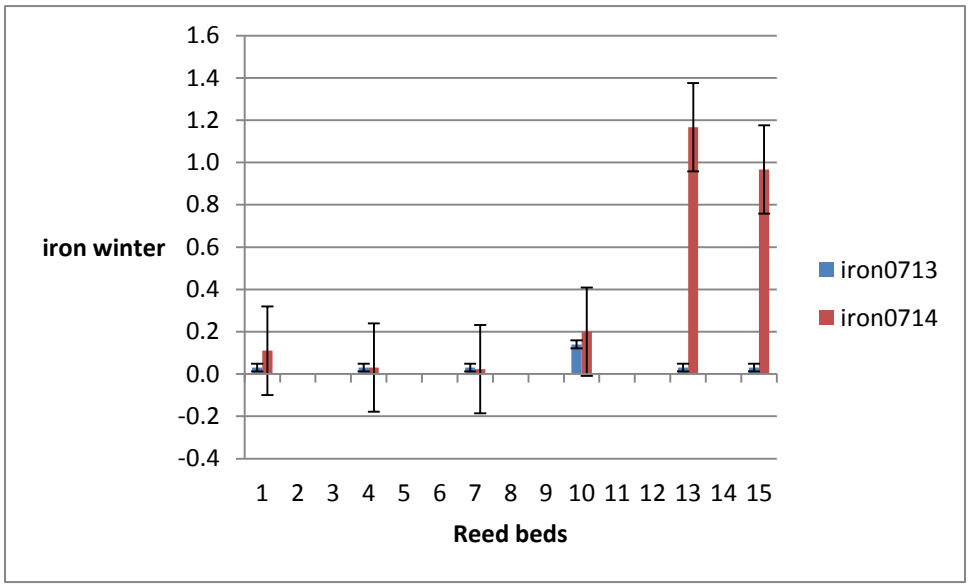

Figure 59: Bar chart (±SE) for iron in winter for July, 2013 and July, 2014

Figure 59 shows a drastic increase in the iron concentrations, in the three lower reed beds in winter 2014 (but not in 2013), exceeding the TWQR for aquatic ecosystems. The iron levels at the rest of the reed beds were still within acceptable limits in July, 2013 and July, 2014.

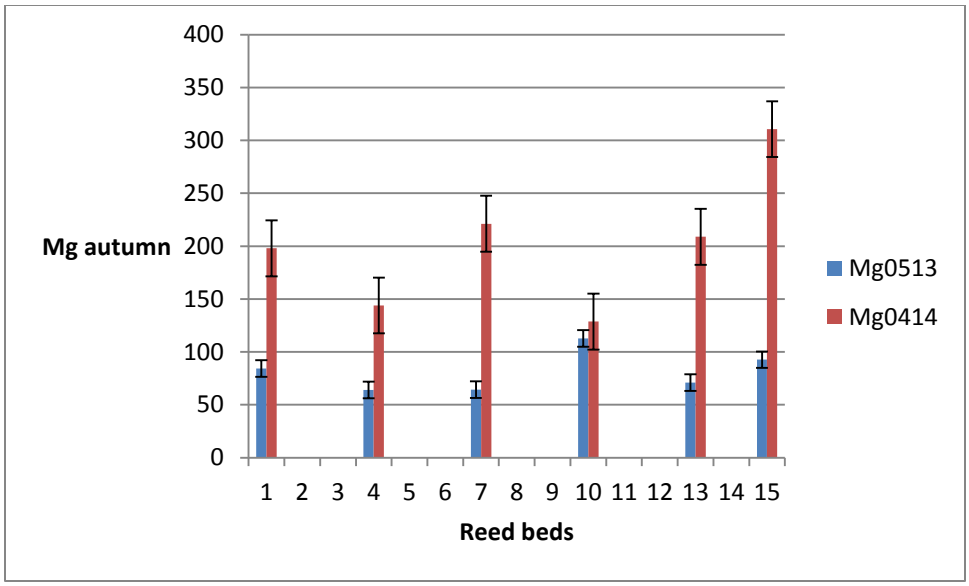

Figure 60: Bar chart (±SE) for magnesium in autumn for May, 2013 and April, 2014

Figure 60 shows that at each of the individual reed beds, the Mg concentrations in autumn, 2014 were much higher than the Mg concentrations in autumn, 2013, but with no clear spatial pattern in either year.

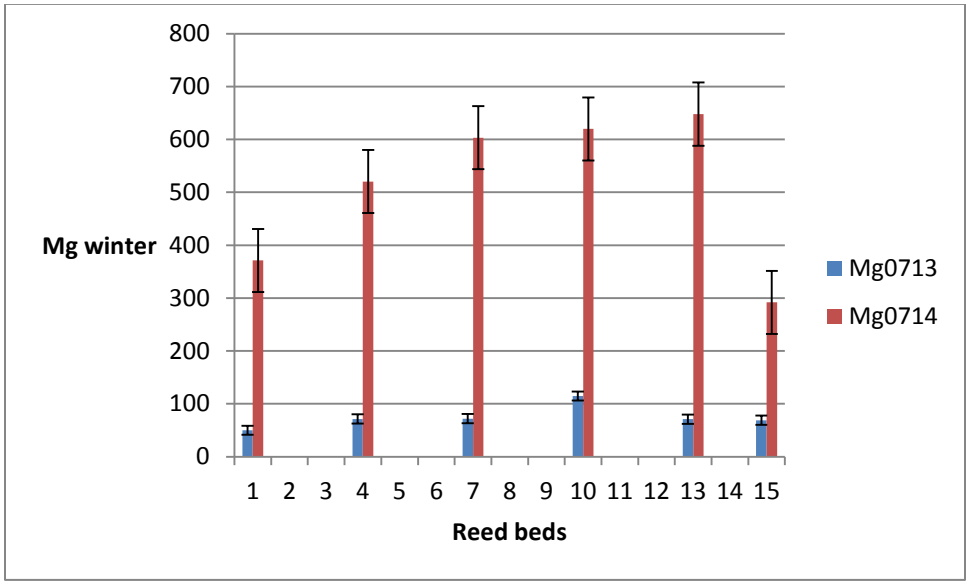

Figure 61: Bar chart (±SE) for magnesium in winter for July, 2013 and July, 2014

The concentrations of Mg recorded across the reed beds, during winter, 2014 were triple the Mg concentrations recorded across the reed beds in winter, 2013 (Figure 61). Both years showed higher Mg concentrations in the middle reed beds.

Chapter 5: Discussion

This chapter presents the discussion surrounding the key findings in this study. The patterns observed in the previous chapter have been explained and logical interpretations have been proffered.

5.1 Key findings

1. The research questions posited at the beginning of the study; i.e.
i). is there a spatial variation in the water quality parameters (pH, EC, Eh) and concentrations of ions and elements in solution across the reed beds? and is there a temporal variation (April versus July) in the water quality and contaminants storage (sediment) within the engineered reed beds?, have been answered, as the box plots and the statistical analyses performed e.g. the analysis of variance (ANOVA) and the Pearson correlation analysis showed some significant patterns in the water and sediment data in terms of the different reed beds, i.e. between reed beds at the upstream, middle and downstream sections of the system (spatial variation) and obvious changes in contaminant concentrations were observed from April to July (temporal variation between seasons).

2. The results from the study showed some evidence of a remediation pattern taking place, especially in the phase 1 reed beds. It can also be inferred from the results that the lateral influx of untreated AMD containing groundwater in the lower phase 2 reed beds noted in previous studies and observed here in the field is adversely affecting the overall performance of the reed beds system as an AMD remediation technique. However, an experimental design during future studies, set in such a way to accommodate analyses of the reed beds in terms of the phases in which they were constructed, would be extremely valuable to allow evaluation of the performance of the reed bed system as an AMD amelioration technique.

3. Principal component analyses, a multivariate technique that shows the variables contributing most to the variation in the complex datasets, in this case, from the two survey years, 2013 and 2014, were performed. The results obtained from the analyses of the inter-annual variations of the two survey years using PCAs showed that EC and sulphate were the most influential variables that were responsible for most of the information from the datasets e.g. Figure 45 (May, 2013), Figure 47 (July, 2013) and Figure 49a &b (April, 2014). The dataset from May, 2013 (Figure 45) showed that pH and these trace and major elements Mg, Mn and Zn (Figure 49a) were also sources of variation. The dataset from July, 2014 (Figure 51) showed that, sulphate, chloride and EC played great roles in terms of variability, with EC being the most responsible, as it has the highest positive loading value on component 1 (the component with the highest cumulative percentage of variation). The major and trace elements were also sources of variation, as Ca, Zn, Mg and K, all had moderate to strong positive loadings on the other axis, component 2 (Figure 51). This multivariate technique helped to further illustrate that EC and sulphate are key indicators of AMD contamination in water, in conjunction with trace and major elements, regardless of the sampling period/era. AMD contaminated effluents usually have characteristic high EC and high sulphate concentrations (Fadiran *et al*., 2014).

4. i) The PCAs performed on the data from the previous and present surveys (2013 and 2014) showed that the PCA for May, 2013 (Figure 45) illustrated that the variables with the highest loadings on the component with the highest cumulative percentage of variation (74.33 %, i.e. component 1) were EC, Mg and sulphate. They were responsible for most of the variation in the data from May, 2013 (autumn period in survey 1) (Figure 45), contrastingly, the PCA for April, 2014 showed that EC, chloride and ammonium had the strongest loadings on axis 1, while Mg and sulphate had weaker associations. These suggest that contaminants are largely associated with many factors.

ii) An evaporation/concentration signal was observed from the PCA for July, 2013, where most contaminants loaded more positively on the first principal component suggesting the strong influence of a common factor which increases all concentrations together (Figure 47). The trend could be related to the high incidence of evaporation rates that occur during winter, while in the PCA for July, 2014 (Figure 51), in comparison with July 2013 (Figure 47), many contaminants showed strong positive loadings along principal component 1, but some contaminants;

ammonium, Co, Ca showed negative loadings. This suggests that although evaporation and subsequent concentration of contaminants may explain elevated winter levels in both years, there might be some other processes at play.

5. The bar charts (Figures 52 – 61) helped to depict some major differences between and/or similarities in the survey years, 2013 and 2014. Some of these differences and/or similarities include: i) The slightly higher pH values in the autumn period of the second survey year, April, 2014 (Figure 52) suggests a decline in acidity over time; this may be an indication of the gradual effectiveness of the reed beds in sequestering contaminants from the effluent flowing across it and thereby improving the water quality leaving the reed bed system, as evident in the higher pH values recorded after a space of one year. The slight rise in pH at each of the respective reed beds (in comparison with the pH at those specific reed beds, in 2013) is one of the differences observed between the sampling years; ii) The pH values recorded at the reed beds downstream (RBs 10, 13 and 15), i.e. the phase 2 reed beds and where lateral seepage is also possibly occurring, were lower than the pH values recorded in the reed beds upstream (RBs 1, 4 and 7, i.e. phase 1 reed beds) during the autumn period in 2013 and also in 2014) (Figure 52). This is one similarity observed for the same season in the two survey years. The lower pH values in the phase 2 reed beds could be possibly due to the lateral seepage occurrence there; iii) Another similar pattern was observed in the same seasons in 2013 and 2014; where slightly lower winter pH values were recorded overall, across the reed beds in July, 2013 and also in July, 2014 (Figure 53), as against the slight higher pH values recorded across the reed beds in May, 2013 and April, 2014 (autumn/wet period) (Figure 52). This trend lends support to the hypothesis that the rate of evaporation exceeds the rate of dilution during extreme dry periods such as winter, thereby decreasing pH; iv) The EC values recorded at the reed beds downstream in the winter sampling period of 2014 (Figure 55) were the highest, exceeding the EC values recorded in the two sampling periods of 2013 (Figure 54). This EC trend over a space of one year might be evidence that the reed beds are accumulating more contaminants over time; v) another difference that was observed between the different years (for autumn), was that no distinct pattern in the sulphate concentrations across the reed beds was seen in May, 2013 (Figure 56), whereas, a distinct pattern of a progressive increase in sulphate across the reed beds was observed in the autumn period of the following year (April, 2014) (Figure 56), while higher sulphate concentrations were recorded in autumn of 2014 than in autumn of 2013. It was also similarly

observed that the sulphate concentrations across the reed beds, during winter, 2014, by far exceeded (doubled) the sulphate concentrations across the reed beds during winter, 2013 (Figure 57). This could be due to the fact that the one year gap allowed for the increased efficiency of the reed beds in accumulating contaminants. The magnesium concentrations at the different reed beds were higher in autumn, 2014 than in autumn, 2013 (Figure 60) and also higher in winter, 2014 than in winter, 2013 (Figure 61), which also supports the claim of a one-year improved efficiency of the reed beds and that more evaporation/less rain might have occurred in 2014 than in 2013.

5.1.1 Trends in the water data

The reed beds have been constructed to attenuate AMD on two aspects (the Northern and Western aspects) and they receive AMD. Hence it may not be expected to find linear changes moving downstream through the system. The pH was high and increased slightly through RBs 1, 4 and 7 in the water in April 2014 but then decreased drastically thereafter (Figure 8), possibly, as a result of lateral inflow. This may also suggest a gradual pattern of AMD attenuation in the older reed beds (RBs 1, 4 and 7). The pH in the water in April 2014 and the Eh in the water in April and July 2014 showed statistically significant differences between the reed beds ($P < 0.05$) (Tables 4 and 7). The Tukey multicomparison tests were performed for the pH (Table 5) and the Eh (Table 8) in the water in April. The multicomparison test (Table 5) showed that in terms of the pH in the water in April 2014, that RBs 13 and 15 are significantly different from the rest of the reed beds, having much lower pH. RBs 13 and 15 are situated furthest downstream in the reed bed system and are part of the phase 2 reed beds, which are still relatively new when compared with the reed beds upstream (phase 1 reed beds) i.e. RBs 1 and 4. In 2013, the pH values were also higher at RBs 1 and 4 than at the latter reed beds (Joubert, 2013). It was suggested in that study, that a gradual attenuation pattern was seemingly taking place at the phase 1 reed beds. The multicomparison test (Table 8) showed that in terms of the Eh in the water in April 2014, three significantly different groups of reed beds were identified. Each group was made up of a pair of reed beds, where within-group differences were not significant. These groups were; A (uppermost sites, RB1 and RB 4), B (furthest downstream sites, RB 13 and RB 15) and C (middle sites, RB 7 and RB 10), which are evident in the box plots for these samples

(Figure 12). The least oxidizing conditions were observed at the middle reed beds (RBs 7 and 10) (Figure 12), which also showed higher pH values than RBs 13 and 15 (Figure 8). The oxidizing condition increased drastically (high Eh; Figure 12) with lower pH (Figure 8) at the reed beds downstream (RBs 13 and 15). pH is usually inversely related to the Eh (Fadiran *et al*., 2014), which is in agreement with the inverse correlation between pH and Eh in the water in April (r = -0.4889) (Table 14).

Lateral seepage was observed during sampling. It was found to be occurring at the reed beds, furthest downstream (phase 2 reed beds) (Figure 5). This could be one of the possible reasons why pH decreased downstream. Another causative factor may be age. Phase 1 reed beds are already maturing and beginning to show gradual attenuation patterns whereas the phase 2 reed beds have not stabilized. Another possible reason why the pH of the water decreased downstream through the reed beds in April (almost end of wet season), could be due to the fact that secondary efflorescence minerals present in drainage channels have a significant influence on the chemistry of surface waters (Harris *et al*., 2003). This significant influence exists because acidity, metals and mineral efflorescence are generated and deposited along mine surface areas and drainage channels during dry periods (Demchak *et al*., 2004; Harris *et al*., 2003). During dry periods, dramatic evaporation occurs causing the formation of mineral efflorescence or encrustations along mine surfaces and drainage areas. This feature is more prominent in areas of seasonal or irregular rainfall, as in the current study area (Harris *et al*., 2003). Mineral efflorescence was observed along the Varkenslaagte drainage area as white encrustations. During the wet season, sulphide oxidation and mineral dissolution of some of the previously formed mineral encrustations or efflorescence (formed during dry periods) will generate AMD waters that enter local surface waters, drainage areas and aquifers, causing acidity and subsequently lowering the pH (Harris *et al*., 2003). Put in another way, the rainfall events dissolves some of the previously formed efflorescence, this results in the remobilization and transport of sulphate and metals downstream (pH decreases, acidity, metal and metal oxides' concentrations are increased downstream) (Harris *et al*., 2003; Demchak *et al*., 2004).

The remobilization of contaminants from previously accumulated metals in the sediment phase contributes to the contamination of the water column (Utete *et al*., 2013). The phenomenon of the remobilization and transport of metals and sulphate downstream during rainfall events i.e.

during the wet season (Harris *et al*., 2003; Demchak *et al*., 2004) could be used to explain the correlations observed in the physico-chemical and ionic parameters of water in April, 2014 (wet season) (Table 14 (upper section)). In the water in April, the pH decreased downstream along the reed beds (Figure 8). Following the remobilization and transport of metals and sulphate downstream and the subsequent decreasing pH, during the wet season, anionic contaminants (e.g. sulphate and chloride) and metals such as Mn and Mg will be remobilized and transported downstream (increasing the concentration of these contaminants downstream). This proffers an explanation as to why in Table 14, there was a positive correlation between sulphate and chloride in the water in April (r = 0.7528), as both anionic contaminants are expected to increase simultaneously with decreasing pH. Chloride is known for its conservative nature,

Also in Table 14, it was observed that the pH in the water in April was inversely correlated with Mn (r = -0.9120) and Mg (r = -0.6325), and there was also a positive correlation between Mn and Mg (r = 0.7594). One possible explanation is that at low pH, there is a greater concentration of hydrogen ions around the plant root (the reeds, in this case) which causes the roots to pump out protons in order to exchange with other mono and diatomic metal cations other than Mn^{2+} resulting in a strong inhibitory effect on the uptake of Mn ion by the plants (Linge, 2008; Carrillo-Gonzalez *et al*., 2006). When adsorption of Mn and other metal ions onto plant surfaces do not occur, these contaminants remain in solution, thus maintaining the concentration of the pollutants in the water column. The reed beds are in place to create evapotranspiration and filter out metals, and to contribute to chemical precipitation. Manganese and other metal contaminants are expected to be adsorbed on the surface of the rhizomes and root mass once the engineered reed beds have fully developed, over time.

For plants to take up metals, the metals have to be bio-accessible and/bioavailable to them, in the first place (Marques *et al*., 2009; Linge, 2008; Carrillo-Gonzalez et al., 2006). The other possible explanation for the inverse correlation between pH and Mn; is that most metals form insoluble hydroxide precipitates under basic conditions (Ritter *et al*., 2002; Nicholson *et al*., 1990) but as the pH decreases, the hydroxide precipitates increase in solubility and therefore dissolution of precipitates takes place. This leads to increasing concentrations of contaminants downstream through the reed beds. At low pH, metals and metal oxides will increase in solubility (Linge,

2008). Also, according to Saria *et al.* (2006), dissolution of metals from rocks and sediments occurs with decreasing pH.

In the water in July**,** 2014, pH was very high at RB 1 before decreasing drastically at RB 4, with a general increase in pH thereafter through the rest of the reed beds (Figure 9). This dry season pattern is almost the reverse of the pattern in pH in April (wet season). While an expected opposing pattern of pH and Eh in RB1 was observed in the water in July (Figure 9 and Figure 13), thereafter, both parameters then showed a similar increasing trend in lower reed beds. This pattern in the lower reed beds is counter-intuitive as Eh is expected to decrease with increasing pH. However, this could be due to the fact that Eh is variable and is also affected by many factors other than pH (Vance, 1996). The multicomparison test of the Eh in the water in July (Table 8) showed distinct groups, where within-group differences were not significant; A (RB 13; RB 15), B (RB 10; RB 15), AB (RB 15), C (RB 7) and D (RB 1; RB 4) i.e. RB 15 was not significantly different from RB 13 and it was not also significantly different from RB 10. RB 7 was significantly different from all the other reed beds. The EC values in the water in July were higher than the EC values in the water in April (Table 6) though this was not statistically significant ($P > 0.05$). The results show that in the water in July, the physico-chemical parameters (pH, EC and Eh), anionic contaminants (chloride and sulphate) and other metal elements like Mn and Mg all increased in the water down through the reed beds. This could be due to the fact that, at extreme dry periods like winter (July is mid-winter in South Africa), pyrite oxidation and dissolution ceases owing to the absence of rain events. Simultaneously, pH is increased and evaporation occurs, causing what is known as 'dramatic evaporation' thereby increasing contaminants downstream (Demchak *et al*., 2004; Harris *et al*., 2003; Sracek *et al*., 2010).

The pH increase downwards through the reed beds in the water in July (Figure 9) could be due to two possible reasons, one of which is the cessation of pyrite oxidation (and subsequent acid generation) at dry periods due to absence of rain. Alternatively, the increase in pH in the water in July could also be attributed to the fact that less effluent comes into the reed beds on the Varkenslaagte drainage during dry periods. But because of the dramatic evaporation that will occur at this extreme dry period, most contaminants are expected to present high concentrations in the water in July. This was observed, as EC, Eh, Mn, Fe, chloride and sulphate were all higher

in the water in July than in April. Although the concentrations of the contaminants were also high in April, the ranges of the concentrations were higher in the dry month of July.

In July, (Table 14 lower section) there were some positive correlations between; (i) pH and Mn (r = 0.5052), and (ii) Fe and Mn (r = 0.8181). These patterns can be related to the close association of pH and Mn in AMD contaminated waters (Johnson, 2003; Linge, 2008), while the removal of Mn from mine waters is largely dependent on the pH of the water amidst other factors (Younger et al., 2002; Linge, 2008). Manganese requires a very high pH for precipitation relative to iron and also the kinetics of Mn oxidation are much slower for precipitation (Morgan and Stumm, 1964). Manganese will be removed from AMD contaminated water at very high pH, only if iron is not present in the influent water, but where iron is present manganese will remain in solution (Johnson, 2003; Linge, 2008). Iron oxide will dissolve at both low pH and high pH causing iron to be present in a solution until a condition(s) brings about its precipitation or removal from solution (Linge, 2008). Current Mn removal systems fail with the presence of iron (Younger *et al*., 2002).

Table 14 (lower section) also shows that EC was positively correlated with many parameters in the water in July, 2014 e.g. EC and: Eh (r = 0.9607), Fe (r = 0.5942), Mn (r = 0.6140), chloride (r = 0.6002) and sulphate (r = 0.8226). This is evidence for evaporation occurrence in the water in July, a claim also supported by the PCAs and the bar charts of the two datasets. It was also observed from the correlations of the parameters in the water in July, 2014 (Table 14) that there were positive correlations between (i) K and Mg (r = 0.6473); (ii) Mn and sulphate (r = 0.5896); (iii) chloride and sulphate (r = 0.8642); and (iv) Fe and sulphate (r = 0.5757). From the results obtained in this study, it is inferred that strong correlations between contaminants suggest common sources, or that these contaminants are being released/ remobilized by common processes. Contaminant remobilization occurs when altered conditions e.g. pH and Eh create a gradient to drive remobilization (Linge, 2008). While contaminants increase in the water in April is possibly due to the occurrence of mineral dissolution and subsequent low pH, the contaminant increase in the water in July is possibly due to the occurrence of dramatic evaporation and subsequent high EC. Inverse correlations between seasons were observed for the pH and the Eh (Table 15), indicating opposing spatial patterns. The EC values in July were higher than the EC

values in April (Table 6) though the differences in the mean values were not statistically significant.

From the water sample results, it can be observed that most of the contaminants had their highest concentrations at RBs 13 and 15. EC values were also relatively high at RBs 13 and 15 in July (Figure 11). Overall, pH range in the water is moderately acidic and it is close to the TWQR (DWAF, 1996). The pH range in the water in 2014 is higher than the pH 3 – 6 range in the water in 2013 (Joubert, 2013) at similar reed beds and at similar seasons. This may be indicative of an ongoing though slow AMD attenuation pattern, although differences in rainfall/evaporation may also be a factor. In the same vein, the EC values recorded in the water samples in this study, although high, are not as high as the EC values (about 5000 ms/cm or 5 000 000 µs/cm) typical of AMD sites on the Witwatersrand gold fields (Makgae, 2012).

Sulphate was highest at RBs 13 and 15 in April (Figure 22) and July (Figure 23). Mg was high in the water in April at RBs 13 and 15 (Figure 26) and in July at RB 13 (Figure 27). Fe was high in the water in July at RBs 13 and 15 (Figure 29). Mn concentration was highest at RBs 13 and 15 in April (Figure 30) and July (Figure 31). Statistical analyses showed significant differences ($P < 0.05$) among the reed beds in terms of the pH in the water in April. The Tukey multicomparison test further showed that these differences lie at RBs 13 and 15 in terms of the pH in the water in April. A possible explanation for this is the lateral seepage entering at RBs 13 and 15 from the adjacent TSF. Lateral influx was visually observed during sampling 1 and 2, specifically around RBs 13 and 15 (as shown by the green arrow in Figure 5). Another possible reason might be that these reed beds (RBs 13 and 15) are the phase 2/ youngest reed beds, just under 9 months old as at the time of this study.

Generally, two patterns were common in the water data; (i) chloride, sulphate and Mn concentrations were high relative to target water quality ranges of DWAF (1996) and water quality guidelines of WHO (2004) in the water flowing across the reed beds in April and also in July. This can be observed from the box plots (Figures 20, 21, 22, 23, 30 and 31).

(ii) Several analytes showed positive correlations between seasons (Table 15), including Mn ($r=0.70$), chloride ($r = 0.45$), sulphate ($r = 0.48$).

The results obtained in this study show that, in the water, in spite of the engineered reed beds in place, for 1 to 2 years at the time of the study, the high concentrations of contaminants e.g. chloride, sulphate and metals (far above World Health Standards ((WHO), 2004) (Table 18) persisted, in both the wet and dry months.

5.1.2 Trends in the sediment data

Sediments often play an important role in maintaining water quality by removing contaminants from the water column through metal sequestration (Linge, 2008). Sequestration is the ability to form complex bonds with metal ions that allow these metal ions to remain firmly within the sediment matrix. However, subsequent contaminant remobilization from the sediment matrix can occur due to changes in soil pH and this can keep dissolved metal concentrations elevated in the water column long after the initial source has been removed (Linge, 2008).

The sediment sample results showed pH values similar to those found in the water samples, in both seasons and in both years (2013 and 2014) (Joubert, 2013) though the pH range in the sediment in 2014 was higher than that in 2013. It was observed from this study that the pH was marginally acidic and close to standards for 'normal' stream pH ranges (Table 19). They were not as low as the pH of typical AMD contaminated sites. The pH decreased across the reed beds from RBs 1 to 10 to 15 in April (Figure 14) and similarly, in July (Figure 15) hence the pH in the sediment in April was positively correlated with the pH in the sediment in July ($r = 0.75$) (Table 16). In spite of this similar pH-pattern, the pH values in the sediment profiles of the reed beds in April were lower than the pH values in July (Table 9). Changes in the soil Eh (from reducing to oxidizing conditions) were observed in the sediment profile down through the reed beds in both April and July (Figures 18 and 19). It is known that Eh values are useful in explaining metal mobility in both water and sediments. In spite of this, it has also been observed that Eh depends on other limnochemical species that fluctuate rapidly in lotic waters. Thus Eh alone might not adequately explain metal concentrations and toxicity (Utete *et al*., 2013). It was observed from the box plots that EC values in the sediment profile of the reed beds in April were higher than the EC values in the sediment in July (Figures 16 and 17) (Table 10). The highest EC value in the sediment profile of the reed beds was observed in April (Figure 16). This is an indication that there could more soluble substances in the sediment matrix.

A possible explanation for the reduced pH and higher EC values in the sediment in April (autumn/wet period) is the greater occurrence of mineral dissolution, soil erosion and runoff in the wet season which increase ions in solution in the sediment matrix through increased transport of contaminated/polluted water from TSFs and other sources into the Varkenslaagte stream i.e. onto the reed bed system. The rain events during the wet season cause mineral dissolution of previously adsorbed metals and the re-suspension of iron oxide and its co-precipitates, thereby increasing acidity (reduced pH) and metal concentrations in the sediment and these contaminants eventually enter back into water column (Carrillo-Gonzalez et al., 2006; Linge, 2008). Also, contaminants previously collected in senescing tissues of wetland plants during dry periods may be released back into the sediment matrix in autumn (Wuana and Okieimen, 2011). Soil erosion and surface water runoff during the wet season are some of the mechanisms that can mobilize trace elements into different environments (Carrillo-Gonzalez et al., 2006). Therefore, the combination of slightly reduced pH values and relatively high EC values (presence of soluble and dissolved particles) in the sediment in April can account for the greater concentrations of metals and metal oxides observed in the sediment in April i.e. Co (80 µg/g), Ni (100 µg/g), Cu (65 µg/g), Mg (630 µg/g), Mn (7500 µg/g) and Fe (7000 µg/g) (Figures 32, 34, 36, 38, 40 and 42). These high concentrations in the sediment profiles are expected as sediments act as sinks in wetlands, sequestering and retaining metal and metal-like contaminants in a bid to release cleaner water downstream. Trace elements like Co, Ni, Cu and Zn are associated with metal oxides in the sediment (Carrillo- Gonzalez *et al*., 2006; Linge, 2008), as both will simultaneously increase/decrease within the sediment matrix.

Hence, a host of significant strong positive correlations are observed in the inter-metallic associations e.g. between Co and Ni (r = 0.734), Co and Zn (r = 0.887), Ni and Cu (r = 0.846), Ni and Zn (r = 0.825), Cu and Zn (r = 0.722), Co and Mg (r = 0.853), Ni and Mg (r = 0.845), Cu and Mg (r = 0.761) and Zn and Mg (r = 0.977) (Table 16).

Inter-metallic correlation associations (as seen above) indicate that these elements travel in pathways through the aquatic ecosystem in a manner that is determined by other metals present (Iwegbu *et al*., 2007). Miller and Miller (2000) also state that positive correlations between metals show an association or interaction between the metals in a particular study area and these metals might have similar sources of input. A strong positive correlation between two metals

may be an occurrence of strong dependence of both metals on the same causal factor (Ashraf *et al*., 2012) or they may simply be part of the same mineral phase – e.g. metal sulphates.

Most significant inter-metallic associations in the sediments usually occur during the wet season (Utete *et al*., 2013), as observed from the correlation analysis of the parameters in the sediment in April (Table 15 (upper section). Heavy rainfall events during the wet season after long dry seasons are one of the causes for elevated metal concentrations (Carrillo-Gonzalez *et al*., 2006).

Generally, in the sediment data, these patterns were common;

(i) The pH decreased downstream in April (Figure 14) and also in July (Figure 15) with a positive seasonal correlation of r = 0.75 (Table 15).

(ii) It was observed from the surface sediment profiles that in as much as Ni, Co and Cu had increasing concentrations in both April and July, the concentrations were generally higher in April. The significant inverse correlations observed i.e. Co (r = -0.74), Ni (r = -0.62) and Zn (r = -0.71) (Table 17) could be driven by the changes in the middle reed bed (RB 10), where it was observed that the trace elements concentrations were lowest at RB 10 in April but highest at this same reed bed in July (Figures 32 – 35). The causal factors are unknown at this stage.

The need for measuring water depth, soil seepage, flow volume and rate in this study cannot be overemphasized. Very little flow between reed beds was observed in the 2014 survey. When the flow rate is slow, this slow water movement through soil columns will allow the elements affected by flow rate to be adsorbed onto soil surfaces thereby reducing their concentrations in the water phase. If the movement of water is fast, the adsorption onto soil surfaces of elements affected by flow rate e.g. Fe and Cu is prevented, thereby leaving these elements in high concentrations in the water phase. Hence when water flow increases, increased concentrations of Fe and Cu are still expected (Carrillo-Gonzalez et al., 2006). On the other hand, when the movement of water is fast, this fast flow rate does not affect the rate of adsorption (onto soil surfaces) of elements that flow rate has negligible effect on e.g. Zn, Cr and Mn. So in essence, while some ions are sensitive to flow rates, others are not. This could be due to selectivity coefficients which influence competitive sorption and cation exchange capacity between target cations (trace elements) and cations present in the flowing water (Carrillo-Gonzalez et al., 2006). Part of the system under review i.e. the sediment of the study site, has high clayey wetland soils,

and therefore impeded internal drainage. High clay and organic matter brings about a higher net negative charge –i.e. cation exchange capacity than a normal draining soil. The rate of flow of water also affects the extent of diffusion of trace elements into soil aggregates thus affecting the chances of adsorption of these elements onto soil surfaces (Carrillo-Gonzalez et al., 2006).

Although, EC values in the range of 3000 – 4000 µs/cm were observed in this study (Tables 25 and 26), they are relatively low when compared to the recorded EC values from AMD hotspots in the Witwatersrand gold fields. The effluent water quality of the Witwatersrand gold fields have been found to have a pH of about 3-4 (this is lower than the pH ranges observed in this study, in both water and sediment at both seasons), with EC of about 5000 ms/cm (i.e. 5 000 000 µs/cm), - this is 1000 times higher than the EC values observed in this study in both water and sediment at both seasons (Makgae, 2012).

The results obtained in this study suggest that metals previously stored/accumulated in the sediment may be remobilized from the sediment phase into the water phase by natural processes like rainfall and evaporation and man-made processes e.g. acid mine drainage, thereby posing a risk to the aquatic ecosystem as described by Carrillo-Gonzalez *et al*., (2006), Utete *et al*., (2013) and Linge (2008). Though most of the metal concentrations in the water in both April and July 2014 exceeded the target water quality ranges for aquatic ecosystems according to DWAF (1996) and WHO (2004) (Table 18), they are not as high as those typical of the Witbank coal fields and other AMD sites. The sediment data from this study show that metal retention in the sediment is occurring (this is key for AMD attenuation in the water column and downstream), and pH mitigation of AMD in the water (a pH range of 5.5 to 6.8 is within the normal TWQR or close to it; Table 19) is evident as well. Hence there is some evidence to conclude that the young engineered reed beds are effective, though not yet fully functional. More time, monitoring and studies on the study site are required to further elucidate the efficacy of the reed beds in retarding AMD. The wetlands and reed beds periodically burn on the Highveld, and the AMD impacted reed beds need to be assessed for the consequent loss of more volatile elements like N, S, Hg and Cr.

The high concentrations of contaminants recorded across the reed beds in the sediment can be attributed to the fact that reed beds are designed as containment and filtration systems. Since metals are expected to accumulate in the sediments and organic materials, if the reed beds are

working, then this should be reflected as lower concentrations of contaminants in the water flowing across the reed beds and out of the system (water exiting the property). However, if the water is not flowing and is also evaporating simultaneously, ultimately the pollutants will not be transported out of the reed beds. The reed beds are a retention and evapotranspiration system. *Phragmites australis* water-use is around 1400 mm on the Highveld gold mines (Dye et al., 2008).

Many metal-metal associations were observed from the correlation analysis performed in this study. Various metal pairs e.g. Mn and Mg, Co and Ni, Ni and Cu, Co and Zn, Zn and Mg associate in both water and sediment phases, especially in heavily contaminated sites (Carrillo-Gonzalez *et al*., 2006; Utete *et al*., 2013; Linge, 2008). The inter-metallic associations make the contamination at a particular site more obvious (Utete *et al*., 2013). The inter-metallic phases abound in heavily contaminated sites possibly because they have similar chemistry. These metallic associations in the water and sediment phases, influence metal bioavailability, mobility and toxicity and thus have potential long term deleterious implications on aquatic fauna (Carrillo-Gonzalez *et al*., 2006; Utete *et al*., 2013; Linge, 2008).

When choosing an AMD treatment option, an understanding of how the contaminants bind to the sediment and the conditions under which the contaminants will be released back into the water column is needed (Linge, 2008). Although, there are more powerful water-sediment extraction methods that could improve future results, this present study on the site has shown that the reed beds have retained contaminants and are on the gradual path of retarding AMD. Time and future monitoring are also important factors i.e. time will tell, if other AMD treatment options should be used in conjunction with the reed beds, to effectively and rapidly tackle the issue of AMD on the Varkenslaagte stream.

Chapter 6: Conclusions and Recommendations

This chapter presents the conclusions that can be drawn from this study. Recommendations for future studies on the study site are also given.

The objectives set at the beginning of the study were met, i.e.

i) To test the early performance of the 6- to 18-month old engineered reed beds in mitigating water acidity, sequestering contaminants in the sediment, and reducing contaminant transport downstream;

ii) To determine whether selected water quality parameters (pH, EC and salt and metal concentrations) leaving the AGA's mining facility are within relevant compliance limits; and

iii) To serve as a baseline post clean-up for periodic evaluation of the reed beds in containing AMD, so as to assist AGA in management decisions (e.g. when to harvest or desludge the reed beds if necessary) and determining whether the investment in wetlands for AMD treatment is cost-effective and justified in the long term.

However, during future studies, to ensure a better evaluation of the performance of the reed bed system and to better inform the management of the system; there is the need for improvements and adjustments of the current experimental design, sampling technique and statistical analyses. These have been put forward below, as recommendations for future studies.

6.1 Key conclusions

The spatial variations in the water quality through the reed beds were generally complex, possibly as a result of the simultaneous interplay of many factors e.g. evapotranspiration, rainfall, run off and lateral seepage. There is a possibility that these external factors may actually be outweighing the gradual attenuation pattern of the engineered reed beds, at the time of this study, because the systems were new (ranging from 6 months to 24 months of age, from bottom to top of the upper Varkenslaagte).

Differences in the survey years, 2013 and 2014 were observed by the patterns depicted in the PCAs (Figures 45 - 51) and in the bar charts for the survey years (Figures 52 – 61). The different

patterns observed in the survey years lent support to some hypotheses such as these: i) evapotranspiration exceeding dilution during dry periods; ii) an incidence or occurrence of lateral seepage at some reed beds will increase the concentrations of the contaminants at these reed beds; iii) time is key in a phytotechnology effort, as phase 1 reed beds performed better, in the role of taking up contaminants from the effluent by the sequestering and subsequent accumulation of contaminants at these reed beds and iv) pH, EC, sulphate, Mg and Fe are key indicators of AMD in this system.

The pH values of the water in April and July were similar and were in the range of 5.0 – 6.6. This pH range, though acidic, is not as low as values typical of AMD waters. The water in July showed elevated concentrations of anionic contaminants e.g. chloride and sulphate and most metal elements e.g. Mg, Mn, K and Fe, relative to the April samples. The water in July also presented higher EC values than in April. This could be attributed to the lack of rain during winter which results in lower inflows to the system, and higher concentrations due to evapotranspiration. On the South African High veld, April is the autumn period, and though this period is close to the start of dry season, rain fall still occurs sometimes. On the other hand, July is mid-winter and mid-dry season when rainfall is not expected. In dry periods, when evaporation is higher, moisture content is drastically reduced, resulting in a lower out-flow, and retaining a more concentrated medium (Sracek *et al*., 2010). The EC values were moderately high in the water in both April and July, although, July presented higher EC values, most likely as a result of lower inflows and higher evaporation from the stream. The consistent increases in EC observed at the lowest (furthest downstream) reed beds (RBs 13 and 15) have been suggested in this study as an occurrence due to a combination of evaporative processes and lateral inputs from the New North Complex TSFs parallel to the stream in this area, as this was visually observed during sampling and the younger age of these reed beds, as they were implemented from top to bottom of the site over a 2-year period. However, the relative importance of evaporative processes and lateral inputs in increasing the concentration of salts could not be quantified in this study. Quantification would require collection of the inflow along a broad front of the stream bank, and measurement of volume and seepage rates. The total flow rates have been measured at the upper and lower weirs since 2006, but by 2014 the surface flows were too low to be measurable. Therefore different instrumentation needs to be considered for accurate determination of the site water balance moving forward post-cleanup (I. Weiersbye, Personal Communication).

The pH range in the sediment in both April and July was also in the range of 5.0 – 6.7, i.e. very similar to the waters. There were elevated concentrations of Co, Ni, copper, Mn, Mg and Fe in the sediment of the reed beds in both April and July, indicating that the reed beds are successful in acting to precipitate, retain and concentrate these metals and minerals. There is the combined role of oxygen, water, sulphur oxidising bacteria and sulphate reducing bacteria in anaerobic wetland sediments. Reed bed phytoremediation involves not only reeds, but mainly a function of the population of algae, micro-organisms, decaying organic matter and clays in the superficial sediments.

Despite the AMD treatment option (engineered reed beds) in place, it was observed from the results, that in the water in April and July, the concentrations of chloride, sulphate, Mg, Mn, K (in July) and Fe (in July) were still above the target water quality range for aquatic ecosystems as set by DWAF (1996). Furthermore, a decreasing trend in overall water contaminant concentrations down through the entire reed beds is not evident, this may be due to a combination (i) of there being two catenal influences and sources of AMD (with AMD seeping from both the Northern TSFs down the canal, and seeping into the lower part of the stream from the Western TSFs parallel), and (ii) to the progressively younger age of the reed beds with distance downstream. In contrast, the high concentrations of Ni, Cu, Co, Zn and metal oxides retained in the sediment of the reed beds in both April and July demonstrate that the reed beds are effective in the precipitation and removal of some metals.

It was concluded in the previous study (immediately after the reed beds had been planted) (Joubert, 2013), that the patterns of attenuation (showing decreasing contaminants down the reed beds system) may never be developed, due to these large sources of AMD, the Old and New North Complexes TSFs, entering the reed beds system (Joubert, 2013). It was also recommended in that study, that there was the need for future monitoring on the site to further investigate the seasonal differences, if any, in terms of the contaminant concentrations and to fully ascertain the effects of evaporation, rainfall and lateral inputs occurring on the study site.

However, the pH of the water, 5.17 to 6.51 in April and the slightly higher values of pH 5.45 to 6.82 in July suggest that the pH of AMD is being strongly ameliorated by the reed beds. The

water quality is almost at, or within the TWQR for pH and Eh. Also, it was observed that metals have been retained in the sediments. All these indicate there is gradual AMD amelioration taking place on the engineered reed beds in the Varkenslaagte stream. Probably, as time elapses, with continual assessment, conspicuous and better attenuation patterns by the reed beds may be observed, as the process of phytoremediation is continuous and not finite.

6.2 Key lessons from this study and recommendations for future studies

1) The flow of contaminated ground water into the phase 2 reed beds can be controlled by the addition of extra reed beds in the best possible locations to check the influx of the lateral seepage.

2) The need for further phases of reed beds to control the underground flow of contaminated water in the phase 2 lower Varkenslaagte may involve the use of investigative methods to map the groundwater flow and better inform the current geo-hydrological and hydro-logical-mass balance models, including estimates of evapotranspiration and losses to groundwater.

3) Flow measurements (subsurface if there are inadequate surface flows) into and out of the reed beds, laterally and downstream, in addition to water sampling could be performed. Continued measurement of the flow volumes in the Varkenslaagte will be required to fully quantify the role of the reed beds in enhancing evapotranspiration and filtration or precipitation processes. Evapotranspiration measurements have determined that *Phragmites* (reed beds) growing on AMD in the Highveld (Dye *et al*., 2008; WRC report by Dye, Jarmain et al- cited in Dye *et al*., 2008). Future studies including evapotranspiration measurements, will allow this to be determined specifically for the Varkenslaagte.

4) The residence time of AMD within the reed beds is another critical factor that should be taken into consideration during future studies, if measureable flows are present, because an increase in residence time (e.g. slower flows) can be expected to result in an increase in metal complexation and mineral precipitation in biomass and sediments. Complexation, precipitation, evapotranspiration, mineral dissolution, sedimentation, water residence time, pooling and flow

velocity variations must be taken into account, in addition to rainfall regime and AMD neutralization technique (Lemière, 2010). Fast and turbulent flow regimes promote oxygenation and exchanges with the sediment (Lemière, 2010) whereas slow and non-turbulent regimes (as is the case on the study site) promote anaerobic conditions, sulphate reduction and metal immobilization within the sediment (Lemière, 2010).

5) Parallel studies have, or are being conducted, which used sequential chemical extraction steps to determine the mobility of metals in the reed beds (Lusilao, 2012) and infer bioavailability of sediment-bound contaminants to the plants. Laboratory examination of the plants' roots and shoots is being conducted to ascertain if metals are taken up or accumulated (S. Mthombeni, MSc in progress).

6) A future sampling technique may involve multiple samplings to improve the statistical evaluation of the performance of the reed beds, for instance, a future sampling campaign of hourly sampling over say, 2-3 days each season, is recommended. This will help to verify whether the contaminants in the water enter the reed bed system at a constant concentration or in pulses.

6.3 Limitations of the present study

1) Time/duration is a limiting factor in this study, considering the fact that the full benefits of a phytoremediation intervention cannot be viewed over a short period. The reed beds may take some years to establish and with less than 2 years since planting, they are not yet fully established on the study site. The system is still establishing and developing biomass for evapotranspiration and organic layers for complexation. This present study in 2014 is a second monitoring period on a young developing system, as time goes on, the catchment trees will grow up, the reed beds will develop organic layers, and the monitoring of water and sediment quality can then be conducted at timed periods. A longer time is required when using evapotranspiration and aquatic plants to control flow, pH and AMD-borne contaminants, as the technology is dependent on plant growth rates, i.e. for the establishment of an extensive root mat system,

micro-organism populations in sediment, algal mats or significant above-ground biomass (Pivetz, 2001).

2) Sampling during the winter and summer periods is done to determine the performance of the remediation system at the driest and wettest time of year, when above-ground green biomass and plant transpiration is lowest. However, it is important to note that, the remediation agent, which is the reed plant, could die off or lose effectiveness during extreme dry periods, like winter, due to harshness or severity of the weather (Pivetz, 2001).

In summary, the PCA analyses performed in this study showed that EC and sulphate were the variables responsible for most of the variation in the data from both survey years. The results from the other statistical analyses performed in this study have also confirmed that EC, sulphate, Mg and Fe are key indicators of AMD; and that wetland development is a gradual mode of remediation and, as such, some length of time (years) is needed for the attenuation capability of engineered reed beds to be fully established. Even though concentrations increased down through the reed bed systems, the flow of water may have decreased or stopped, so that there was little transport of these contaminants further downstream.

Hence future studies would be needed to quantify AMD inflow and outflow concentrations and volumes, including subsurface, to calculate transport fluxes. Additional AMD remediation efforts on the site need to simultaneously address the occurrence of lateral inputs from the western TSFs to the Varkenslaagte, in the region of reed beds 13 and 15.

References

AGA. (2009). *AngloGold Ashanti (AGA) Environmental Management Programme.* Retrieved April 3, 2015, from AGA West Wits Operations: http://www.anglogold.co.za/subwebs/InformationForInvestors/ReportToSociety04/values_bus_principles/Environment/e_cs_sa_7_11.htm

AGA. (2013, April). *Environment.* Retrieved November 17, 2014, from AngloGold Ashanti: http://www.aga-reports.com/13/os

AGA. (2015, February). *Quarterly Water Quality Report.* Retrieved September 29, 2015, from AngloGoldAshanti:http://www.anglogoldashanti.com/en/Media/Reports/Quarterly%20Reports/Q12015Results.pdf

Akcil, A., Koldas, S. (2006). Acid Mine Drainage(AMD): causes, treatment and case studies. *Journal of Cleaner Production*, 14, 1139 - 1145.

Ashraf, M.A., Maah, M.J., Yussof, I. (2012). Chemical speciation and potential mobility of heavy metals in the soil of a former tin mining catchment. *The Scientific World Journal*, 1, 1-11.

Barton-Bridge. J.P, Robertson, A.M. (1989). Design and reclamation of mine waste facilities to control acid mine drainage. Presentation at the Canadian Land Reclamation Association and the American Society for Surface Mining and Reclamation, Calgary.

Battaglia, M., Hose, G.C., Turak, E., Warden, B. (2005). Depauperate macroinvertebrates in a mine affected stream: clean water may be the key to recovery. *Environmental Pollution*, 138, 132-141.

Bell, F.G., Donnelly, L.J. (2006). *Mining and its Impact on the Environment.* Taylor & Francis, London.

Berger, A.C., Bethke, C.M., Krumhansi,J.L. (2000). A process model of natural attenuation in drainage from a historic mining district. *Applied Geochemistry*, 15, 655-666.

Carrillo-Gonzalez, R., Simunek, J., Sauve, S., Adriano, D. (2006). Mechanisms and Pathways of Trace Elements Mobility in Soils. In *Advances in Agronomy* (pp. 91, 111-178). Sparks, D.L (Editor): San Diego Academic Publishers.

Chadwick, J.W., Canton, S.P., Dent, R.L. (1986). Recovery of benthic invertebrate communities in Silver Bow Creek, Montana, following improved metal mine wastewater treatment. *Water, Air and Soil Pollution*, 28, 427-438.

Chapman, P.J., Kay, P., Mitchell, G., Pitts, C. (2013). Surface Water Quality. In J. Holden, *Water Resources: An Integrated Approach* (pp. 79-122). Routledge, Taylor and Francis Group, London and Newyork.

Coetzee, H. (2004). *An assessment of sources, pathways, mechanisms and risks of current and potential future pollution of water and sediments in gold-mining areas of the Wonderfonteinspruit catchment.* Council for Geosciences: A Report for Water Research Commission, Pretoria.

Concas, A., Ardau, C., Cristini, A., Zuddas,P., CaO. G. (2006). Mobility of heavy metals from tailings to stream water in a mining activity contaminated site. *Chemosphere*, 63, 244-253.

Coulton, R., Bullen, C., Hallet, C. (2003). The design and optimization of active mine water treatment plants. *Land, Contamination and Reclamation*, 11, 273-279.

Cravotta III, C. (2008). Dissolved metals and associated constituents in the abandoned coal mine discharges. *Applied Geochemistry*, 23, 203-226. Pennslyvannia, USA.

CSIR. (2009). *Council for Scientific and Industrial Research (CSIR): Acid mine drainage in South Africa, briefing note 02/2009.* CSIR Natural Resources and the Environment, Pretoria, South Africa.

Dallas, H.F., Day, J.A. (1994). *The effect of water quality variables on riverine biotas.* Water Research Commission (WRC) Report, WRC, Pretoria.

Dancey, C., Reidy, J. (2004). Statistics without Maths for Psychology: using SPSS for Windows, London: Prentice Hall.

De Waard, K. C. (2012). *Waste discharge charge system: The practical implication from a gold mining perspective.* Mini dissertation report, Potchefstroom Campus, North West University.

Diamond, J.M., Bower, W., Gruber, D. (1993). Use of man-made impoundment in mitigating acid mine drainage in the North Branch Potomac River. *Environmental Management*, 17, 225-238.

Demchak, J., Skousen, J., McDonald, L.M. . (2004). Longevity of acid discharges from underground mines located above the regional water table. *Journal of Environmental Quality*, 33, 656-668.

Downing, B.W., Gravel, J., Mills, C. (1998). *Trace Element Geochemistry in Acid Rock Drainage.* Retrieved October 30, 2014, from Trace Element Geochemistry: http://technology.infomine.com/enviromine/ard/introduction/trace.htm

Durand, J. (2012). The impact of gold mining on the Witwatersrand on the rivers and karst system of Gauteng and North West Province, South Africa. *Journal of African Earth Sciences*, 68, 24-43.

DWAF. (1996).The *South African Water Quality Guidelines (2nd edition). Volume 7: Aquatic Ecosystems*. Department of Water Affairs and Forestry (DWAF), Pretoria.Retrieved November 15, 2014, from South African Water Quality Guidelines: http://www.dwaf.gov.za/IWQS/aquaticecosystems.pdf

Dye, P.J., Jarmain, C., Oageng, B., Xaba, J., Weiersbye, I.M. (2008). The potential of woodlands and reed beds for control of acid mine drainage in the Witwatersrand gold fields, South Africa. *Mine Closure 2008, Johannesburg, South Africa*, (pp. 487 - 489). Fourie, A.B., Tibbett, M., Weiersbye, I.M., Dye, P.J. (editors).

Dye, P., Weierbye, I. (2013). *Summary on water management and monitoring in the upper catchment of the Varkenslaagte stream, within the West Wits mining operations of AngloGold Ashanti Ltd.* Ecological Engineering and Phytotechnology Programme, University of the Witwatersrand, Johannesburg.

Environment. (2014, November 13). Retrieved from Anglo Gold Ashanti: http://www.anglogoldashanti.com/en/sustainability/Pages/Environment.aspx

Evangelou, V. (1995). *Pyrite Oxidation and its Control.* Florida: CRC Press, Inc.

Evangelou, V. (1998). Pyrite Chemistry: the key for abatement of acid mine drainage. In *Acidic Mining Lakes: Acid Mine Drainage, Limnology and Reclamation* (pp. 197-222). Geller, A., Klapper,H., Salomons, W. (Editors), Berlin, Springer.

Fadiran, A.O., Dlamini, C.L., Thwala, J.M. (2014). Environmental assessment of acid mine drainage pollution on surface water bodies around Ngwenya mine, Swaziland. *Journal of Environmental Protection*, 5, 164-173.

Fennessy, M. S., Mitsch, W.J. (1989). Design and use of wetlands for renovation of drainage from coal mines. In *Ecological Engineering: An Introduction to Ecotechnology* (pp. 231-254). John Wiley & Sons, New York, Mitsch.W.J. and Jorgensen S.E. (Editors).

Ferreira da Silva, E., Almeida, S.F., Nunes, M.L., Luis, A., Borg, F., Hedlund, M., Patinha, E., Teixeira, P. (2009). Heavy metal pollution downstream the abandoned Coval da Mo nine, Portugal and associated effects on epilethic diatom communities. *Science of the Total Environment*, 407, 5620-5636.

Galpin, J.S., Krommenhoek, R.E. (2014). *Course notes for Statistical research design and analysis.* School of Statistics and Actuarial science, University of the Witwatersrand, Johannesburg.

Gray, L.J., Ward, J.V. (1983). Leaf litter breakdown in streams receiving treated and untreated metal mine drainage. *Environment International*, 9, 135-138.

Harris, D.L., Lottermoser, B.G., Duchesne, J. (2003). Ephemeral acid mine drainage at the Montalbion silver mine, north Queensland. *Australian Journal of Earth Sciences*, 50, 797-809.

He, M., Wang, Z., Tang, H. (1997). Spatial and temporal patterns of acidity and heavy metals in predicting the potential for the ecological impact on the Le An river polluted by acid mine drainage. *The Science of the Total Environment*, 206, 67-77.

Horowitz, A. (1991). *A Primer on sediment – trace element Chemistry.* 136pp. Chelsea, Lewis Publishers.

Hounslow, A. W. (1995). *Water Quality Data: Analysis and Interpretation.* Boca Raton, FL, CRC Lewis.

Hutter, J. (2011). *Performance characteristics of analytical tests.* Intersol, 6-9: AL Control Laboratories.

Iwegbu, C.M., Nwajei, G.E., Isirimah, N.O. (2007). Characteristic levels of heavy metals in sediments and dredged sediments of a municipal creek in Nigeria. *Environmentalist*, 26, 139-141.

Johnson, K. (2003). Enhanced in situ bioremediation techniques for Mn removal from mine waters. *Contaminated Land: Applications in Real Environments (CL: AIRE) Research Bulletin*, pp. 1, 1-4.

Johnson, D.B., Hallberg, K.B. (2005). Acid mine drainage remediation options: a review. *Science of the Total Environment*, 338, 3-14.

Johnston, D., Potter, H., Jones, C., Rolley, S., Watson, I., Pritchard, J. (2008). *Abandoned mines and the water Environment.* Environment Agency, Bristol.

Joubert, M. (2013). *The transport of acid mine drainage contaminants through remediation reed beds in the Varkenslaagte stream: a baseline study.* Honours Project Report, Faculty of Science, University of the Witwatersrand, Johannesburg.

Jung, M., Ahn, J., Chon., H. (2001). Environmental contamination and sequential extraction of trace elements from mine wastes around various metalliferous mines in Korea. *Geosystem Engineering, 4*, 50 – 60.

Kalin, M. (2004). Passive mine water treatment: the correct approach? *Ecological Engineering*, 22, 299-304.

Karbassi, A.R, Nabi-Bidhendi, G.H, Bayati, I. (2005). Environmental geochemistry of heavy metals in a sediment core off Bushehr, Persian Gulf. *Environmental Health Science and Engineering*, 2: 255-260.

Kelly, M. (1988). *Mining and the freshwater Environment.* Elsevier Applied Science, (pp.231) , London.

Kimball, Briant A. (1994). Coupling of hydrologic transport and chemical reactions in a stream affected by acid mine drainage. *Environmental Science Technology*, 28, 2065-2073.

Kleinmann, R. (1985). Control of Acid Mine Drainage: Treatment of acid mine water by wetlands. *Proceedings of a technology transfer seminar.* (pp. 48-52). US Dept. of Interior, Bureau of Mines #9027. Kleinmann, R.L.P (Editor).

Kleinmann, R.L.P., Crerar, D.A., Pacelli, R.R. (1981). Biogeochemistry of acid mine drainage and a method to control acid formation. *Mining Engineering*, 33, 300-305.

Kleinmann, R.L.P., Hedin, R.S., Nairn, R.W. (1998). Treatment of mine drainage by anoxic limestone drains and constructed wetlands . In *Acidic Mining Lakes: Acid Mine Drainage, Limnology and Reclamation* (pp. 303-319). Geller, A., Klapper, H., Salomons, W. (Editors), Springer, Berlin.

Koryak, M., Reilly, R.J. (1984). Vascular riffle flora of Appalachian streams: the ecology and effects of acid mine drainage on Justicia americana (L.) Vahl. *Proceedings of the Pennslyvannia Academy of Science*, 58, 55-60.

Laine, D.M., Dudeney, A.W. (2000). Bull house mine water project. *Transactions of the Institution of Mining and Metallurgy*, 109, 224-227.

Lampkin, A.J. III., Sommerfield, M.R. (1982). Algal distribution in a small, intermittent stream receiving acid mine drainage. *Journal of Phycology*, 18, 196-199.

Larsen, D., Mann, R. (2005). Origin of high Mn concentrations in coal mine drainage, eastern Tennessee. *Journal of Geochemical Exploration*, 86, 143-163.

Lasat, M. (2002). Phytoextraction of toxic metals: a review of biological mechanisms. *Journal of Environmental Quality*, 31, 109-210.

Legislation. (Act 108 of 1996). *Constitution of the Republic of South Africa* .

Lemière, B. (2010). Neutralisation distance of acid drainage and migration range of pollutants. In *Mine Water and Innovative Thinking* (pp. 371-374). Wolkersdorfer and Freund (Editors), Sydney, NS.

Letterman, R.D., Mitsch, W.J. (1978). Impact of mine drainage on a mountain stream in Pennslyvannia. *Environmental Pollution*, 17, 53-73.

Li, M.G., Aube, B.C, St-Arnaud.L.C. (1997). Considerations in the use of shallow water covers for decommissioning reactive tailings. *Proceedings of the Fourth International Conference on Acid Rock Drainage, Volume 1*, (pp. 115-130). Vancouver, BC.

Linge, K. (2008). Methods for investigating trace element binding in sediments. *Environmental Science and Technology*, 38, 165-196.

Liu, C.W., Lin, K.H., Kuo, Y.M. (2003). Application of factor analysis in the assessment of groundwater quality in a Blackfoot disease area in Taiwan. *Science of the Total Environment*, 313, 77-89.

Lusilao Julien, G. (2012). *Characterization and modelling of mercury speciation in industrially polluted areas due to energy production and mineral processing in South Africa.* PhD thesis, Environmental and Analytical Chemistry Group, School of Chemistry, Faculty of Science, University of Witwatersrand, Johannesburg, South Africa.

Makgae, M. (2012). The status and implications of AMD legacy facing South Africa. *International Minewater Association, Annual Conference, 2012*, (pp. 327-334). Council for Geoscience, Environmental Geoscience Unit, Pretoria. McCullough, Lund and Wyse (Editors).

Marques, A.P., Rangel, A.O., Castro, P.M. (2009). Remediation of heavy metal contaminated soils: phytoremediation as a potentially promising clean-up technology. *Environmental Science and Technology*, 39, 622-654.

Mayes, W.M., Batty, L.C., Younger, P.L., Jarvis, A.P., Koiv, M., Vohla, C., Mander, U. (2009). Wetland treatment at extremes of pH. *Science of the Total Environment*, 407, 3944-3957.

McCarthy, T. (2011). The impact of acid mine drainage in South Africa. *South African Journal of Science*, 107(5/6), 1-7.

Mehling, P.E., Day, S.J., Sexsmith, K.S. (1997). Blending and layering waste rock to delay, mitigate or prevent acid generation: a case review study. *Proceedings of the Fourth International Conference on Acid Rock Drainage, Volume 2*, (pp. 953-970). Vancouver, BC.

Metesh, J.J., Jarrell, T., Oravetz, S. (1998.). Treating Acid Mine Drainage from abandoned mines in remote areas. *Tech. Rep.*, 9871-2821-MTDC. Missoula, MT: United States.

Miller, J.N., Miller, J.C. (2000). *Statistics in the Chemometrics for Analytical Chemistry, fourth edition.* Miller, J.N. (Editor), Pearson Education Limited, Harlow, England.

Miller, R. (1996). Phtyoremediation technology overview report. *Groundwater Remediation Technologies Analysis Centre, Series O, Vol.3*.

Morgan, J.J., Stumm, W. (1964). Colloid-chemical properties of Mn dioxide. *Journal of Colloid Science*, 19, 347-359.

Morrison, R. (2004). *Environmental information systems: a challenge to meet corporate Environmental strategy in the South Africa mining industry, MSc Thesis.* Retrieved October 22, 2014, from Department of Geography, Environmental Management & Energy Studies (ETDs), University of Johannesburg, South Africa, UJDigispace: https://ujdigispace.uj.ac.za/handle/10210/2032.

Mucina, L., Rutherford, M.C. (2006). *The vegetation of South Africa, Lesotho and Swaziland.* Strelitzia 19. Tien Wah Press (PTE) Limited, Singapore.

Naicker, K., Cukrowska, E., MvCarthy, T.S. (2003). Acid mine drainage arising from gold mining activity in Johannesburg, South Africa and envFes. *Environmental Pollution*, 122, 29-40.

Navarro, M.C., Perez-Sirvent, C., Martinez-Sanchez, M.J., Vidal, J., Trovar, P.J., Bech, J. (2008). Abandoned mine sites as a source of contamination by heavy metals: a case study in a semi-arid zone. *Journal of Geochemical Exploration*, 96, 183-193.

Neal, C., Whitehead, P.G., Jeffery, H., Neal., M. (2005). The water quality of the River Carnon, West Cornwall, November 1992 to March 1994: the impacts of Wheal Jane discharges. *Science of the Total Environment*, 338, 23-39.

Ngigi, S. (2009). *Establishing effective, appropriate and applicable technologies in treating contaminated surface water as part of a rehabilitation strategy for the Princess Dump in Roodeport, West of Johannesburg.* MSc Thesis, University of the Witwatersrand.

Nicholson, R.V., Gillham, R.W., Reardon, E.J. (1990). Pyrite oxidation in carbonate-buffered solution: 2. Rate control by oxide coatings. *Geochimica et Cosmochimica Acta*, 54, 395-402.

Nsimba, E. (2013). *Development of a biophysical system based on bentonite, zeolite and micro-organisms for remediating gold mine wastewaters and tailings ponds, Witwatersrand.* PhD Thesis, University of the Witwatersrand, Johannesburg.

O'Sullivan, A., Conlon, R., Moran, B., Otte, M. (2005). Characterization of constructed wetland substrates by chemical sequential extraction and x-ray diffraction analyses. *Biology and Environment*, 105B, 87-94.

Owen, T. (2008, Spring). *Acid Mine Drainage.* Retrieved November 15, 2014, from Global Water Pollution: http://web1.cnre.vt.edu/lsg/3104/GEOG%20Proj/Tim-AMD%20Pollution/AMD-General%20information.html

Perkins, E.H., Nesbitt, H.W., Gunter, W.D., St-Arnaud, L.C. and Mycroft, J.R. . (1995). *Critical review of geochemical processes and geochemical models adaptable for prediction of acidic drainage from waste rock.* Mine Environment Neutral Drainage (MEND) Report, No. 1.42.1, MEND, Ottawa, ON, 120pp.

Perry, A., Kleinmann, R.L.P. (1991). The use of constructed wetlands in the treatment of acid mine drainage. *Natural Resources Forum*, 15, 178-184.

Pivetz, B. (2001). *Phytoremediaton of contaminated soil and groundwater at hazardous waste sites.* United States Environmental Protection Agency (USEPA) : Groundwater Issue. Oklahoma, U.S.A.

Ritter, L., Solomon, K., Sibley, P., Hall, K., Keen, P., Mattu, G., Linton, B. (2002). Sources, pathways and relative risks of contaminants in surface water and ground water: a perspective prepared for the Walkerton inquiry. *Journal of Toxicology and Environmental Health*, 65, 1- 142.

Robins, M. (2004). *Closure of tailings facilities: Current practice review and guidelines for success.* MSc. Thesis, Engineering Faculty, University of the Witwatersrand.

Saria, L., Shimaoka, T., Miyawaki, K. (2006). Leaching of heavy metals in acid mine drainage. *Waste Management and Research*, 24, 134-140.

Sarmiento, A.M., Nieto, J.M., Olias, M., CANOVAs, C.R. (2009). Hydrochemical characteristics and seasonal influences on pollution by acid mine drainage in the Odiel River basin, Spain. *Applied Geochemistry*, 24, 697-714.

Singer, P.C., Stumm, W. (1970). Acidic mine drainage: the rate determining step. *Science*, 167, 1121-1123.

Smit, E.A., Freeman, J.L. (2006). Environmental cleanup using plants: biotechnological advannces and ecological considerations. *Frontier in Ecology and the Environment*, 4,203-210.

Smith, K. (1997). *Restoration and Reclamation Review.* Department of Horticultural Science, University of Minnesota, St. Paul, MN, Vol.2, 1-7.

Snyder, C.D., Aharrah, E.C. (1985). The typha community: a positive influence on mine drainage and mine restoration. *Wetlands and Water Management on Mined Lands* (pp. 187-188). The Pennsylvania State University, Pennsylvania, Snyder, C and Aharrah, E (Editors).

Sracek, O., Veselovsky, F., Kribek, B., Malec, J., Jehlicka, J. (2010). Geochemistry, mineralogy and Environmental impact of precipitated efflorescent salts at the Kabwe Cu-Co chemical leaching plant in Zambia. *Applied Geochemistry*, 25, 1815-1824.

Stumm, W., Morgan, J.J. (1996). Chemical equlibria and rates in natural waters. In *Aquatic Chemistry* (p. 1022). John Wiley & Sons, Inc. New York, Stumm, W. (Editor).

Swanson, D.A., Barbour, S.L., Wilson, G.W. (1997). Dry-site versus wet-side cover design. *Proceedings of the Fourth International Conference on Acid Rock Drainage, Volume 4*, (pp. 1595-1610). Vancouver, BC.

Swart, E. (2003). The South African legislative framework for mine closure. *The Journal of the South African Institute of Mining and Metallurgy*, pp. 489-492.

Tremaine, S.C., Mills, A.L. (1991). Impact of water column acidification on protozoan bacterivory at the lake sediment-water interface. *Applied and Environmental Microbiology*, 57, 775-784.

Tutu, H., McCarthy, T.S., Cukrowska, E. (2008). The chemical characteristics of acid mine drainage with particular reference to sources, distribution and remediation: The Witwatersrand Basin, South Africa, as a case study. *Applied Geochemistry*, 23, 3666–3684.

UNEP. (2010). *Phytoremediation processes*. Retrieved November 23, 2014, from United Nations Environmental Programme: Newsletter and Technical Publications, Freshwater management series No. 2: http://www.unep.or.jp/ietc/publications/freshwater/FMS2/2.asp

USEPA. (1999). *Phytoremediation Resource Guide.* Retrieved July 29, 2014, from United States Environmental Protection Agency, Solid waste and emergency (5102G): http//: www.epa.gov/ tioclu-in.org

Utete, B., Nhiwatiwa, T., Barson, M., Mabika, N. (2013). Metal correlations and mobility in sediment and water from the Gwebi River in the Upper Manyame Catchment, Zimbabwe. *International Journal of Water Sciences*, 2, 1-8.

Van Damme, P.A., Hamel, C., Ayala, A., Bervoets, L. (2008). Macroinvertebrate community response to acid mine drainage in the rivers of the High Andes (Bolivia). *Environmental Pollution*, 156, 1061-1068.

Vance, D. (1996). Redox reactions in remediation. *Environmental Technology*, 6, 24-25.

Water Resource Characterization (WRC). (2014a). Retrieved November 20, 2014, from NCSU Water Quality Group - WaterShedss - pH: http://www.water.ncsu.edu/watershedss/info/ph.html

Water Resource Characterization(WRC). (2014b). Retrieved November 20, 2014, from NCSU Water Quality Group - WaterShedss - heavy metals: http://www.water.ncsu.edu/watershedss/info/hmetals.html

WHO. (2004). *World Health Organization (WHO), Guidelines for drinking water quality, third edition.* 3, 23-56, WHO publications, Geneva, Switzerland.

Wildman, T. R., Laudon, L. S. (1989). Use of wetlands for treatment of Environmental problems in mining non-coal-mining applications. In *Constructed wetlands for wastewater treatment* (pp. 221-231). Chelsea, Michigan: D. A. Hammer (ed.), Lewis.

Winde, F., Stoch, E.J. (2010). Threats and opportunities for post-closure development in dolomitic gold mining areas of the West Rand and the Far West Rand (South Africa) - a hydraulic view: mining legacy and future threats. *Water SA*, 36, 69 -74.

Wiseman, I.M., Edwards, P.J., Rutt,G.P. (2003). Recovery of an aquatic ecosystem following treament of abandoned mine drainage with constructed wetlands. *Land Contamination and Reclamation*, 11, 221-229.

Wren, C.D., Stephenson, G.L. (1991). The effect of acidification on the accumulationand toxicity of metals to freshwater invertebrates. *Environmental Pollution*, 71, 205-241.

Wuana, R., Okleimen, F.E. (2011). Heavy metals in contaminated soils: A review of sources, chemistry, risks and best available strategies for remediation. *ISRN Ecology, 20pp*.

Younger, P.L., Banwart, S.A., Hedin, R.S. (2002). *Mine Water: Hydrology, Pollution, Remediation.* Kluwer Academic Publishers, Dordrecht.

Zamzow, K. (2014). *Acid Rock Drainage and Metal Leaching at the Pebble Prospect.* Retrieved November 13, 2014, from Pebble Science: http://pebblescience.org/Pebble-Mine/acid_drainage.html

Ziemkiewicz, P., Skousen, J. (1996). Overview of acid mine drainage at source: control strategies. In *Acid Mine Drainage: Control and Treatment. Second edition* (pp. 69-78). West Virginia University and the National Mine Reclamation Center, Morgantown, WV.

Ziemkiewicz, P.F., Skousen, J.G., Simmons, J. (2003). Long-term performance of passive acid mine drainage treatment systems. *Mine Water Environment*, 22, 118-129.

Appendices

Appendix 1. Descriptive statistics and statistical tests for water samples

1 - pH

A. Descriptive statistics

A-1: Descriptive statistics for pH in April, 2014

Analysis Variable : pH						
RB	Mean	StdDev	Std Error	Min mum	Maximum	Median
1	6.29	0.19	0.11	6.15	6.51	6.21
4	6.36	0.09	0.05	6.29	6.47	6.33
7	6.40	0.05	0.03	6.34	6.44	6.41
10	6.07	0.05	0.03	6.02	6.11	6.09
13	5.56	0.07	0.04	5.48	5.62	5.57
15	5.23	0.06	0.03	5.17	5.29	5.22

A-2: Descriptive statistics for pH in July, 2014

Analysis Variable : pH						
RB	Mean	Std Dev	Std Error	Minimum	Maximum	Median
1	6.80	0.02	0.01	6.79	6.82	6.79
4	5.47	0.02	0.01	5.45	5.49	5.47
7	6.01	0.08	0.05	5.92	6.06	6.05
10	6.36	0.01	0.01	6.35	6.37	6.36
13	6.57	0.02	0.01	6.55	6.58	6.57
15	6.43	0.01	0.00	6.42	6.43	6.43

B. Test for Normality

B-1: Test for normality in pH in April, 2014

R-Square	CoeffVar	Root MSE	pH Mean

R-Square	CoeffVar	Root MSE	pH Mean
0.967173	1.666351	0.099722	5.984444

B-2: Test for normality in pH in July, 2014

R-Square	CoeffVar	Root MSE	pH Mean
0.995711	0.551013	0.034561	6.272222

C. Equality test for pH in April, 2014

C-1: Test for equality of variances (Bartlett and Levene Tests) for pH in April

Levene's Test for Homogeneity of pH Variance ANOVA of Squared Deviations from Group Means					
Source	DF	Sum of Squares	Mean Square	F Value	Pr > F
RB	5	0.00123	0.000246	2.92	**0.0596**
Error	12	0.00101	0.000084		

Bartlett's Test for Homogeneity of pH Variance			
Source	DF	Chi-Square	Pr > ChiSq
RB	5	5.5222	**0.3555**

$H_{0:}$ $\delta_1 = \delta_2 = \delta_3$ or equal variances or there is no difference among the groups, δ stands for variance

H_A: unequal variances or there is a difference among the groups

P (Levene) = 0.0596

P (Bartlett) = 0.3555

Alpha = 0.05

Both P values are greater than 0.05, so we fail to reject the null hypothesis therefore the groups have equal variances, so we can go on to perform ANOVA for pH in April

C-2: Test for equality of variances (Bartlett and Levene Tests) for pH in July, 2014

Levene's Test for Homogeneity of pH Variance ANOVA of Squared Deviations from Group Means					
Source	DF	Sum of Squares	Mean Square	F Value	Pr > F

RB	5	0.000039	7.724E-6	3.71**0.0293**
Error	12	0.000025	2.085E-6	

Bartlett's Test for Homogeneity of pH Variance			
Source	DF	Chi-Square	Pr > ChiSq
RB	5	14.2947	**0.0138**

H_0: $\delta_1 = \delta_2 = \delta_3$ or equal variances or there is no difference among the groups, δ stands for variance

H_A: unequal variances or there is a difference among the groups

P (Levene) = 0.0293

P (Bartlett) = 0.0138

Alpha = 0.05

Both P values are less than 0.05, so we reject the null hypothesis therefore the groups have unequal variances, so we do not progress to ANOVA parametric test, as the assumption of ANOVA, homogeneity of Variances has not been upheld. Since ANOVA is not carried out therefore multicomparison test (Tukey) would not be carried out as well. Rather the Kruskal-Wallis non parametric test is now performed for pH in July.

D. ANOVA test for pH in April, 2014

One Way ANOVA parametric test (Test for the Means of the groups) for pH in April.

Source	DF	ANOVA SS	Mean Square	F Value	Pr > F
RB	5	3.51591111	0.70318222	70.71	**<.0001**

$H_0 = \mu_1 = \mu_2 = \mu_3$ or there is no difference in the means of the groups, μ stands for the means

H_A = at least two μs are different or there is a difference among the groups

Alpha = 0.05

ANOVA from above **P (F) = 0.0001**, this is less than 0.05, so we reject the null hypothesis and conclude that there is a difference amongst the groups (reed beds), also, ANOVA is significant i.e. less than 0.05 so we go on to do the Tukey multicomparison test to ascertain where the differences lie.

E. Tukey test for pH in April, 2014

The Tukey test (multicomparison test) for pH in April.

TUKEY TEST Means with the same letter are not significantly different.				
Grouping		Mean	N	RB
	A	6.39667	3	7
	A			
B	A	6.36333	3	4
B	A			
B	A	6.29000	3	1
	B	6.07333	3	10
	C	5.55667	3	13
	D	5.22667	3	15

RBs 1, 4 and 7 all have the same letters

RBs 1, 4 and 7 are not significantly different from one another

RB 10 is significantly different from RB 7 but not for RB 1 and RB 4

RBs 13 and 15 are individually significantly different from all the other reed beds

Significant differences lie in RBs 10, 13 and 15.

F. Kruskal-Wallis non parametric test for pH in July, 2014

Kruskal-Wallis Test	
Chi-Square	16.6132

DF	5
Pr> Chi-Square	**0.0053**

H_0: $M_1 = M_2 = M_3$ or there is no difference among the groups, M stands for median

H_A: at least two medians are different or there is a difference among the groups

Alpha = 0.05

P (Chi square) = 0.0053, this is less than 0.05, so we reject H_0 and conclude that there is sufficient evidence to say that at least two medians/ there is a difference among the groups.

2- EC

A-1 Descriptive statistics for EC in April, 2014

Analysis Variable : EC (µs/cm) for April, 2014						
RB	Mean	StdDev	Std Error	Minimum	Maximum	Median
1	3664.00	91.15	52.62	3598.00	3768.00	3626.00
4	3987.67	10.02	5.78	3980.00	3999.00	3984.00
7	4563.33	49.33	28.48	4530.00	4620.00	4540.00
10	3786.00	33.15	19.14	3763.00	3824.00	3771.00
13	3951.00	7.00	4.04	3944.00	3958.00	3951.00
15	3841.33	14.50	8.37	3827.00	3856.00	3841.00

A-2 Descriptive statistics for EC in July, 2014

Analysis Variable : EC (µs/cm) for July, 2014						
RB	Mean	StdDev	Std Error	Minimum	Maximum	Median
1	2624.00	23.64	13.65	2602.00	2649.00	2621.00
4	3312.33	3.51	2.03	3309.00	3316.00	3312.00
7	4197.67	6.51	3.76	4191.00	4204.00	4198.00
10	5210.67	6.51	3.76	5204.00	5217.00	5211.00
13	5346.33	65.04	37.55	5302.00	5421.00	5316.00
15	5323.33	12.10	6.98	5314.00	5337.00	5319.00

3 – Eh

A-1 Descriptive statistics for Eh in April, 2014

Analysis Variable : Eh(mV)						
RB	Mean	StdDev	Std Error	Minimum	Maximum	Median
1	215.30	10.28	5.94	203.80	223.60	218.50
4	232.57	12.97	7.49	218.20	243.40	236.10
7	102.57	13.49	7.79	92.50	117.90	97.30
10	106.27	3.16	1.83	103.70	109.80	105.30
13	185.97	12.64	7.30	171.50	194.90	191.50
15	182.87	3.42	1.98	179.70	186.50	182.40

A-2: Descriptive statistics for Eh in July, 2014

Analysis Variable : Eh (mV)					
RB	Mean	StdDev	Minimum	Maximum	Median
1	142.23	14.74	132.60	159.20	134.90
4	135.43	11.87	122.70	146.20	137.40
7	277.30	9.53	266.30	283.20	282.40
10	318.57	3.97	314.10	321.70	319.90
13	351.80	5.17	346.90	357.20	351.30
15	332.87	5.67	329.30	339.40	329.90

Appendix 2. Descriptive statistics and statistical tests for sediment samples

1 – pH

A: Descriptive statistics

A-1: Descriptive statistics for pH in sediment sample in April, 2014

Analysis Variable : pH							
RB	Mean	Std Dev	Std Error	Minimum	Maximum	N	Median
1	6.13	0.50	0.29	5.55	6.43	3	6.40
10	6.14	0.08	0.04	6.10	6.23	3	6.10
15	5.95	0.29	0.17	5.63	6.20	3	6.01

A-2: Descriptive statistics for pH in sediment sample in July, 2014

Analysis Variable : pH							
RB	Mean	Std Dev	Std Error	Minimum	Maximum	N	Median
1	6.45	0.26	0.15	6.16	6.66	3	6.53
10	6.48	0.08	0.04	6.41	6.56	3	6.46
15	6.44	0.06	0.04	6.37	6.49	3	6.46

B. Test for Normality

B-1: Test for Normality for pH in sediment sample in April, 2014

R-Square	Coeff Var	Root MSE	pH Mean
0.095096	5.540023	0.336403	6.072222

B-2: Test for Normality for pH in sediment sample in July, 2014

R-Square	Coeff Var	Root MSE	pH Mean
0.013798	2.482248	0.160243	6.455556

Both R-Square values in April and July are low and therefore poor models.

C. Test for Equality of variances

C-1: Test for Equality of variances in pH in sediment sample in April, 2014

Levene's Test for Homogeneity of pH Variance ANOVA of Squared Deviations from Group Means					
Source	DF	Sum of Squares	Mean Square	F Value	Pr > F
RB	2	0.0414	0.0207	2.68	0.1473
Error	6	0.0463	0.00772		

Bartlett's Test for Homogeneity of pH Variance			
Source	DF	Chi-Square	Pr > ChiSq
RB	2	4.0979	0.1289

Both P values in Bartlett and Levene tests are greater than 0.05, hence there is homogeneity of variances, so ANOVA can be performed.

C-2: Test for Equality of variances in pH in sediment sample in July, 2014

Levene's Test for Homogeneity of pH Variance ANOVA of Squared Deviations from Group Means					
Source	DF	Sum of Squares	Mean Square	F Value	Pr > F
RB	2	0.00347	0.00173	3.41	0.1026
Error	6	0.00305	0.000509		

Bartlett's Test for Homogeneity of pH Variance			
Source	DF	Chi-Square	Pr > ChiSq
RB	2	3.9324	0.1400

Both P values in Bartlett and Levene tests are greater than 0.05, hence there is homogeneity of variances, so ANOVA can be performed.

D. ANOVA parametric test

D-1: ANOVA for pH in sediment sample in April, 2014

Source	DF	ANOVA SS	Mean Square	F Value	Pr > F
RB	2	0.07135556	0.03567778	0.32	0.7410

ANOVA has a P-value greater than 0.05, so it is not significant, therefore Tukey test cannot be performed as they would not be any significant differences to show amongst the reed beds.

D-2: ANOVA for pH in sediment sample in July, 2014

Source	DF	ANOVA SS	Mean Square	F Value	Pr > F
RB	2	0.00215556	0.00107778	0.04	0.9592

ANOVA has a P-value greater than 0.05, so it is not significant, therefore Tukey test cannot be performed as they would not be any significant differences to show amongst the reed beds.

2 – EC

A: Descriptive statistics

A-1: Descriptive statistics for EC in sediment sample in April, 2014

Analysis Variable : EC							
RB	Mean	Std Dev	Std Error	Minimum	Maximum	N	Median
1	1005.00	15.39	8.89	988.00	1018.00	3	1009.00
10	1628.67	163.03	94.12	1464.00	1790.00	3	1632.00
15	1013.67	3.79	2.19	1011.00	1018.00	3	1012.00

A-2: Descriptive statistics for EC in sediment sample in July, 2014

Analysis Variable : EC							
RB	Mean	Std Dev	Std Error	Minimum	Maximum	N	Median
1	1194.67	88.64	51.17	1127.00	1295.00	3	1162.00
10	1116.67	152.02	87.77	966.00	1270.00	3	1114.00
15	1038.33	148.06	85.48	888.00	1184.00	3	1043.00

3 – Eh

A: Descriptive statistics

A-1: Descriptive statistics for Eh in sediment sample in April, 2014

Analysis Variable : Eh							
RB	Mean	Std Dev	Std Error	Minimum	Maximum	N	Median
1	-78.67	242.81	140.18	-284.30	189.20	3	-140.90
10	149.97	149.76	86.47	-21.90	252.50	3	219.30
15	51.63	76.78	44.33	-23.90	129.60	3	49.20

A-2: Descriptive statistics for Eh in sediment sample in July, 2014

Analysis Variable : Eh							
RB	Mean	Std Dev	Std Error	Minimum	Maximum	N	Median
1	9.50	158.14	91.30	-173.10	101.90	3	99.70
10	87.10	16.47	9.51	69.80	102.60	3	88.90
15	36.93	215.05	124.16	-211.20	169.30	3	152.70

Appendix 3: Mean concentrations (ppm) of trace and major elements in water samples, April, 2014, measured by ICP-OES

	Ti	V	Co	Cu	As	Se	Cd	Sn	Sb	Au	U	Cl	Hg	Al	Ca	Fe	K	Mg	Mn	Na	Ni	P	S	Zn	Sum conc	Sum conc
RB	ppm	ppm	ppm	ppm	ppm	ppm	ppm	ppm	ppm	ppm	ppm	ppm	ppm	ppm	ppm	ppm	ppm	ppm	ppm	ppm	ppm	ppm	ppm	ppm	ppm	%
RB 1.1	0.00	0.00	0.14	0.00	0.00	0.00	0.00	0.00	0.00	0.00	0.00	360.00	0.00	0.07	261.70	0.15	14.60	254.90	0.06	291.60	0.07	0.00	732.00	0.03	1915.32	0.19
RB 1.2	0.00	0.00	0.29	0.00	0.00	0.00	0.00	0.00	0.00	0.00	0.00	280.00	0.00	0.14	272.40	0.07	18.40	219.80	3.00	294.80	0.04	0.00	928.00	0.02	2016.96	0.20
RB 1.3	0.00	0.00	0.21	0.00	0.00	0.00	0.00	0.00	0.00	0.00	0.00	180.00	0.00	0.15	147.00	0.03	15.40	119.00	2.05	228.80	0.02	0.00	681.80	0.01	1374.47	0.14
RB 4.1	0.00	0.00	0.19	0.00	0.00	0.00	0.00	0.00	0.00	0.00	0.00	360.00	0.00	0.09	222.10	0.06	14.10	212.80	1.08	264.80	0.01	0.00	918.50	0.01	1993.74	0.20
RB 4.2	0.00	0.00	0.11	0.00	0.00	0.00	0.00	0.00	0.00	0.00	0.00	210.00	0.00	0.06	176.20	0.03	10.20	123.20	0.49	241.30	0.00	0.00	820.50	0.01	1582.10	0.16
RB 4.3	0.00	0.00	0.04	0.00	0.00	0.00	0.00	0.00	0.00	0.00	0.00	440.00	0.00	0.12	157.10	0.03	10.60	95.70	0.23	214.70	0.00	0.00	675.00	0.01	1593.53	0.16
RB 7.1	0.00	0.00	0.21	0.00	0.00	0.00	0.00	0.00	0.00	0.00	0.00	380.00	0.00	0.14	304.20	0.24	16.80	282.30	4.80	357.90	0.06	0.00	1229.80	0.06	2576.51	0.26
RB 7.2	0.00	0.00	0.11	0.00	0.00	0.00	0.00	0.00	0.00	0.00	0.00	340.00	0.00	0.08	210.00	0.04	15.50	181.20	0.35	290.10	0.01	0.00	959.40	0.02	1996.80	0.20
RB 7.3	0.00	0.00	0.10	0.00	0.00	0.00	0.00	0.00	0.00	0.00	0.00	440.00	0.00	0.14	268.40	0.02	16.20	200.00	0.11	310.50	0.01	0.00	1051.90	0.02	2287.40	0.23
RB 10.1	0.00	0.00	0.05	0.00	0.00	0.00	0.00	0.00	0.00	0.00	0.00	340.00	0.00	0.11	168.20	0.06	13.00	145.30	0.19	273.70	0.00	0.00	765.20	0.01	1705.82	0.17
RB 10.2	0.00	0.00	0.04	0.00	0.00	0.00	0.00	0.00	0.00	0.00	0.00	380.00	0.00	0.00	204.20	0.09	12.00	139.20	0.61	211.60	0.00	0.00	705.00	0.01	1652.75	0.17
RB10.3	0.00	0.00	0.02	0.00	0.00	0.00	0.00	0.00	0.00	0.00	0.00	500.00	0.00	0.00	195.40	0.08	10.00	101.40	0.35	195.40	0.00	0.00	637.10	0.01	1639.76	0.16
RB 13.1	0.00	0.00	0.06	0.00	0.00	0.00	0.00	0.00	0.00	0.00	0.00	360.00	0.00	0.00	194.00	0.02	11.30	192.10	8.50	175.20	0.02	0.00	782.00	0.01	1723.21	0.17
RB 13.2	0.00	0.00	0.04	0.00	0.00	0.00	0.00	0.00	0.00	0.00	0.00	340.00	0.00	0.10	190.30	0.01	9.70	169.80	7.90	174.00	0.02	0.00	738.30	0.02	1630.19	0.16
RB 13.3	0.00	0.00	0.05	0.00	0.00	0.00	0.00	0.00	0.00	0.00	0.00	230.00	0.00	0.12	248.50	0.03	11.40	264.60	12.40	195.20	0.02	0.00	1024.30	0.02	1986.64	0.20
RB 15.1	0.00	0.00	0.07	0.00	0.00	0.00	0.00	0.00	0.00	0.00	0.00	360.00	0.00	0.00	309.50	0.04	13.30	321.20	20.60	213.00	0.05	0.00	1325.30	0.04	2563.10	0.26
RB 15.2	0.00	0.00	0.06	0.00	0.00	0.00	0.00	0.00	0.00	0.00	0.00	360.00	0.00	0.13	226.30	0.08	12.30	269.10	17.00	192.60	0.06	0.00	987.80	0.05	2065.47	0.21
RB 15.3	0.00	0.00	0.05	0.00	0.00	0.00	0.00	0.00	0.00	0.00	0.00	200.00	0.00	0.09	287.70	0.07	13.70	341.50	20.20	226.00	0.07	0.00	1229.40	0.06	2318.84	0.23

- Sum concentration is the total sum of the concentrations of all the contaminants present in each reed bed in 'ppm'.
- Sum concentration (%) was calculated by dividing each 'total ppm value' per reed bed by 10000 to get a' %' value.

Appendix 4: Mean concentrations (ppm) of trace and major elements and nitrate, in water samples, July, 2014, measured by ICP-MS and IC.

	Al	Ti	V	Co	Cu	As	Se	Cd	Sn	Sb	Au	Pb	U	Nitrate	Cl	Hg	Ca	Fe	K	Mg	Mn	Si	Ni	P	S	Zn	Sum conc	Sum conc
RB	ppm	ppm	ppm	ppm	ppm	ppm	ppm	ppm	ppm	ppm	ppm	ppm	ppm	ppm	ppm	ppm	ppm	ppm	ppm	ppm	ppm	ppm	ppm	ppm	ppm	ppm	ppm	%
RB 1.1	0.01	0.00	0.00	0.32	0.00	0.00	0.00	0.00	0.00	0.00	0.00	0.00	0.00	18.10	251.00	0.00	302.80	0.08	21.94	324.00	1.55	0.57	0.03	0.00	1034.20	0.04	1954.62	0.20
RB 1.2	0.00	0.00	0.00	0.31	0.00	0.00	0.00	0.00	0.00	0.00	0.00	0.00	0.00	16.00	280.40	0.00	412.00	0.03	27.00	403.00	7.00	0.55	0.03	0.00	1532.60	0.04	2678.93	0.27
RB 1.3	0.01	0.00	0.00	0.22	0.01	0.00	0.00	0.00	0.00	0.00	0.00	0.03	0.00	16.40	263.10	0.00	356.20	0.20	32.60	386.60	7.20	0.63	0.04	0.00	1362.00	0.05	2425.24	0.24
RB 4.1	0.02	0.00	0.00	0.61	0.01	0.00	0.00	0.00	0.00	0.00	0.00	0.00	0.00	34.40	317.60	0.00	524.20	0.03	48.20	699.60	0.73	0.80	0.03	0.00	2158.80	0.04	3785.03	0.38
RB 4.2	0.00	0.00	0.00	0.45	0.00	0.00	0.00	0.00	0.00	0.00	0.00	0.00	0.00	28.80	324.60	0.00	345.30	0.03	58.80	480.30	0.43	0.72	0.02	0.00	1519.20	0.03	2758.65	0.28
RB 4.3	0.00	0.00	0.00	0.50	0.00	0.00	0.00	0.00	0.00	0.00	0.00	0.00	0.00	30.00	347.00	0.00	313.80	0.03	59.70	380.70	0.24	0.61	0.02	0.00	1221.30	0.05	2353.91	0.24
RB 7.1	0.00	0.00	0.00	0.47	0.00	0.00	0.00	0.00	0.00	0.00	0.00	0.00	0.00	15.60	217.60	0.00	350.10	0.02	72.90	512.40	0.53	0.58	0.02	0.00	1678.80	0.04	2849.02	0.28
RB 7.2	0.00	0.00	0.00	0.26	0.00	0.00	0.01	0.00	0.00	0.00	0.00	0.00	0.00	25.00	405.40	0.00	382.20	0.02	75.30	558.60	1.26	0.71	0.04	13.20	1736.10	0.07	3198.11	0.32
RB 7.3	0.00	0.00	0.00	0.25	0.00	0.00	0.00	0.00	0.00	0.00	0.00	0.00	0.00	24.80	379.20	0.00	621.90	0.03	99.60	738.30	1.03	0.74	0.05	0.00	2858.70	0.05	4724.61	0.47
RB 10.1	0.00	0.00	0.00	0.21	0.01	0.00	0.00	0.00	0.00	0.00	0.00	0.00	0.00	27.20	429.20	0.00	341.20	0.18	51.60	522.20	0.57	0.59	0.02	0.00	1592.00	0.03	2964.98	0.30
RB 10.2	0.00	0.00	0.00	0.16	0.00	0.00	0.00	0.00	0.00	0.00	0.00	0.00	0.00	23.60	388.20	0.00	426.20	0.33	51.80	613.80	5.00	0.79	0.01	0.00	2102.20	0.04	3612.10	0.36
RB10.3	0.00	0.00	0.00	0.11	0.00	0.00	0.00	0.00	0.00	0.00	0.00	0.00	0.00	24.20	320.00	0.00	417.00	0.07	52.00	723.60	8.60	0.70	0.01	0.00	1901.80	0.04	3448.09	0.34
RB 13.1	0.09	0.00	0.00	0.23	0.01	0.00	0.00	0.00	0.00	0.00	0.00	0.03	0.00	24.40	334.40	0.00	458.70	0.21	62.70	674.70	27.90	0.62	0.04	0.00	2048.10	0.15	3632.13	0.36
RB 13.2	0.01	0.00	0.00	0.18	0.00	0.00	0.00	0.00	0.00	0.00	0.00	0.00	0.00	21.20	347.20	0.00	487.50	1.80	68.70	735.00	31.20	0.47	0.03	0.00	2188.20	0.03	3881.49	0.39
RB 13.3	0.01	0.00	0.00	0.13	0.00	0.00	0.00	0.00	0.00	0.00	0.00	0.00	0.00	21.40	347.60	0.00	353.10	1.50	68.70	533.70	22.50	0.55	0.04	0.00	1585.80	0.02	2935.02	0.29
RB 15.1	0.47	0.00	0.00	0.15	0.00	0.00	0.00	0.00	0.00	0.00	0.00	0.00	0.00	11.00	364.00	0.00	162.80	0.70	37.60	224.20	14.20	16.60	0.24	0.00	661.20	0.04	1493.16	0.15
RB 15.2	0.00	0.00	0.00	0.08	0.00	0.00	0.00	0.00	0.00	0.00	0.00	0.00	0.00	10.00	395.20	0.00	225.20	1.00	43.60	351.20	21.60	0.64	0.08	0.00	1108.40	0.02	2157.00	0.22
RB 15.3	0.00	0.00	0.00	0.08	0.00	0.00	0.00	0.00	0.00	0.00	0.00	0.00	0.00	10.80	352.20	0.00	219.40	1.20	40.40	300.00	19.00	0.43	0.04	0.00	1099.80	0.03	2043.35	0.20

Appendix 5: Mean concentrations of trace and major elements in the sediment profiles (cm), April, 2014, measured by XRF. Note that Mg, Al, Si, P, K, Ca, Mn and Fe are presented as the oxide for XRF data.

Element	Na_2O	MgO	Al_2O_3	SiO_2	P_2O_5	S	Cl	K2O	CaO	Cr	MnO	FeO	Co	Ni	Cu	Zn	Pb	U
Unit	%	%	%	%	µg/g	µg/g	µg/g	%	%	µg/g	µg/g	%	µg/g	µg/g	µg/g	µg/g	µg/g	µg/g
CRM 2	<0.14	1.381	15.13	74.82	1325	2224	261	2.727	0.8165	<5.1	1042	4.551	21.5	35.9	111.1	245.4	97.7	<1.3
1.1. 0-2 CM	<0.14	0.344	20.48	69.96	717	8240	696	2.067	0.4559	<5.1	7533	4.502	69.6	82.4	46.8	61.4	54.5	2.4
1.1. 2-5 CM	<0.14	0.444	29.66	82.91	127.6	1247	<101	1.588	0.1632	145.2	534.9	3.44	<6.2	49.3	32.4	31.5	29.6	<1.7
1.1. 5 -10 CM	<0.14	0.503	29.76	82.57	402	4559	302	1.72	0.2953	147.9	2361	3.095	34.7	62.1	34.6	42.1	34.7	<1.8
1.1. 10-20 CM	<0.14	0.252	27.79	71.78	<15	130.4	281	1.283	0.0949	119.9	345.7	3.687	<8.1	43.1	25.7	20.7	6.7	<1.7
1.2 0-2 CM	<0.14	0.279	23.21	65.97	571	4038	656	2.278	0.2583	119.5	1043	5.423	36.7	73.3	42.2	49.2	34.5	3.4
1.2 2-5CM	<0.14	0.488	35.2	89.03	285.4	1505	<171	2.377	0.1932	236.4	809.4	5.763	<7.4	50.4	29.4	38.4	19.5	<1.5
1.2 5-10 CM	<0.14	0.195	23	63.23	310.6	989.2	293	2.15	0.1466	102	386.7	5.833	14.9	61.7	31.1	38.3	25.2	<1.3
1.2 10-20 CM	<0.14	0.245	22.97	63.07	215.4	900.6	197	2.102	0.1343	109.4	174.7	5.679	13.8	61.6	31.8	37.2	22.5	<1.3
1.2 20-30 CM	<0.14	0.31	22.78	63.67	529.3	3869	586	2.23	0.2892	96	2903	5.402	56	86.4	46.5	61.7	31.4	2
1.3 0-2 CM	<0.14	0.241	23.19	61.07	382	2408	445	2.401	0.2392	116	1730	6.506	41.2	76.8	41.1	48.7	44.3	1.4
1.3 2-5 CM	<0.14	0.207	25.17	64.51	354.4	1280	374	2.63	0.1955	124.8	1359	7.44	33.2	75.7	39.9	47.4	34.7	1.9
1.3 5-10 CM	<0.14	0.197	24.4	60.74	310.4	1010	323	2.463	0.1581	117.5	344.5	6.396	22	67.8	36.8	42.1	32	<1.3
10.1 0-2 CM	<0.14	0.16	19.49	79.32	437.3	1238	267	2.313	0.2342	<5.1	96.1	4.773	16.7	42.5	38.1	30.6	34.7	<1.3
10.1 2-5 CM	<0.14	0.22	19.36	77.55	469.1	1775	1128	2.164	0.2458	<5.1	121.1	4.134	8.5	39.8	35.7	31.4	69.4	<1.3
10.1 5-10CM	<0.14	0.275	23.88	66.12	519.3	3077	317	2.433	0.268	110.6	121.9	5.695	16.4	66.9	40.6	43.8	28.6	2.1
10.1 10-20 CM	<0.14	0.327	28.22	61.14	411	2520	247	2.7	0.2387	140.5	127.1	6.624	20	85.5	51.4	50.6	29.5	<1.5
10.1 20-30 CM	<0.14	0.228	24.93	58.23	385.3	2060	476	2.752	0.1908	159.8	162.6	7.286	25	81.1	47	46.7	30.3	<1.4
10.2 0-2 CM	<0.14	0.216	26	65.11	547	3631	281	2.82	0.188	147.7	113	6.092	17	69.1	51.6	38.3	41.9	3.7
10.2 2-5 CM	<0.14	<0.067	10.22	32.84	293.5	1206	<101	2.721	0.1514	112.9	56.6	5.493	10.6	60.1	45.1	31.2	33.4	<1.5
10.2 5-10 CM	<0.14	0.382	39.52	86.54	533	2318	<170	3.259	0.1799	145.6	17.8	6.288	5.2	60.3	41.9	33.9	30.3	<1.7
10.2 10-20 CM	<0.14	0.209	25.79	58.56	515	2134	339	2.801	0.161	147.3	19.3	7.192	18.1	74.8	46.6	39.9	29.6	1.8
10.3 0-2 CM	<0.14	0.244	27.23	56.93	402.1	2107	203	2.688	0.1607	155.8	212.3	6.821	25.4	91.4	56.9	48.2	31.1	<1.5
10.3 2-5 CM	<0.14	0.227	27.18	56.1	402.1	1710	298	2.674	0.1634	157.4	198.2	6.709	20.5	90.4	52.5	48.3	30.8	<1.5
10.3 5-10 CM	<0.14	0.208	27.65	55.9	375.9	2283	174	2.718	0.1795	151.1	152	6.267	17.7	92	48.1	46	29.1	<1.5
10.3 10-20 CM	<0.14	0.195	24.82	58.45	434	3098	378	2.625	0.1822	133.3	133.6	6.99	24.8	69.4	42.3	36.2	29.3	<1.5
10.3 20-30 CM	<0.14	0.212	22.57	69.05	452	4270	214	2.613	0.1929	<5.1	40	4.441	12.3	50.2	38.7	27.5	26.2	<1.3

Continuation of Appendix 5

Element	Na_2O	MgO	Al_2O_3	SiO_2	P_2O_5	S	Cl	K2O	CaO	Cr	MnO	FeO	Co	Ni	Cu	Zn	Pb	U
15.1 0-2 CM	<0.14	0.432	22.73	67.09	760	7393	813	2.064	0.4617	<5.1	354.8	4.311	80.6	94	53.7	87.4	64.3	7.4
15.1 2-5 CM	<0.14	0.371	22.42	65.68	777	9995	628	2.183	0.431	122.7	303.5	5.788	57.3	86.7	50.8	69.5	80.6	11
15.1 5-10 CM	<0.14	0.148	22.14	58.22	574	2800	318	2.256	0.2001	134.3	103.2	9.427	30.9	58.4	41	30.6	32	<1.4
15.1 10-20 CM	<0.14	0.148	23.87	55.47	481	1621	377	2.454	0.1848	161.9	<3.9	9.571	25.8	71.3	35.6	31	37.6	<1.5
15.1 20-30 CM	<0.14	0.179	23.26	62.73	481.1	2249	309	2.525	0.1796	112.8	<3.9	7.161	17.6	55.5	30.3	28.6	26.8	<1.4
15.2 0-2 CM	<0.14	0.63	23.47	75.93	1160	9021	1332	2.567	0.5644	<5.1	640.3	6.127	72.9	107.5	65.9	105.2	112.5	22.5
15.2 2-5 CM	<0.14	0.385	20.69	68.59	576	4821	473	2.235	0.3163	<5.1	228	5.041	30.3	68.5	42.9	55.6	36.9	14.8
15.2 5-10 CM	<0.14	0.258	20.97	67.9	454.8	3329	496	2.218	0.2206	<5.1	112	5.679	24.3	51.6	28.3	33.2	34.4	2.2
15.2 10-20 CM	<0.14	0.18	21.53	64.15	401.5	1909	130	2.349	0.1759	<5.1	10	6.647	11.6	49.5	30.6	27.3	26.8	<1.4
15.2 20-30 CM	<0.14	0.158	27.35	70.83	481	1640	219	2.617	0.1704	160.8	<3.9	10.32	11.1	52.9	35.2	25.9	28.2	<1.6
15.3 0-2 CM	<0.14	0.506	21.3	67.47	989	6128	1057	2.357	0.4869	119.7	734.9	5.429	70.9	92.7	54.6	102	57.4	17.5
15.3 2-5 CM	<0.14	0.512	20.92	68.46	692	4432	591	2.272	0.4007	<5.1	379.8	4.827	45.1	81.1	54.6	79.1	39.4	23.3
15.3 5-10 CM	<0.14	0.26	20.54	69.79	344.6	2063	254	2.255	0.2315	<5.1	176.6	4.496	23.5	52.1	30.9	33.7	29.8	2.3
15.3 10-20 CM	<0.14	0.241	20.08	69.49	287.7	2176	180	2.247	0.1991	<5.1	128.1	4.982	10.3	44.4	25.9	27.4	28.2	<1.3

Appendix 6: Mean concentrations of trace and major elements in the sediment profiles (cm), July, 2014, measured by XRF. Note that Mg, Al, Si, P, K, Ca, Mn and Fe are presented as the oxide for XRF data.

Element	Na2O	MgO	Al2O3	SiO2	P2O5	S	Cl	K2O	CaO	Cr	MnO	FeO	Co	Ni	Cu	Zn	Pb	U
Unit	%	%	%	%	µg/g	µg/g	µg/g	%	%	µg/g	µg/g	%	µg/g	µg/g	µg/g	µg/g	µg/g	µg/g
CRM- SED	<0.14	1.425	15.16	72.02	1323	2175	286	2.847	0.8681	<5.1	1060	4.547	17.7	35.3	107.4	242.1	96	<1.3
1.1 0-2 CM	<0.14	0.4	21.62	66.42	551	5536	503	2.311	0.4203	<5.1	2671	4.851	46.6	79.5	45.1	51.8	31.4	6.3
1.1 2-5 CM	<0.14	0.286	21.33	66.55	407.4	3590	253	2.185	0.2967	<5.1	939.8	4.994	26.9	69.5	42.1	46	26.2	4.6
1.1 5-10 CM	<0.14	0.275	20.83	64.89	275.9	2596	254	2.065	0.2434	108.8	470.7	5.032	18.5	64.3	40.3	48.1	23.6	3.9
1.1 10-20 CM	<0.14	0.228	23.13	67.39	154.6	1443	312	2.039	0.1716	94.8	621.5	5.559	14.8	54.6	30.3	33.4	18.1	<1.2
1.2 0-2 CM	<0.14	0.341	21.64	62.96	436.8	5332	509	2.346	0.3572	<5.1	1714	5.234	45.1	82.5	48.6	53.3	30.5	6.5
1.2 2-5 CM	<0.14	0.228	22.24	62.54	249.4	2473	350	2.216	0.2302	97	656.4	5.425	16.7	69.5	40.6	46	23.2	3.1
1.2 5-10 CM	<0.14	0.191	23.24	61.39	224.1	1363	173	2.248	0.1886	<5.1	645	5.574	15.7	65.9	36.5	41.1	22.3	<1.3
1.2 10-20 CM	<0.14	0.263	23.29	62.83	139.6	811.3	373	2.205	0.13	107.3	306.5	5.254	11.3	61.6	32.7	37	18.9	<1.3
1.3 0-2 CM	<0.14	0.474	21.03	69.53	716	10120	3188	2.538	0.5865	104.4	12290	5.47	150.2	107.6	44.1	62.6	31	1.7
1.3 2-5 CM	<0.14	0.252	23.32	63.97	399	2843	344	2.549	0.2288	114.1	566.6	5.964	34	69.2	36.5	43.5	24.9	<1.4
1.3 5-10 CM	<0.14	0.201	23.28	61.43	326.3	1447	242	2.468	0.1837	122	362.5	6.206	17.6	65.6	36.4	40.6	25.1	<1.3
1.3 10-20 CM	<0.14	0.149	23.44	58.64	268.2	1330	181	2.555	0.1436	128.6	562.7	7.585	19.8	65.3	36.1	37.4	24.6	<1.4
10.1 0-2CM	<0.14	0.369	23.47	61.1	507	3449	744	2.614	0.2779	117.7	596.3	5.942	23.7	82.2	47.4	55.4	27	2.7
10.1 2-5CM	<0.14	0.254	25.9	57.94	384.1	2155	385	2.759	0.2339	130.7	195.2	6.86	31.6	88.7	44.4	52.5	25.6	<1.5
10.1 5-10CM	<0.14	0.254	25.47	56.73	327.5	1843	455	2.754	0.2268	139.5	200.8	6.895	20	90.6	46.7	53.4	27.8	<1.5
10.1 10-20CM	<0.14	0.247	25.9	56.54	318.9	909.4	357	2.811	0.1988	159	226.8	7.197	22.1	86.9	47.5	49.4	28.6	<1.5
10.1 20-30CM	<0.14	0.296	25.26	58.48	265.2	999.6	290	2.792	0.1848	145.2	229.1	6.639	23.4	79.5	44.1	46	26.7	<1.4
10.2 0-2 CM	<0.14	0.223	24.98	61.71	441	2183	473	2.871	0.2074	129.7	125	5.989	13.8	65.6	43.1	39.7	27.3	<1.4
10.2 2-5 CM	<0.14	0.29	25.06	61.6	423.1	2273	444	2.889	0.1928	123	84.7	5.582	20.6	64.3	40.6	37.4	25.2	<1.4
10.2 5- 10 CM	<0.14	0.238	25.04	63.72	452	1534	133	3.013	0.1649	<5.1	81.1	5.387	15.4	62.9	42.5	36.4	24.6	<1.4
10.2 10-20 CM	<0.14	0.254	26.46	66.25	449.1	1398	213	3.211	0.1733	129.9	37.5	5.896	16.9	65.7	32.6	37.1	24.7	<1.5
10.3 0-2 CM	<0.14	0.223	21.03	70.32	349.8	4279	470	2.434	0.2625	<5.1	24.2	4.005	12.3	49	40	33.5	26.2	1.6
10.3 2-5 CM	<0.14	0.253	22.3	66.88	385.6	3848	312	2.457	0.2047	<5.1	21	4.515	14.1	50.3	43.7	29.3	25.8	<1.3

Continuation of Appendix 6

Element	Na2O	MgO	Al2O3	SiO2	P2O5	S	Cl	K2O	CaO	Cr	MnO	FeO	Co	Ni	Cu	Zn	Pb	U
10.3 5-10 CM	<0.14	0.19	23.65	61.58	461.1	2895	257	2.487	0.2	125.2	15.7	5.737	15.1	55	48.5	31.7	26.3	<1.4
10.3 10-20 CM	<0.14	0.191	26.2	58.91	441.2	2368	388	2.871	0.1847	131.9	<6.7	6.69	20.3	70.9	43.5	37.7	28.1	<1.5
15.1 0-2 CM	<0.14	0.394	19.53	64.82	605	8133	517	1.914	0.4977	<5.1	358.1	4.083	47.2	77.7	49.6	74.1	31	9.8
15.1 2-5 CM	<0.14	0.26	21.46	65.61	432.5	4808	564	2.266	0.3221	123.8	168.8	6.185	33.2	64.1	39.8	44.8	28.8	3.7
15.1 5-10 CM	<0.14	0.143	21.86	61.93	329.3	2115	190	2.401	0.2023	122.3	45.4	7.252	20	54.5	36.6	30.5	28.3	<1.4
15.1 10-20 CM	<0.14	0.154	26.14	67.09	422.6	1582	<133	2.722	0.1874	143.5	<3.9	8.457	12.8	57.7	36	29.4	27.6	<1.5
15.2 0-2 CM	<0.14	0.302	29.06	84.31	75.5	1386	<199	2.038	0.1679	173.7	243.7	4.963	<7.9	36.2	23.3	23.3	13.6	<1.7
15.2 2-5 CM	<0.14	0.221	21.57	70.89	230.4	1875	<101	2.388	0.1898	<5.1	49.7	5.143	15.3	44.8	22.6	27.6	26	<1.3
15.2 5-10 CM	<0.14	0.181	21.46	63.41	262.4	1325	<123	2.371	0.1927	100.6	<3.9	7.565	12.8	48	31.6	28.4	28.2	<1.4
15.2 10-20 CM	<0.14	0.187	22.76	64.52	340	1574	272	2.422	0.1932	119	<3.9	7.22	13.8	53.6	37.7	29.6	29.2	<1.4
15.3 0-2 CM	<0.14	0.341	19.94	66.5	396.7	2823	908	2.297	0.3392	<5.1	593.6	4.802	41.7	65.3	32.6	57.5	29.6	6.5
15.3 2-5 CM	<0.14	0.665	27.61	86.3	436.3	5691	<101	2.514	0.4265	<5.1	280.5	4.602	43.8	80	49.5	70.6	29.6	15.1
15.3 5-10 CM	<0.14	0.322	23.59	73.59	303.2	3087	151	2.378	0.2853	<5.1	180.1	5.756	6.9	50.7	32.4	29.4	27.8	1.6
15.3 10-20 CM	<0.14	0.296	21.83	74.17	323.2	2946	<101	2.311	0.2536	<5.1	94.2	4.188	7.7	45	26.3	27.2	27	<1.3

Appendix 7: *In situ* measurements of pH, Eh, EC and temperature, April, 2014.

REED BED	Eh(mV)	pH	EC (µs/cm)	TEMP (°C)
1.1	218.5	6.15	3768	15.9
1.2	203.8	6.21	3626	16.7
1.3	223.6	6.51	3598	16.9
2.1	256.1	6.11	3637	15.6
2.2	231.3	6.43	3631	15.9
2.3	263.5	6.54	3628	16.2
3.1	269.5	6.31	3991	16.1
3.2	244.5	6.39	3978	17.3
3.3	252.2	6.42	3972	17.3
4.1	236.1	6.29	3999	17.6
4.2	218.2	6.33	3984	18.1
4.3	243.4	6.47	3980	18.3
5.1	211.3	6.01	4180	19.6
5.2	209.2	6.09	4119	20.3
5.3	210.7	6.07	4089	21.3

Reed beds 1-5

REED BED	Eh(mV)	pH	EC (µs/cm)	TEMP (°C)
6.1	92.6	6.04	4530	20.1
6.2	90.2	6.02	4420	20.6
6.3	91.7	6.11	4390	20.9
7.1	97.3	6.34	4620	21.6
7.2	92.5	6.44	4540	23.4
7.3	117.9	6.41	4530	23.9
8.1	108.4	6.66	4680	20.9
8.2	109.2	6.71	4610	22.3
8.3	99.5	6.95	4560	23.6
9.1	102.4	6.34	4540	21.4
9.2	102.3	6.73	4510	21.8
9.3	91.4	6.78	4440	21.8
10.1	105.3	6.02	3824	21.6
10.2	109.8	6.09	3771	21.9
10.3	103.7	6.11	3763	22.3

Reed beds 6 - 10

REED BED	Eh(mV)	pH	EC (µs/cm)	TEMP (°C)
11.1	102.4	6.21	3772	20.6
11.2	114.7	5.97	3769	21.3
11.3	116.5	5.49	3742	22.4
12.1	171.9	6.32	3902	21.2
12.2	177.3	5.78	3882	19.9
12.3	188.5	5.69	3827	19.2
13.1	191.5	5.62	3958	17.1
13.2	171.5	5.57	3951	18.4
13.3	194.9	5.48	3944	19.3
14.1	196.8	5.51	3992	16.2
14.2	185.9	5.46	3844	17.4
14.3	199.7	5.33	3841	17.6
15.1	182.4	5.29	3856	16.8
15.2	179.7	5.22	3841	17.2
15.3	186.5	5.17	3827	18.1

Reed beds 11- 15

Appendix 8: *In situ* measurements of pH, Eh, EC, temperature and DO, July, 2014.

REED BED	Eh (mV)	pH	EC (µs/cm)	TEMP (°C)	DO (mg/L)
1.1	159.2	6.8	2602	8.9	5.38
1.2	134.9	6.8	2621	9.4	5.51
1.3	132.6	6.8	2649	9.4	5.67
2.1	199.2	5.4	3221	10.8	4.92
2.2	167.1	5.5	3210	10.9	5.21
2.3	148.4	5.5	3319	11.2	5.24
3.1	165.2	5.5	3117	10.1	5.01
3.2	157.1	5.5	3124	10.3	5.11
3.3	151.9	5.4	3148	10.7	5.17
4.1	146.2	5.5	3316	11.5	6.14
4.2	137.4	5.5	3312	11.7	6.09
4.3	122.7	5.5	3309	11.7	6.11
5.1	261.4	5.9	4149	11.1	6.03
5.2	277.4	6.0	4152	11.3	6.13
5.3	282.1	6.0	4216	11.6	6.16

Reed beds 1- 5

REED BED	Eh (mV)	pH	EC (µs/cm)	TEMP (°C)	DO (mg/L)
6.1	252.9	5.9	4172	12.3	7.21
6.2	264.2	5.9	4183	12.2	7.19
6.3	272.4	5.9	4226	12.6	7.24
7.1	266.3	5.9	4191	11.9	7.14
7.2	282.4	6.1	4198	12.4	7.27
7.3	283.2	6.1	4204	12.7	7.31
8.1	248.2	5.8	4021	12.5	7.19
8.2	259.1	5.9	4065	12.7	7.28
8.3	262.9	5.9	4110	12.8	7.26
9.1	266.3	5.9	4152	13.1	8.11
9.2	281.2	6.0	4178	13.4	8.17
9.3	284.6	6.1	4193	13.5	8.13
10.1	314.1	6.4	5217	13.8	8.21
10.2	321.7	6.4	5204	13.8	8.18
10.3	319.9	6.4	5211	14.1	8.19

Reed beds 6 -10

REED BED	Eh (mV)	pH	EC (µs/cm)	TEMP (°C)	DO (mg/L)
11.1	326.1	6.4	5209	12.7	7.35
11.2	338.6	6.4	5254	12.8	7.37
11.3	327.4	6.4	5228	12.8	7.35
12.1	333.7	6.4	5251	13.6	8.18
12.2	329.1	6.4	5301	13.8	8.24
12.3	337.2	6.4	5297	13.8	8.21
13.1	351.3	6.6	5316	12.6	7.24
13.2	346.9	6.6	5302	12.8	7.29
13.3	357.2	6.6	5421	12.8	7.26
14.1	314.3	6.4	5211	11.9	6.56
14.2	326.4	6.4	5294	12.1	6.82
14.3	331.7	6.4	5297	12.3	6.84
15.1	329.3	6.4	5314	12.4	6.79
15.2	339.4	6.4	5337	12.7	7.02
15.3	329.9	6.4	5319	12.6	7.13

Reed beds 11 -15

4

Appendix 9: *In situ* measurements of pH, Eh, EC and temperature, May, 2013 (Source: Joubert, 2013)

RBs	Temp (°C)	DO (mg/L)	EC (µs/cm)	pH
1.1	12.2	9.58	3450	6.24
1.2	15	8.64	3905	6.28
1.3	14	11.28	3642	6.49
2.1	14.3	4.21	4430	5.66
2.3	10.7	6.12	4333	4.21
3.1	12.1	8.54	3708	4.81
3.2	14.2	6.89	4065	4.51
3.3	13.2	5.77	4561	4.34
4.1	17.8	6.81	3816	5.75
4.3	14.7	7.6	3801	4.99
5.1	15.1	6.86	3708	5
5.3	15	7.33	3502	6.01
6.1	17	7.43	4128	4.23
6.2	14.7	7.44	3967	3.85
6.3	15.5	8.43	4093	3.77
7.1	16.8	6.84	3804	6.81
7.3	17.1	6.93	3726	6.03
8.1	21.4	6.27	4760	4.43

RBs	Temp (°C)	DO (mg/L)	EC (µs/cm)	pH
8.3	14.2	8.43	3870	5.47
9.1	15	8.03	3717	4.7
9.2	18.1	8.22	4139	4.41
9.3	18.1	8.32	3056	4.35
10.1	12.8	9.35	3383	4.72
10.3	18	9.4	3823	4.9
11.1	17.1	8.21	3620	6.84
11.3	17.7	8.61	3746	6.46
12.1	12.8	9.76	3443	7.25
12.2	22.5	6.54	4083	7.55
12.3	19.9	6.56	2473	7.15
13.1	13.9	6.9	3170	7
13.3	16.3	8.74	3436	7.12
14.1	16.2	6.91	3227	7.3
14.3	18.6	6.66	3780	6.95
15.1	12.8	6.95	2907	7.06
15.2	16.3	6.34	3240	6.76
15.3	16	7.27	3178	7.17

Appendix 10: *In situ* measurements of pH, Eh, EC and temperature, July, 2013 (Source: Joubert, 2013)

RBs	Temp (°C)	DO (mg/L)	EC (µs/cm)	pH	Eh
1.1	8.8	8.58	3295	6.13	185.7
1.2	10.6	8.35	4577	6.25	176.1
1.3	8.9	8.71	3278	6.44	237.6
2.1	11.7	6.26	3402	5.88	226.6
2.3	8.9	7.93	3360	5.88	322.3
3.1	10	10.21	3612	6.23	176
3.2	11	9.61	3670	5.79	187.2
3.3	11.1	8.83	3713	6.03	282.1
4.1	14.8	7.77	3730	6.25	205.5
4.3	13.6	10.28	4081	6.16	196.1
5.1	13.3	7.8	3754	5.76	163.4
5.3	14.5	8.05	4119	6.03	188.5
6.1	14.7	8.82	4500	5.6	216.6
6.2	12.2	8.22	4243	4.82	230.6
6.3	12.4	8.65	4254	4.35	330.6
7.1	13.4	7.96	4336	6.07	209.1
7.3	14.2	7.29	4472	6	215.3
8.1	19.5	7.14	3943	6.42	217.8

RBs	Temp (°C)	DO (mg/L)	EC (µs/cm)	pH	Eh
8.3	12.3	8.95	4086	6.17	220.7
9.1	11.7	10.07	3395	6.34	264.2
9.2	14.3	9.32	3596	6.33	256.8
9.3	14	10.08	3543	6.7	212.4
10.1	9.3	10.82	3214	6.46	195.4
10.3	14.3	9.72	3344	6.58	235.7
11.1	14.3	7.47	4893	6.04	225.5
11.3	14.2	9.65	3230	6.73	220.3
12.1	10.9	9.82	3002	6.97	117.8
12.2	16.4	7.97	3476	6.88	219.5
12.3	19.8	7.56	3652	6.72	201.4
13.1	12.1	7.16	4729	6.61	197.6
13.3	14.2	7.33	3381	6.7	209
14.1	16.8	8.18	3030	6.93	214.6
14.3	18	7.5	3844	6.75	210.4
15.1	14.1	8.05	2979	6.51	156.5
15.2	13.5	6.42	3028	6.41	199.2
15.3	16.2	7.45	2937	6.08	203.2

Appendix 11: Certified Values of Stream Sediment Reference Materials (Approved by China National Analysis Center for Iron and Steel (Beijing, China, Issued in 2010).

μg/g	NCS DC73315a	μg/g	NCS DC73315a	μg/g	NCS DC73315a	μg/g	NCS DC73315a
P	575±23	Sr	78±2	W	5.5±0.3	CaO	0.77±0.02
Pb	102±4	Ta	1.3±0.1	Y	29±2	Na_2O	0.64±0.03
Pr	9.3±0.2	Tb	0.90±0.06	Yb	3.1±0.3	K_2O	2.59±0.05
Rb	129±4	Te	(0.3)	Zn	263±5	H_2O	3.97±0.26
S	0.24±0.03*	Th	14.8±0.7	Zr	275±17	CO_2	(0.45)
Sb	8.9±0.7	Ti(%)	0.46±0.02	SiO_2(%)	69.33±0.20	Corg	(0.51) **
Sc	12.1±0.5	Tl	0.84±0.06	Al_2O_3	13.40±0.09	TC	(0.7)
Se	0.37±0.04	Tm	0.48±0.03	TFe_2O_3	5.27±0.07		
Sm	6.1±0.1	U	3.9±0.2	FeO	(0.78)		
Sn	5.0±0.5	V	99±3	MgO	1.29±0.03		